

**INVESTIGATION OF BIOMARKERS USING  
LIPIDOME-BASED RESEARCH ANALYSIS IN  
SIALIDOSIS**

**A Thesis Submitted to  
the Graduate School of Engineering and Sciences of  
İzmir Institute of Technology  
in Partial Fulfillment of the Requirements for the Degree of**

**MASTER OF SCIENCE**

**in Molecular Biology and Genetics**

**by  
İlker GÜMÜŞ**

**March 2024  
İZMİR**

We approve the thesis of **İlker GÜMÜŞ**

**Examining Committee Members:**

---

**Prof. Dr. Volkan SEYRANTEPE**

Department of Molecular Biology and Genetics, Izmir Institute of Technology

---

**Prof. Dr. Özden YALÇIN ÖZUYSAL**

Department of Molecular Biology and Genetics, Izmir Institute of Technology

---

**Assoc. Prof. Dr. Kemal Uğur TÜFEKÇİ**

Vocational School of Health Services, Izmir Democracy University

**20 March 2024**

---

**Prof. Dr. Volkan SEYRANTEPE**

Supervisor, Department of Molecular Biology and Genetics  
Izmir Institute of Technology

---

**Prof. Dr. Özden YALÇIN ÖZUYSAL**

Head of Department of Molecular  
Biology and Genetics

---

**Prof. Dr. Mehtap EANES**

Dean of Graduate School of  
Engineering and Sciences

## ACKNOWLEDGMENTS

First, I would like to express my deepest regards and respect to my supervisor Prof. Dr. Volkan SEYRANTEPE for his support, guidance, and extensive knowledge in my research and thesis studies.

I would like to thank The Scientific and Technological Research Council of Turkey (TUBITAK) (121Z099) for the financial support of the Project and for providing me with a scholarship. I would like to extend my sincere thanks to my colleagues as family members of SEYRANTEPE Laboratory. I am grateful to my supportive friends, Orhan Kerim İNCİ, Selman YANBUL, Tufan Utku ÇALIŞKAN, Ebru ADA, Hatice Hande BASIRLI, Melike CAN ÖZGÜR, Nurselin ATEŞ, Beyza KAYA, Tuğçe ŞENGÜL for their mentoring, support and kindness during my research and thesis work. I especially thank Seçil AKYILDIZ DEMİR for her assistance and help during my graduate studies. I am also appreciative of all undergraduate members of SEYRANTEPE Laboratory for their motivation and infinite help. In a nutshell, I am so appreciative of my family members, my father Yüksel GÜMÜŞ, my mother Hasibe GÜMÜŞ, my sister Hande GÜMÜŞ for their infinite love and their infinite trust for my entire career, and their infinite support during my thesis. I am also so grateful to my wife Melike GÜMÜŞ for her passion love, understanding, endless and infinite support, and trust during this thesis.

# ABSTRACT

## INVESTIGATION OF BIOMARKERS USING LIPIDOME-BASED RESEARCH ANALYSIS IN SIALIDOSIS

Neuraminidase 1, also known as N-acetyl- $\alpha$ -neuraminidase, is an enzyme found in lysosomes and encoded by the NEU1 gene. This enzyme is responsible for eliminating terminal sialic acids from glycoproteins and oligosaccharides. When mutations occur in the NEU1 gene, it leads to a particular lysosomal storage disorder known as sialidosis. Sialidosis is a rare genetic disorder that is inherited in an autosomal recessive manner. Sialidosis is classified into two subtypes: Type I, which has a later onset, and Type II, which presents with an early onset. In previous studies, an increase in glycolipid levels in visceral organs, and accumulation of sialyloligosaccharides and sialoglycoproteins were reported. However, the effect of NEU1 sialidase on secondary lipid expression levels in sialidosis pathology remains unknown. The relationship between lipid expression levels and inflammation of human and mouse sialidosis fibroblast cell lines was analyzed for the first time in this study. To understand the connection between secondary lipid alterations and inflammation in sialidosis molecular biological approaches and shotgun lipidome analysis were followed. The link between the secondary lipid alterations and their association with sialidosis was determined in our research. We have concluded that the findings not only provide the elucidation of the lipidome characteristics in sialidosis models of mice and patients, but they also have the potential to establish a connection between the lipidome and the occurrence of inflammation in sialidosis. Grasping the correlation between the changes in secondary lipids and inflammation may offer therapeutic strategies for sialidosis patients by modulating the expression of secondary lipids.

# ÖZET

## SİALİDOZ HASTALIĞINDA LİPİDOM ANALİZİ İLE BİYOBELİRTEÇLERİN BELİRLENMESİ

N-asetil-a-nöraminidaz olarak da bilinen Neuraminidaz 1, lizozomlarda bulunan ve NEU1 geni tarafından kodlanan bir enzimdir. Bu enzim, terminal sialik asitlerin glikoproteinlerden ve oligosakaritlerden elimine edilmesinden sorumludur. NEU1 geninde mutasyonlar meydana geldiğinde, sialidoz olarak bilinen özel bir lizozomal depo bozukluğuna yol açar. Sialidoz, otozomal resesif bir şekilde kalıtsal olan nadir bir genetik hastalıktır. Sialidoz iki alt tipe ayrılır: Daha geç başlayan Tip I ve erken başlayan Tip II. Önceki çalışmalarda iç organlarda glikolipid düzeylerinde artış ve sialiloligosakkaritler ile sialoglikoproteinlerin birikimi rapor edilmiştir. Ancak NEU1 sialidazın sialidoz patolojisinde sekonder lipid ekspresyon seviyeleri üzerindeki etkisi bilinmemektedir. İnsan ve fare sialidosis fibroblast hücre dizilerinin lipid ekspresyon düzeyleri ile inflamasyonu arasındaki ilişki ilk kez bu çalışmada analiz edildi. Sialidozda ikincil lipid değişiklikleri ile inflamasyon arasındaki bağlantıyı anlamak için moleküler biyolojik yaklaşımlar ve Shotgun Lipidome analizi takip edildi. Araştırmamızda sekonder lipid değişiklikleri ile sialidoz arasındaki ilişki belirlendi. Bulguların, fare ve hastaların sialidoz modellerinde lipidom özelliklerinin aydınlatılmasının yanı sıra, lipidom özellikleri ile sialidozda inflamasyon oluşumu arasında bağlantı kurma potansiyeline sahip olduğu sonucuna vardık. Sekonder lipidlerdeki değişiklikler ile inflamasyon arasındaki korelasyonun anlaşılması, sekonder lipidlerin ekspresyonunu modüle ederek sialidoz hastaları için terapötik stratejiler sunabilir.

*Dedicated to my precious family...*

# TABLE OF CONTENTS

LIST OF FIGURES .....	ix
LIST OF TABLES .....	xiii
CHAPTER 1. INTRODUCTION .....	1
1.1. Lipids .....	1
1.2. Glycoconjugates in Eukaryotes .....	1
1.2.1. Glycolipids .....	2
1.2.2. Glycosphingolipids .....	2
1.3. Sialidases .....	3
1.3.1. Neu1 (Neuraminidase 1) Sialidase .....	5
1.4. Lysosomal Storage Diseases .....	6
1.4.1. Sialidosis .....	8
1.4.2. Mice Models of Neu1 (Neuraminidase I) Sialidase Deficiency .....	9
1.5. Inflammation .....	9
1.5.1. Inflammation in Lysosomal Storage Disease .....	11
1.6. Secondary Lipid Alterations in Lysosomal Storage Diseases .....	13
1.7. Aim of the Thesis Study .....	14
CHAPTER 2. MATERIAL & METHODS .....	16
2.1. Animals .....	16
2.2. Mouse Genotyping .....	16
2.2.1. Genotyping of Mice for Neu1 Allele .....	17
2.3. Isolating Fibroblasts from Animals .....	18
2.4. Human Cell Lines .....	19
2.5. Immortalization of Fibroblast Cell Lines .....	19
2.6. Real-Time PCR .....	20
2.6.1. RNA Isolation .....	20
2.6.2. cDNA Synthesis .....	21
2.6.3. RT-PCR .....	22
2.7. QPCR Array .....	23

2.7.1. RNA Isolation with Qiagen RNase Plus Mini Kit.....	24
2.7.2. cDNA Conversion for Real-Time PCR Array .....	25
2.7.3. RT <sup>2</sup> Profiler PCR Array .....	25
2.8. Western Blot .....	27
2.8.1. Protein Isolation.....	27
2.8.2. Bradford Assay and Protein Preparation.....	27
2.8.3. SDS-PAGE Gel Electrophoresis .....	29
2.9. Lipidome Analysis.....	31
2.9.1. Preparing Samples for Shotgun Lipidome Analysis.....	31
 CHAPTER 3. RESULTS .....	 32
3.1. Genotyping of Mice for Neu1 .....	32
3.2. Lipidome Analysis.....	32
3.3. RT-PCR.....	38
3.3.1 Array Results .....	38
3.3.2. qPCR Results .....	48
3.4. Western Blot .....	50
3.5. Histological Analysis.....	53
3.5.1. Oil-RED-O Staining .....	53
3.5.2. Periodic acid – Schiff Stain (PAS) Staining .....	53
 CHAPTER 4. DISCUSSION.....	 57
 CHAPTER 5. CONCLUSION .....	 66
5.1. Future Directions .....	67
 REFERENCES .....	 68

## LIST OF FIGURES

<u>Figure</u>	<u>Page</u>
Figure 1.1. Representative of the asymmetry of membrane with the location of glycoproteins and glycolipids. (Source: N.V. Bhagavan and Chung-Eun Ha, 2011) .....	2
Figure 1.2. Scheme of how to work Neu1 enzyme on the Glycoprotein and Glycolipid molecules. (Source: Mohammad et al. 2018).....	3
Figure 1.3. Schematic of the potential loss of the neurons during the lysosomal storage disease. (Source: Bosch, M.E and Kielian, T., 2015).....	12
Figure 2.1. Figure 2.1. Representative of <i>Neu1</i> <sup>-/-</sup> Mouse Breeding.....	17
Figure 2.2. Figure 2.2. RT2 profiler PCR Array Format.....	24
Figure 3.1. Neu1 gene alleles genotyping which is coming from the tails of mice by conducting PCR protocols. Amplification of the mutant allele was monitored at 180 bp and wild type allele was monitored at 400 bp.....	32
Figure 3.2. Glycerophospholipid lipidome assays from 2-month-old <i>WT</i> and <i>Neu1</i> <sup>-/-</sup> mice (A, B, and C) and 5-month-old <i>WT</i> and <i>Neu1</i> <sup>-/-</sup> mouse fibroblasts (D, E, and F) were shown in Figure 3.2. The comparison between <i>WT</i> and <i>Neu1</i> <sup>-/-</sup> was determined with the GraphPad analysis and the One-way ANOVA test was conducted. Each sample was conducted with n=3.....	33
Figure 3.3. Glycerophospholipid lipidome assays from human fibroblast cell lines. Orderly, GM01719, GM02921, and GM01718 are human fibroblast cell lines. GM01719 is called C1, control 1. GM02921 is counted as a P1, patient 1. GM01718 is counted as P2, patient 2. The analysis was conducted according to the comparison between <i>WT</i> and <i>Neu1</i> <sup>-/-</sup> was determined with the GraphPad analysis and a One-way ANOVA test was conducted. Each sample was conducted with n=3.....	35
Figure 3.4. Glycerolipid lipidome assays from 2-month-old <i>WT</i> and <i>Neu1</i> <sup>-/-</sup> mouse (A) and 5-month-old <i>WT</i> and <i>Neu1</i> <sup>-/-</sup> mouse fibroblast cell line samples (B), and human fibroblast cell lines (C). Orderly, GM01719, GM02921, and GM01718 which are human fibroblast cell lines. GM01719 is called C1, control 1. GM02921 is counted as a P1, patient 1. GM01718 is counted as P2, patient 2. The amount of each lipid was added, and a one-way-ANOVA analysis was used to determine p-values by using GraphPad. Data were reported as means SEM (n=3, *p<0,05, **p<0,01, ***p<0,001). Each sample was conducted with n=3.....	36

<u>Figure</u>	<u>Page</u>
Figure 3.5. Sterol lipids lipidome assays from 2-month-old <i>WT</i> and <i>Neu1</i> <sup>-/-</sup> mouse (A) and 5-month-old <i>WT</i> and <i>Neu1</i> <sup>-/-</sup> mouse fibroblast cell line samples (B), and human fibroblast cell lines (C). Orderly, GM01719, GM02921, and GM01718 which are human fibroblast cell lines. GM01719 is called C1, control 1. GM02921 is counted as a P1, patient 1. GM01718 is counted as P2, patient 2. The amount of each lipid was added, and a 2-way ANOVA analysis was used to determine p-values by using GraphPad. Data were reported as means SEM (n=3, *p<0,05, **p<0,01, ***p<0,001). Each sample was conducted with n=3.....	37
Figure 3.6. Gene expression ratio of chemokines in 2-month-old <i>WT</i> and <i>Neu1</i> <sup>-/-</sup> mouse fibroblasts (A) and 5-month-old <i>WT</i> and <i>Neu1</i> <sup>-/-</sup> mouse fibroblasts (B) also Orderly, GM01719, GM02921 and GM01718 which are human fibroblast cell lines. GM01719 is called C1, control 1. GM02921 is counted as a P1, patient 1. GM01718 is counted as P2, patient 2 (C). Expression ratios were calculated with $\Delta$ CT method and 2-way-ANOVA analysis was used to determine p-values by using GraphPad. Data were reported as means SEM (n=3, *p<0,05, **p<0,01, ***p<0,001).....	39
Figure 3.7. Gene expression ratio of interleukins in 2-month-old <i>WT</i> and <i>Neu1</i> <sup>-/-</sup> mouse fibroblasts (A) and 5-month-old <i>WT</i> and <i>Neu1</i> <sup>-/-</sup> mouse fibroblasts (B) also orderly, GM01719, GM02921, and GM01718 which are human fibroblast cell lines. GM01719 is called C1, control 1. GM02921 is counted as a P1, patient 1. GM01718 is counted as P2, patient 2 (C). Expression ratios were calculated with the $\Delta$ CT method and 2-way-ANOVA analysis was used to determine p-values by using GraphPad.....	41
Figure 3.8. Gene expression ratio of interferons and TNF Receptor Family Members in 2-month-old <i>WT</i> and <i>Neu1</i> <sup>-/-</sup> mouse fibroblasts (A and B) and 5-month-old <i>WT</i> and <i>Neu1</i> <sup>-/-</sup> mouse fibroblasts (C and D) also Orderly, GM01719, GM02921 and GM01718 which are human fibroblast cell lines. GM01719 is called C1, control 1. GM02921 is counted as a P1, patient 1. GM01718 is counted as P2, patient 2 (E and F).....	43
Figure 3.9. Gene expression ratio of Growth Factors in 2-month-old <i>WT</i> and <i>Neu1</i> <sup>-/-</sup> mouse fibroblasts (A) and 5-month-old <i>WT</i> and <i>Neu1</i> <sup>-/-</sup> mouse fibroblasts (B) also orderly, GM01719, GM02921, and GM01718 which are human fibroblast cell lines.....	45

<u>Figure</u>	<u>Page</u>
Figure 3.10. Gene expression ratio of Other Cytokines in 2-month-old <i>WT</i> and <i>Neu1</i> <sup>-/-</sup> mouse fibroblasts (A) and 5-month-old <i>WT</i> and <i>Neu1</i> <sup>-/-</sup> mouse fibroblasts (B) also Orderly, GM01719, GM02921 and GM01718 which are human fibroblast cell lines. GM01719 is called C1, control 1. GM02921 is counted as a P1, patient 1. GM01718 is counted as P2, patient 2 (C). Expression ratios were calculated with $\Delta$ CT method and 2-way-ANOVA analysis was used to determine p-values by using GraphPad. Data were reported as means SEM (n=3, *p<0,05, **p<0,01, ***p<0,001).....	46
Figure 3.11. Gene expression ratio of Ccl2, Ccl5, and Cxcl10 in 2-month-old <i>WT</i> and <i>Neu1</i> <sup>-/-</sup> mouse fibroblasts and 5-month-old <i>WT</i> and <i>Neu1</i> <sup>-/-</sup> mouse fibroblasts was shown orderly in A, B, and C part of the figure. Expression ratios were calculated with $\Delta$ CT method and 2-way-ANOVA analysis was used to determine p-values by using GraphPad. Data were reported as means SEM (n=3, *p<0,05, **p<0,01, ***p<0,001).....	48
Figure 3.12. Gene expression ratio of Ccl2, Ccl3, Ccl5, and Cxcl10 in GM01719, GM02921, and GM01718 which are human fibroblast cell lines. GM01719 is called C1, control 1. GM02921 is counted as a P1, patient 1. GM01718 is counted as P2, patient 2 (C). Expression ratios were calculated with $\Delta$ CT method and 2-way-ANOVA analysis was used to determine p-values by using GraphPad. Data were reported as means SEM (n=3, *p<0,05, **p<0,01, ***p<0,001).....	49
Figure 3.13. The representative Western Blot analysis for inflammatory detection of 2- and 5-month-old <i>WT</i> and <i>Neu1</i> <sup>-/-</sup> mice fibroblast cells. Analyses of immunoblot were monitored in Figure 3.12A for IKB- $\alpha$ and $\beta$ -actin (A). Analyses of immunoblot were monitored in Figure 3.12B for NF- $\kappa$ B and $\beta$ -actin (B). Analysis of the intensity of IKB- $\alpha$ for 2- and 5-month-old <i>WT</i> and <i>Neu1</i> <sup>-/-</sup> mice fibroblast cells (C). Analysis of the intensity of NF- $\kappa$ B for 2-month (2M) and 5-month-old (5M) <i>WT</i> and <i>Neu1</i> <sup>-/-</sup> mice fibroblast cells (D).....	51
Figure 3.14. The representative Western Blot analysis for inflammatory detection of orderly, GM01719, GM02921, and GM01718 which are human fibroblast cell lines. One of the <i>WT</i> controls of the human fibroblast cell line from our laboratory used GM01719 is called C1, control 1. GM02921 is counted as a P1, patient 1. GM01718 is counted as P2, patient 2, these are human fibroblast cells. Analyses of immunoblot were monitored in Figure 3.13A for IKB- $\alpha$ and $\beta$ -actin (A). Analyses of immunoblot were monitored in Figure 3.13B for NF- $\kappa$ B and $\beta$ -actin (B). Analysis of the intensity of IKB- $\alpha$ and intensity of NF- $\kappa$ B for human fibroblast cells (D).....	52

<b><u>Figure</u></b>	<b><u>Page</u></b>
Figure 3.15. Oil-Red-O staining and Periodic acid-Schiff stain (PAS) staining in 2-month-old WT, <i>Neu1</i> <sup>-/-</sup> mice fibroblast samples (Figure 3.15A, B, C and D), and 5-month-old WT, <i>Neu1</i> <sup>-/-</sup> mice fibroblast samples (Figure 3.15E, F, G and H). Images were taken at 40X magnification by Olympus light microscope.....	55
Figure 3.16. Oil-Red-O staining and Periodic acid - Schiff Stain (PAS) staining in human fibroblast samples which are orderly, one of the human control fibroblasts from our laboratory as a Control 1, also GM01719, GM02921, and GM01718 which are human fibroblast cell lines. One of the <i>WT</i> controls of the human fibroblast cell line from our laboratory used GM01719 is called C2, control 2. GM02921 is counted as a P1, patient 1. GM01718 is counted as P2, patient 2, these are human fibroblast cells (Figure 3.15A, B, C, D, E, F, G, and H). Images were taken at 40X magnification by Olympus light microscope.....	56

# LIST OF TABLES

<b><u>Table</u></b>	<b><u>Page</u></b>
Table 1.1. Human Sialidases Properties.....	5
Table 2.1. Primer sequences that were conducted while genotyping of mice.....	18
Table 2.2. Primer of the forward and reverse of the inflammation marker genes .....	22
Table 2.3. PCR component mix .....	26
Table 2.4. Cycling conditions for Roche LightCycler 96 .....	26

# CHAPTER 1

## INTRODUCTION

### 1.1. Lipids

Lipids have a tremendous impact on cellular events such as the storage of energy, cellular transport, and also formation of cellular membranes (Liu et al., 2021). According to the role of lipids in the structure of cellular membranes, cholesterol, glycerophospholipids, and sphingolipids have also different impacts on the synaptogenesis, conduction of impulses, and maintenance of myelin sheaths (Cermenati et al., 2015). The regulation of neuroinflammation is adjusted from these lipids (Fuller and Futerman, 2018). The lipids have different subgroups, and these subgroups are fatty acyls, glycerolipids, glycerophospholipids, prenol lipids, polyketides, saccharolipids, sphingolipids and sterol lipids (Stephenson et al., 2017).

### 1.2. Glycoconjugates in Eukaryotes

Glycoconjugates are a family of carbohydrates which are also known as glycans, and they are covalently linked to the non-sugar moieties such as lipids or proteins (Broussard, Alex C, and Michael Boyce, 2019). Some of the main glycoconjugates are glycoproteins, glycolipids, lipopolysaccharides, glycopeptides, peptidoglycans, and proteoglycans. These carbohydrates have an important role in acting as an informational carrier in the migration of cells, cell-cell recognition, and adhesion of cell-to-cell connectivity and glycoconjugates have an impact on the immune system which responds to the environment (Broussard, Alex C, and Michael Boyce, 2019). In nature, each cell possesses a glycocalyx which consists of the interface of the cell with the environment and this glycocalyx has a rich glycan coat surface of the cells (Schnaar, Gerardy-Schahn, and Hildebrandt 2014).

### 1.2.1. Glycolipids

Glycolipids are embedded in the membrane of the cell plasma. Glycolipids occur from glycosylated lipids. They are derivatives of glycosylated lipids. They are called a family member of the glycoconjugates. They contain one or more residues of monosaccharides which are bounded by a linkage of glycosidic chains. These linkages are moieties that are hydrophobic, and these are some sphingoids, ceramides which are N-acyl sphingoids, or prenyl phosphate or acylglycerols. Glycolipids possess also subgroups. These are Glycoglycerolipids and Glycosphingolipids (Malhotra, 2012). Lipids which come from the derivatives of glycosyl, have a critical impact on the fluidity of the cell membrane and the formation of lipid rafts in the cell membrane (Brandenburg and Holst 2015), (Malhotra, 2012).

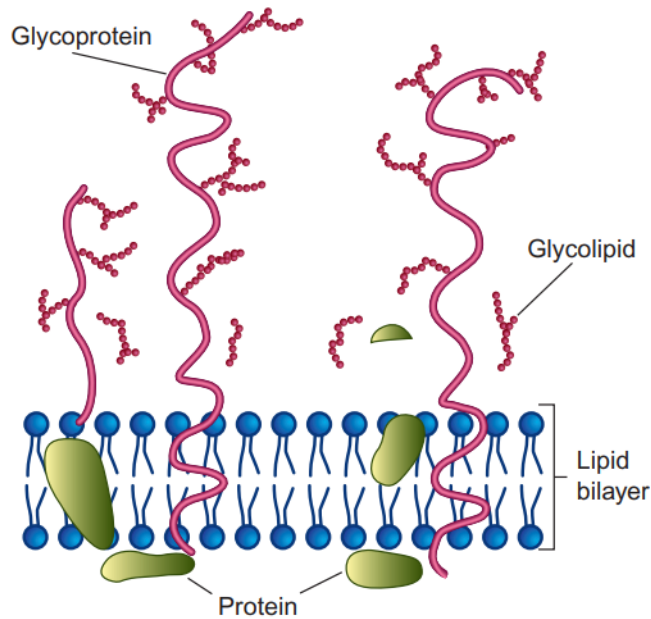


Figure 1.1. Representative of the asymmetry of membrane with the location of glycoproteins and glycolipids. These molecules which are carbohydrate-containing are exclusively present and monitored on the plasma membrane surface. (Source: N.V. Bhagavan and Chung-Eun Ha, 2011)

### 1.2.2. Glycosphingolipids

Glycosphingolipids are one of the subgroups of glycolipids. They contain an unsaturated hydrophobic part of the hydrocarbon group and occur from the core group of sphingosines (Carter et al. 1947). The unsaturated hydrophobic hydrocarbon part of this

composition is ceramide for Glycosphingolipids (Malhotra, 2012). Glycosphingolipids can be monitored in the membrane of the cells as a lipid raft composition in different species (Kopitz 2017; Schnaar and Kinoshita 2015). Glycosphingolipids play an important role in the adhesion of cells and the transduction of signal initiation in the cell connection (Kopitz 2017). Also, because of their localization parts in the cell membrane, they have an impact on the nervous system differentiation and maturation of the nervous system (Olsen and Færgeman 2017). Glycosphingolipids are monitored in tissues that are mostly related to the central nervous system (Coet et al. 1998).

Glycosphingolipids are differentiated according to their structural differences. These differences are categorized according to the moiety of carbohydrates. These carbohydrate moieties are globo-, lacto/neolacto-, asialo-series, and ganglio- groups (Furukawa et al. 2014).

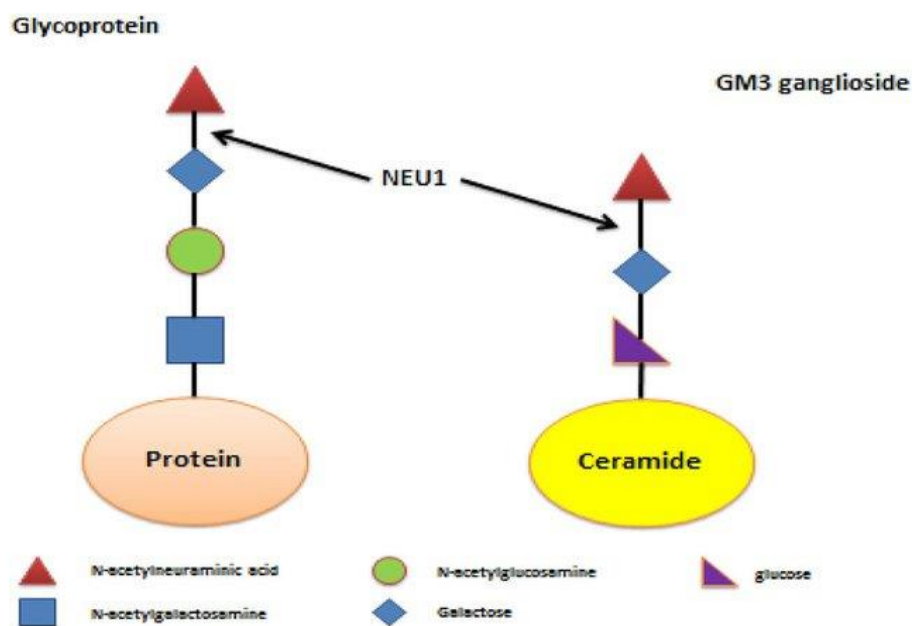


Figure 1.2. Scheme of how to work Neu1 enzyme on the Glycoprotein and Glycolipid molecules. (Source: Mohammad et al. 2018)

### 1.3. Sialidases

Neuraminidases or sialidases are enzymes that have a role in catalyzing sialic acid residues. These sialic acid residues are removed from the glycoproteins, glycolipids, gangliosides, and oligosaccharides (Saito and Sugiyama 2002). These enzymes possess a critical role in cellular functions such as the proliferation of cells, adhesion of cells, and alteration of receptors, or their differentiations. Also, these sialidases have an impact on

the degradation of some glycoconjugates which are gangliosides (Miyagi et al. 2012). Sialidases are categorized according to their localization in the cells.

There are four sialidases for mammalian cells and these enzymes are created by different genes these genes are Neu1, Neu2, Neu3, and Neu4 which are shown in Table 1. These enzymes can be localized in lysosomes which is Neu1 (Miyagi and Tsuiki, 1985) these enzymes can be localized in cytosolic, and these enzymes are encoded by Neu2 (Seyrantepe et al. 2004), enzymes can be associated with the membrane of plasma, and this is Neu3 (Miyagi 1990), also sialidases can be mitochondrial and this is Neu4 (Yamaguchi et al. 2005). On the other hand, moreover, to the localization of subcellular enzymes, their impact on the immune system, and the specificity of each enzyme can vary from each other (Miyagi 1990).

Neu1 sialidase is placed in the lysosomes. Neu1 is counted for the catabolism and degradation of sialoglycoconjugates in lysosomes (Frisch et al. 1979). Glycopeptides and oligosaccharides are some of the substrates of Neu1 sialidases (Schneider et al. 1991).

Neu2 sialidase is monitored in the cytosol and this is called Neuraminidase 2. Neuraminidase 2 possesses an attraction of gangliosides, glycoproteins, and oligosaccharides. Also, in the literature, Neu2 has an affinity for GM3 ganglioside activity (Miyagi and Yamaguchi 2012).

Neu3 sialidase is placed at the membrane of plasma and Neu3 sialidase is known as Neuraminidase 3. Neu3 sialidase is counted as an integral membrane protein. Neu3 sialidase adjusts the interaction of ganglioside oligosaccharide chains. The adhesion of cells, their pathways to apoptosis and differentiation, carcinogenesis, and some pathways that are related to the signaling of insulin are affected by oligosaccharide chain alterations (Miyagi and Yamaguchi 2012). Neu3 sialidase also possesses ganglioside activities for such different gangliosides. These gangliosides are GM1, GM2, and GM3 (Miyagi and Yamaguchi 2012).

Neu4 sialidase (Neuraminidase 4) is placed in the outer and inner membrane of the mitochondria (Yamaguchi et al. 2005) and the lumen of the lysosome (Seyrantepe et al. 2004). Neu4 sialidase has an attraction with glycoproteins and oligosaccharides. Neu4, which is associated with mitochondria, plays a crucial role in the differentiation of neurons and it affects apoptosis. GM2 and GD1a ganglioside activity was monitored according to the Neu4 sialidase (Seyrantepe et al. 2008).

### 1.3.1. Neu1 (Neuraminidase 1) Sialidase

The Neu1 gene, also known as Neuraminidase 1, is a human gene located on chromosome 6p21.3. Neu1 is a lysosomal enzyme belonging to the sialidase family. It plays a crucial role in the catabolism of sialic acid-containing molecules in various tissues and cell types. Sialic acids are important glycoconjugates that participate in cell adhesion, signaling, and recognition processes. The protein from the human Neu1 gene is transcribed. This protein contains 145 amino acids (Pshezhetsky et al. 1997).

Table 1.1. Human Sialidases Properties (Source: Momti et al. 2002)

	NEU1	NEU2	NEU3	NEU4
Cellular Localization	Lysosome	Cytosol Nucleus	Plasma Membrane	Lysosome Intracellular Membrane Mitochondria
Substrate Preference	Oligosaccharides 4MU-Neu5Ac <sup>1</sup>	Glycoproteins Oligosaccharides Gangliosides 4MU-Neu5Ac	Gangliosides	Glycoproteins Oligosaccharides Gangliosides 4MU-Neu5Ac
Optimal pH	4.4-4.6	6.0-6.5	4.6-4.8	4.4-4.5
Deduced Functions/ Processes Involved	Lysosomal catabolism Immune response	Myogenesis	Tumorigenesis Neuronal differentiation	Lysosomal catabolism Neuronal differentiation
Genomic Localization	6p21.31	2p37.1	11q13.4	2p37.3

On the other hand, in the mouse Neu1 gene is in chromosome 17 (Frisch et al. 1979). Neu1 sialidase works in humans systematically and expression of Neu1 sialidase occurs in whole tissues, especially in the pancreas (Bonten et al. 1996). Neu1 gene expression is varied in the mouse however, expression of the Neu1 gene is mostly observed in the kidney, pancreas heart, liver, spleen, lung, and brain (Igdoura et al. 1998).

Sialidase of Neu1 plays a crucial role in sialoglycoconjugate catabolism in lysosomes, and its degradation in lysosomes (Frisch et al. 1979). According to Table 1, the Sialidase of Neu1 substrates are glycopeptides and oligosaccharides. On the other

hand, it was published that Neu1 may have an impact on glycolipid catabolism (Schneider et al. 1991).

The form of the Neu1 sialidase enzyme is comprised of  $\beta$ galactosidase ( $\beta$ -Gal) and lysosomal protective protein Cathepsin A (PPCA) (Horst et al. 1989). The protective protein Cathepsin A supports the stabilization of the glycosidase. Also, PPCA activity deficiency was shown to reason for the galactosialidosis which is named as a disorder of lysosomal storage disease (D'Azzo et al. 1996).

Neu1 sialidase enzymes possess different participations in different processes such as activation of adaptive immune system cells or sialoglycoconjugate catabolism (Seyrantepe et al. 2003; Nan, Carubelli, and Stamatatos 2007). Neu1 sialidase enzyme is also responsible for IL-4 and IFN- $\gamma$  expression. Moreover, in the literature, it was published that IFN- $\gamma$  expression is prevented according to the Neu1 sialidase activity deficiency (Nan et al. 2007). Also, the Neu1 sialidase enzyme participates in the metabolism of elastin (Starcher et al. 2008; Seyrantepe et al. 2008; Bocquet et al. 2021). The activity of Neu1 sialidase supports the Th2 cytokine productions and Toll-like receptor activation (Chen et al. 2014). Neu1 sialidase enzyme has an impact on the activation of TLR2, TLR3, and TLR4 (Amith et al. 2009), macrophage phagocytosis in cells (Seyrantepe et al. 2010), pathogenesis of cancer (Garcia-Dominguez et al. 2022; Lv et al. 2020). The negative correlation between Neu1 sialidase activity and the activity capacity of cancer cells for metastasis was published (Uemura et al. 2009). A high level of GM3 ganglioside in mouse cells of carcinoma was monitored with the lower activity of Neu1 sialidase (Miyagi and Yamaguchi 2012). However, in a recent study, it was published that GM3 ganglioside accumulation was not monitored in all types of cells with the deficiency of Neu1 sialidase (Aerts et al. 2019). Moreover, in the literature, GM3 ganglioside catabolism is correlated with the Neu3 and Neu4 sialidases in the brain of mice (Pan et al. 2016). On the other hand, how deficiency of Neu1 impacts brain ganglioside and other organ oligosaccharides remains unknown (Breiden and Sandhoff 2020).

#### **1.4. Lysosomal Storage Diseases**

Lysosomal storage disorders (LSDs) are uncommon genetic conditions marked by issues with the proper functioning of lysosomes – small compartments enclosed in cell

membranes. These lysosomes hold enzymes essential for breaking down diverse molecules like proteins, lipids, and carbohydrates, breaking them into smaller components to recycle or remove them. In LSDs, a deficiency or malfunction in one of these lysosomal enzymes causes certain substances to build up within the lysosomes (Neufeld 1991; Tardy et al. 2004). This buildup can hinder cell functions and trigger various symptoms based on the disorder.

Lysosomal storage disorders (LSDs) can occur because of the absence of enzymes which are localized in lysosomes, and some of the substances are accumulated according to this absence of enzymes. These substances are substrates or biomolecules which are glycosaminoglycans, gangliosides, sphingolipids, glycosphingolipids, glycoproteins, and other lipids in the lysosomes was shown and their enormous accumulation is the reason for toxicity in the cellular area (Ferreira and Gahl 2017).

Substrate accumulation causes the storage of these substances, and their storage has an impact on different cell types and systems. These cell types are in the nervous system or system of reticuloendothelial, muscle eye, etc. (Boustany 2013). Accumulation of these substrate levels determines how the impact is critical on patients. This effect can be more severe or it can be monitored as a mild effect. Especially, the activity of the enzyme adjusts the substrate level accumulation.

The symptoms and seriousness of LSDs can differ significantly. A number of these conditions are identified during childhood, and it's vital to detect them early and take action to alleviate symptoms and enhance the well-being of those impacted. Potential treatments encompass enzyme replacement therapy, substrate reduction therapy, and additional supportive measures aimed at handling particular symptoms and complications. Since these disorders are rooted in genetics, a definitive cure is currently lacking, prompting ongoing research to advance improved treatment methods and interventions. According to the literature, more accumulation of substances can cause more severe phenotypes and it is monitored at earlier ages (Conzelmann and Sandhoff 1983). In patients with lysosomal storage disorders, non-catabolized substances accumulate gradually and as time goes by time the accumulation progresses. Moreover, alterations not only occur in the substances that are related to the deficiency of genes but also secondary alterations are observed in the lysosomal storage disorders. These such as glycoaminoacids, and oligosaccharides can accumulate in the patient's urinary system and accumulations of these secondary substrates are key for a patient's diagnosis of LSDs (Xia et al. 2013).

### **1.4.1. Sialidosis**

Sialidosis occurs because of the deficiency of Neu1 sialidase. It is a systematic disease, and it affects the whole body. The oligosaccharides accumulation which are sialylated in organs and the accumulation of substances in body fluids or urine is the detection part of sialidosis disease in humans (Pelt et al. 1988). There are two types of sialidosis. The variant of the disease is Type I and Type II clinically.

Type I sialidosis is counted as a mild form which is also called cherry-red-spot myoclonus. In Type I sialidosis symptoms are monitored late on set such as second or third life decade. Impairment of visuality and myoclonus are the indicator symptoms of Type I sialidosis and these symptoms gradually progress according to the disease (d'Azzo et al. 2015). Type I sialidosis may not alter the intellectuality of the patient, however, the problems occur in the movements such as voluntarily, also tremors, seizures, lymphocytes which are vacuolated in peripheral blood, and lysosomes which are swollen in the liver Kupffer cells are monitored in the Type I patients (d'Azzo et al. 2015). Also, the oligosaccharides accumulation in the system of central nervous neurons was observed in the biopsy of brain tissue of sialidosis patients who possess Type I variant salidosis (Sekijima et al. 2013).

Type II sialidosis is the severe variant of the disease. In this variant of the disease, the complete absence of lysosomal neuraminidase is monitored. It is lethal during fetal development or at birth. In this Type II variant of the sialidosis prenatal ascites, hydrops fetalis and hepatosplenomegaly can be monitored in the patients (Khan and Sergi, 2018). Also, in Type II sialidosis, coarse features, dysostosis multiplex, renal involvement, and cardiac anomalies are indicators of this type of variant in sialidosis. The different mutation types such as missense, nonsense mutations, deletions, or insertions can cause the severe type of sialidosis (Seyrantepe et al. 2003). Some of the lipids are accumulated in Type II sialidosis such as GD3, GM4, GM3, and LM1 in the patients' visceral organs. However, this accumulation of the glycolipids has not been monitored in the patient's brain tissue (Breiden and Sandhoff 2020). Type II sialidosis is a rare genetic condition marked by a lack of neuraminidase enzyme, resulting in the buildup of glycoproteins and glycolipids in different body tissues and organs. This disorder is inherited through autosomal

recessive inheritance and exhibits diverse clinical symptoms (d'Azzo et al. 2015). Diagnosis entails a clinical assessment and genetic testing, with treatment primarily centered around providing support. The outlook for affected individuals varies based on the severity of the condition in Type II sialidosis under the mutations on the *Neu1* gene.

#### **1.4.2. Mice Models of Neu1 (Neuraminidase I) Sialidase Deficiency**

To study the function of the *Neu1* gene and to monitor the role of neuraminidase 1 in physiological pathways *Neu1* nullizygous mice were created by d'Azzo et al., 2002. In these created mice this model occurred by the LacZ/PGK/neo expression cassette insertion into the exon1 of the *Neu1* gene (de Geest et al. 2002). In the adaptive immune system cells, vacuolization was observed except for neutrophils in the mice model of *Neu1*<sup>-/-</sup> (de Geest et al. 2002). These mice represent the variant of Type II sialidosis which are suffering from the early set of the symptoms of *Neu1* sialidosis. Complete loss of the *Neu1* gene in mice triggers several symptoms which are edema, spleen enlargement, urinary excretion of oligosaccharides, nephropathy, impairment of neurons, spine deformity, and hematopoiesis (d'Azzo et al. 2002). The size of the mice *Neu1*<sup>-/-</sup> have a smaller proportion of the body and weight compared to the same age of *WT* mice. The life span of *Neu1*<sup>-/-</sup> mice is between 5 to 8 months and these mice stopped breeding at the age of late-onset (d'Azzo et al. 2002).

Mice models have been created to investigate *Neu1* sialidase deficiency, allowing researchers to explore its underlying mechanisms and potential treatment avenues. It's worth noting that although these mouse models are valuable for studying genetic disorders like *Neu1* sialidase deficiency, they don't entirely replicate the complexity of the human condition. Nonetheless, they offer crucial insights into disease mechanisms and possible therapeutic approaches. Researchers frequently employ a combination of cell culture models, animal models, and human studies to gain a comprehensive understanding of rare genetic disorders such as sialidosis.

### **1.5. Inflammation**

Inflammation is the key regulator processes that respond to the body's stimuli. Inflammation occurs because of the pathogen encountered and cell damage or different

exposure to the substances. The response of the immune system's defense is shown as a component of the fundamental result of an inflammatory response. It has a tremendous impact on tissue maintaining homeostasis and supporting healing. During this intricate response, an array of cells, signaling molecules, and intricate mechanisms collaborate to eradicate the initial source of cellular damage, eliminate impaired tissue, and set in motion the procedures needed for tissue restoration.

An inflammatory response occurs according to the white blood cells or leukocytes. One of the white blood cells and the most abundant one is neutrophils. Neutrophils arrive at the inflammation site in front to respond to the damage (Rosales 2018). Neutrophils destroy and engulf the pathogens that are invading, and they release inflammatory mediators. Inflammatory mediators are cytokines and chemokines that impress other immune cells to the site (Nathan 2006). Macrophages are also another important cell of immune involved in inflammation. Pathogens and debris of cells are phagocytosed by macrophages. Its activation is followed by pro-inflammatory cytokine production, and these are interleukin-1(IL-1) and tumor necrosis factor-alpha (TNF- $\alpha$ ) (Gordon 2003). According to the response of these cytokines, this response plays a crucial role in intensifying the response of inflammation and inducing fever in the human body. Inflammation in the human body can occur both in supporting side or harmful side effects. It depends on the duration of inflammation and how intense it is. It is divided into two variants: acute and chronic inflammation. Acute inflammation is an initiation of healing processes and it is monitored in a short-term effect. On the other hand, chronic inflammation occurs over a long period, and chronic inflammation is related to different kinds of diseases or disorders which are autoimmune impacts or different cardiovascular diseases (Sally Hannoodee 2021).

To sum up, inflammation represents a very complicated or detailed and very thoroughly controlled biological reaction that encompasses a variety of immune cells and signaling molecules. While it serves as a critical defense mechanism against detrimental stimuli, its mismanagement can also contribute to the development of diseases (Zigterman and Dubois 2022).

### **1.5.1. Inflammation in Lysosomal Storage Disease**

Substrates that are accumulated because of the deficiency of genes are one of the unwanted materials that lead to the accumulation of unmetabolized depositions in cells. These depositions are glycolipid substrates that activate the pathogenic cascades. This situation triggers the process of the immune system and continues with the activation of inflammation (Rozenfeld and Feriozzi, 2017). The unwanted materials in the cells in lysosomal storage diseases cannot be digested and the response of the inflammation is continued because of this accumulation and deposition of substrates. Elimination of unwanted materials in the cells is important for ameliorating these acute inflammatory responses in Lysosomal storage disorders. However, lysosomal storage disorders possess this continuous chronic inflammatory response because of the deposition of unwanted materials. Lysosomes have an impact on the response of the immune system. For example, in the Fabry disease, scientists have monitored leukocyte perturbation and overexpression of leukocytes. In the Fabry disease, globotriaosylsphingosine (lyso-Gb3) globotriaosylceramide (Gb3), and toll-like receptors interact with each other, and this interaction comes from the dendritic cells (Rozenfeld and Feriozzi, 2017). From the dendritic cells, the signal is released and activates innate immunity. In the literature, Toll-like receptors are monitored to be triggered by these glycolipids and this activation process can cause inflammation and cascades of fibrosis in one of the lysosomal storage disorders (Rozenfeld and Feriozzi, 2017).

Lysosomes play a critical role in the system of immune functions (Vitner, Platt, and Futerman 2010) One of the roles of the lysosomes in the immune system is the presentation of antigens and processing of antigens, perforin secretion by cytotoxic T cells, pro-inflammatory mediators release and phagocytosis(D. Schmid and Münz 2005; Dorothee Schmid et al. 2006). In lysosomal storage disorders, there are remaining pathological conditions, and these conditions are counted as an affecting side of the system of immunity(Castaneda et al. 2008).

Regardless of the substrate specificity involved, studies showed that in lysosomal storage disorders, the immune system is affected and irregularities occur in the immune system of the individuals(Coutinho, Matos, and Alves 2015). According to the substrate deposition and accumulation, if inflammation occurs over long periods, it has a hazardous effect on the cells. Cellular damage occurs because of the longtime exposure to inflammatory responses. This long period of exposure to the inflammation can cause the

failure of therapeutic approaches because of the non-recyclable cellular damage (S. U. Walkley 2009). Without a doubt, natural chemicals known as damage-associated molecular patterns (DAMPs) are generated from injured or dying cells. Pattern recognition receptors on immune cells recognize these chemicals, which then initiate an inflammatory response (Land 2015). Under typical physiological circumstances, inflammation is a quick reaction that ends as the original stimulus is removed. White blood cells migrate into the afflicted tissues because of the production of cytokines and other inflammatory chemicals, which cause inflammation (Land 2015).

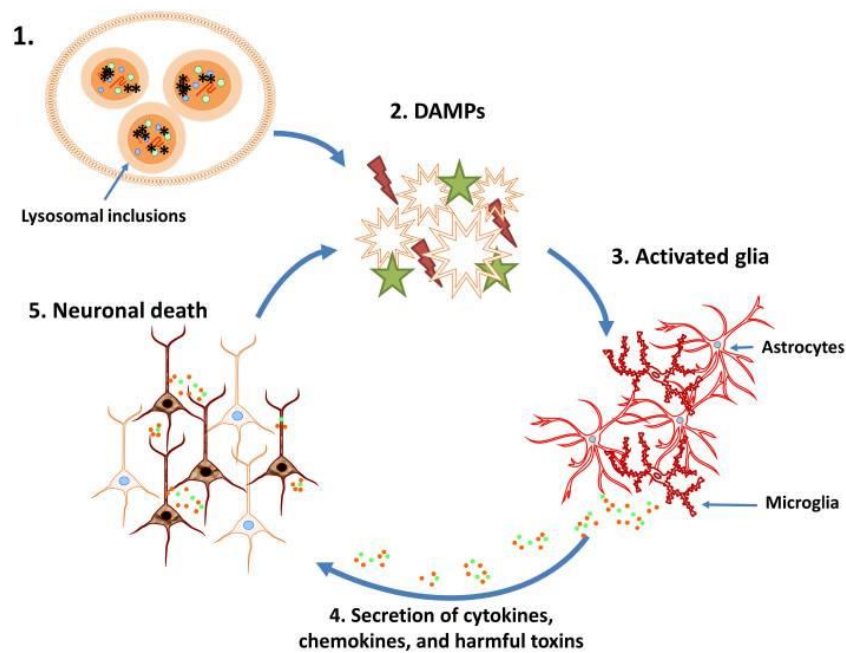


Figure 1.3. Schematic of the potential loss of the neurons during the lysosomal storage disease. (Source: Bosch, M.E and Kielian, T., 2015)

Another one of the lysosomal storage disorders is type 1 Gaucher disease, in this case, lack of central nervous system attending is monitored. Macrophages are stored in this type of lysosomal storage disorder. Macrophages are detected in whole body organs especially prominent in the spleen, liver, and bone marrow. Different cytokine release and activation of macrophages are followed by the storage of GlcCer in macrophages (Jmoudiak and Futerman 2005). This storage in the macrophages serves as a detection key for Gaucher disease in some situations. Most of the central nervous system pathologies in lysosomal storage diseases are observed in brain parts. In particular, inflammatory responses are monitored more commonly. This inflammation in the brain can be the result of disease or trauma by activating the response of inflammation (Ransohoff and Perry 2009). In a normal situation in the healthy individual's

brain, the resting state is monitored in the microglia cell lines however after the infection or traumatic situation occurs in the individuals, microglial cells are affected, and they are activated while the disease continues(Ransohoff and Perry 2009).

According to the unwanted accumulation of substrates in the cells because of the lysosomal storage diseases, an inflammatory response is activated, and this response of inflammation gradually increases in parallel with the amount of the unwanted substances(Jeyakumar et al. 2003). In the literature, most of the studies about the lysosomal storage disorder show that inflammation in the individuals triggers and contributes to the pathogenesis(Jeyakumar et al. 2003). One of the examples of this situation is an accumulation of GM1 and GM2 gangliosides, this accumulation triggers the activation of both the central nervous system and the inflammatory response of the peripheral side with the early onset of clinical cases, and in this situation, it is monitored that a lot of different pro-inflammatory cytokine activations (Jeyakumar et al. 2003). Moreover, another lysosomal storage disease is Sandhoff disease. In the literature, the Sandhoff disease mouse model was treated with non-steroidal anti-inflammatory drugs to prevent the recruitment of peripheral immune cells of the brain, after the application clinical benefits were monitored in the manuscript and the results were promising for future research(Hawkins-Salsbury, Reddy, and Sands 2011; Y. P. Wu and Proia 2004). Also, in another LSD, the mouse model of NPC1 was treated with the non-steroidal anti-inflammatory drug, and this mouse took advantage of the treatment (Smith et al. 2009).

## **1.6. Secondary Lipid Alterations in Lysosomal Storage Diseases**

Lysosomal storage diseases are named after the primary accumulation of substances. These are glycoproteinoses, gangliosidoses, sphingolipidoses, and mucopolysaccharidoses. Moreover, to the primary storage of different materials, the secondary accumulation of other products is also monitored in the lysosomal storage diseases. These are more often not directly linked to the primary storage of the products (Steven U. Walkley and Vanier 2009). Lipids are glycosphingolipids and phospholipids moreover cholesterol is the most appealing and well-comprehended substances of secondary storages in LSDs. For the total understanding of each lysosomal storage disease, the link between the secondary lipid accumulation and pathogenesis of the

disease plays a crucial role in the comprehension of all aspects of the disorders (Steven U. Walkley and Vanier 2009).

The major class of secondary lipid accumulation variants are phospholipids, cholesterol, or glycosphingolipids (GSLs) in both brain and visceral organs. In the same diseases, in both brain and visceral organs, accumulation of secondary lipids can be observed (Steven U. Walkley and Vanier 2009). These alterations are detected by the antibodies against these lipids or cytochemical staining methods can be used for cholesterol detection in the cellular accumulation sites.

One of the examples of secondary lipid accumulation in lysosomal storage diseases is the accumulation of GM2 and GM3 gangliosides. These accumulations in the GM2 and GM3 gangliosides are associated with neuropathological effects. Also, Niemann-Pick diseases and mucopolysaccharidoses, but also deficiency of prosaposin because of the ceroid lipofuscinoses and glycoproteinosis. GM2 and GM3 are monitored in the human brain in very minor amounts which is 1% or a maximum of 2% of the ganglioside amount of the total volume (Kamoshita et al. 1969; Cumings 1962). This ganglioside amount is much smaller in *the WT* mouse brain than the normal human brain's total ganglioside (Kamoshita et al. 1969). In the Niemann-Pick disease type A of the patient's brain's autopsy, especially GM2 ganglioside accumulation was found compared to the other gangliosides and in the Niemann-Pick C disease (NPC) (Harzer et al. 1978).

Secondary lipid accumulation is observed in the visceral organs as well as brain tissue in lysosomal storage disorders. Especially, Hepatosplenomegaly was monitored in some of the specific lysosomal storage diseases such as Niemann-Pick type C or type A and Type B variants. Also, GM3 and GM2 ganglioside accumulation and their increases were monitored. As well as neutral glycolipids, lactosylceramide, glucosylceramide, and globotriaosylceramide, and globoside increases were observed in these lysosomal storage diseases. GM3 is also elevated in the liver and spleen of the Gaucher disease (Nilsson et al. 1982).

## **1.7. Aim of the Thesis Study**

The thesis study aims to investigate the link between secondary lipid alterations and inflammation of human patients and *Neul*<sup>-/-</sup> mice fibroblast cell lines. To comprehend how the link between inflammation and secondary lipid alterations occurs,

fibroblast cell lines were chosen because sialidosis is a systematic disease that is one of the lysosomal storage disorders (Khan and Sergi 2018). To elucidate whether the secondary lipid metabolism could trigger inflammation in human patients and *Neu1*<sup>-/-</sup> mice fibroblast cell line. The findings will not only provide the elucidation of the lipid content in cells from the sialidosis mouse model and patient, but they will also have the potential to establish a connection between the lipids and neuroinflammation in sialidosis (Seyrantepe et al. 2003). Determination of the connection between secondary lipid alterations as well as inflammation markers may suggest developing new therapeutic targets in sialidosis.

## CHAPTER 2

### MATERIALS AND METHODS

#### 2.1. Animals

Neu1 gene knockout mice (*Neu1*<sup>-/-</sup>) were obtained from Prof. Dr. Alessandra d'Azzo (Department of Genetics and Tumor Cell Biology, St. Jude Children's Research Hospital, Memphis, Tennessee). Neu1 gene knockout mice (*Neu1*<sup>-/-</sup>) were donated by Prof. Dr. Alessandra d'Azzo to our laboratory. After these mice came to Turkey, they were accommodated at the Institute of Technology Animal Research Center in Izmir, Turkey. The housing and breeding of these mice were handled in individually ventilated cage systems. They were placed in cages which had a maximum of five mice. 12-hour dark-light cycle, constant humidity, and accurate temperature ratios were maintained. These mice were supplied with water and food and this feeding system counted as ad libitum because there is no restriction to reach water and food. The Institutional Animal Care and Use Committee of the Izmir Institute of Technology approved animal experiments. According to this approval, all experiments were conducted under the control of the Turkish Institute of Animal Health guide which also guides the laboratory animal model used in laboratories.

One male (*Neu1*<sup>+/-</sup>) and two female (*Neu1*<sup>+/-</sup>) mice was mated. Heterozygous mice breeding cages were used to produce Neu1 gene knockout mice (*Neu1*<sup>-/-</sup>). After the first genotyping processes occurred, *WT* female and male mice were also mated to produce *WT* offspring. To follow this section, Neu1 gene knockout mice (*Neu1*<sup>-/-</sup>) and *WT* mice were obtained from the animal breeding processes.

#### 2.2. Mouse Genotyping

Mouse Genotyping was conducted after the mice reached 1-month-old. After the mice reached 1-month-old, they were separated from their parents to the new cages. DNA isolation was conducted from the mouse tail. Weaned mice genotyping was conducted to determine an accurate genotype of mice. DNAs which are obtained from

mice, firstly in a shaking incubator they were incubated at 70 rpm and 55°C for overnight in Eppendorf tubes consisting of 250 µl Lysis Buffer (10% 1M Tris pH 7.6, 2.5% 0.2 EDTA, 20% SDS, 4% 5-month-old NaCl) and also 6 µl Proteinase K (25 µg/µl, Sigma-Aldrich, Germany). After overnight incubation, samples were put in a centrifuge at 13000 rpm for 10 minutes.

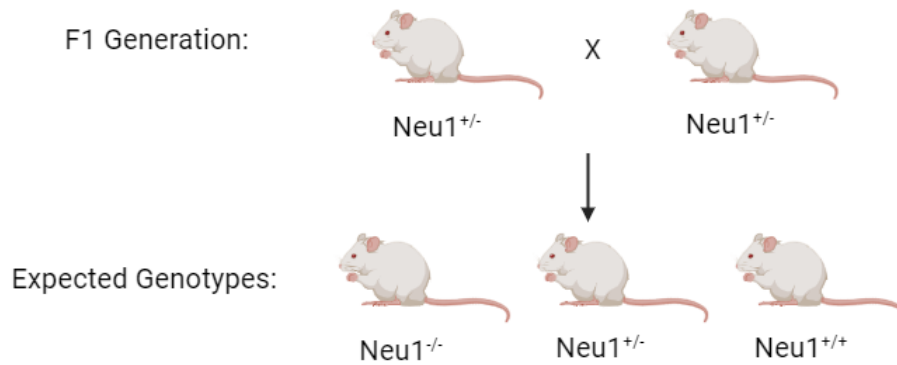


Figure 2.1. Representative of *Neu1*<sup>-/-</sup> Mouse Breeding

After that part, each sample's supernatant was separated from the debris and transferred this supernatant to the new tubes. The supernatant volume of each New Eppendorf tube was also added to the same amount of 100% isopropanol. The tubes were made upside down a couple of times vigorously and after that samples were centrifuged under the 13000 rpm for 1 minute, room temperature conditions. After this centrifugation, each supernatant was discarded and at the bottom of each Eppendorf tube DNA was obtained. 500 µl 70% ethanol for purification of DNA was added onto the Eppendorf tubes and again samples were centrifuged under the 13000 rpm for 1 minute, room temperature conditions. The supernatant was carefully discarded and after that, to get rid of the remaining ethanol, the samples were held in air-dry to remove the remaining ethanol. Incubation was conducted for 10-15 minutes and at room temperature. After all ethanol was removed from the DNA samples, each sample was dissolved in 100 µl ultrapure water, and samples were incubated in an incubator at 55°C for 1 hour to completely dissolve DNA in water.

### 2.2.1. Genotyping of Mice for *Neu1* Allele

Genotyping of the *Neu1* allele with PCR protocol was conducted and isolation of DNAs was used for this PCR protocol. Approximately 100 ng DNAs were required for

PCR. In these PCR conditions, a Reaction Mix was first generated. This reaction mix contained 0.4  $\mu$ M of each forward primer, 0.4  $\mu$ M of reverse primer, 0.4 mM dNTP, 10X PCR buffer including 2 mM MgCl<sub>2</sub> (GeneDireX), 1.25 units of Taq Polymerase (GeneDireX). Also in the PCR machine, the conditions were optimized and for Neu1 PCR conditions were orderly: 3 minutes at 94°C; 30 seconds at 94°C (30 cycles), 30 seconds at 58.1 °C (30 cycles); 2 minutes at 72°C; and 10 minutes at 72°C.

Table 2.1. Primer sequences that were conducted while genotyping of mice.

Gene	Primers	Primer Sequences	Product Size
Neu1	MNTG-1 Forward	5'- GACAGGGATCGCCGGGAGCTATGG -3'	WT Ale1 180 bp
	MNTG-2 Forward	5'- CACCAGGCTGAAGTCATCCTCTGC -3'	
	LacZ Reverse	5'- GATAGGTTACGTTGGTGTAGATGGGCG -3'	Mutant Ale1 400 bp

### 2.3. Isolating Fibroblasts from Animals

Initiation of Fibroblasts from Animals was conducted with the isolation of fibroblasts from each genotype. Mice were taken under the control of the Izmir Institute of Technology Animal Research Center. In the laboratory of Prof. Dr. Volkan SEYRANTEPE, euthanasia was applied to the mice in the laboratory and in the class II laminar cabinet to prevent any contamination. Sterile working environment under the class II laminar cabinet, the mouse was killed with dislocation of the cervical area, and the mouse's chest hair was shaved and cleaned. After that part, %70 ethanol for cleaning and removing hair from the chest was used. 1 cm<sup>2</sup> of clean skin from the mice's chest was cut with a blade and this piece was chopped into tiny pieces to easily release the fibroblast line to the flask. Completely shredded skin piece was separated in the 5ml of DMEM which contained 10%FBS and 1% Penicillin-Streptomycin antibiotics. After that part, according to the attaching to the surface, cells were waited for adhering to the stick to the flask surface. After 2 days, when we saw the morphology of the fibroblast cell lines for each genotype, to get rid of the extra pieces of skin pieces in the T25 flask, gently washed with 1X PBS. The immortalization step was detailly explained in the next section.

## 2.4. Human Cell Lines

Human fibroblast cell lines were selected and bought from the Coriell Institute. Three different human cell lines were bought. GM01718, GM01719, and GM02921 were these cell lines Coriell codes. These cell lines in the results part counted as Patient 1, Control 1, and Patient 2 to easily explain. GM01718 was a cell line that had a *Neu1* gene deficiency, and she was a 2-month-old human sialidosis patient. GM01719 was the mother of GM01718, and she is a 25-year-old female. She was a carrier so the *Neu1* +/- heterozygous allele containing the fibroblast cell line was GM01719. Lastly, GM02921 was a different sialidosis patient fibroblast cell line. He was a 2-year-old patient fibroblast cell line and phenotypic effects were severe as same as the GM01718 fibroblast patient cell line. Each cell line sample was obtained with the dry-ice and each fibroblast cell line was followed in the cell culture under very careful conditions.

## 2.5. Immortalization of Fibroblast Cell Lines

Immortalization of primary cells gave the ability to maintain their function, shape, and properties much longer and remain as a primary for both human and mouse cell lines. Primary fibroblast cell lines were created from this skin part of each genotype of mice. After that part, to create immortal cell lines, virus transfection was used. The precursor fibroblast cell lines were kept in the DMEM (10% FBS and Antibiotics) in a 25 cm<sup>2</sup> flask. To immortalize these cells, the PA317 LXS<sub>N</sub> 16E6E7(ATCC, CRL2203) cell line was used because it contained a retrovirus vector, pLXS<sub>N</sub>16E6E7 and it included the Psi-2 ectotrophic cell line. The cell of packaging holding the vector, antibiotic-free medium at a concentration of 50-75% can grow this vector. This cultured medium was collected and a 0.45 µm filter was used to filter from the cell and medium also dilution ratio was followed according to the instructions from the company. After that part, polybrene (Sigma-Aldrich, TR-1003) was added 8 µg/ml onto the cells. This virus/polybrene mixture was poured onto the mice and human primary fibroblasts to initiate immortalization and incubation was conducted for 2 hours at 37°C. After that in the final part, the polybrene was added to the DMEM solution at a final ratio which is 4 µg/ml also the incubation occurred for at least 5 hours. In the last part, Cells were selected with the

addition of geneticin after the 10 days of treatment (Gibco,10131027) to DMEM (10% FBS, 1%Pen-Step).

## **2.6. Real-Time PCR**

Real-time PCR was used for the analysis of the RNA of each sample. Fibroblasts of 2- and 5-month-old *WT* and Neu1 gene knockout (*Neu1*<sup>-/-</sup>), Human fibroblast cell lines which were GM01718, GM01719, and GM02921 used for real-time PCR analysis. Real-time PCR was followed with some procedures, and it was performed according to the following sections. There was isolation of RNA, synthesis of cDNA from RNA, and lastly, RT-PCR protocols to follow these experiments. For each mouse cell line sample, three independent mice were selected, and isolated fibroblasts of each mouse were to create different cell lines for each genotype for real-time PCR analysis. Also, for human fibroblast cell lines, each sample was three times for each RNA isolation sample, and these human fibroblast cell lines were collected from the cell culture at the same time during each sample preparation period to follow the same passage number to control conditions of cell biology.

### **2.6.1. RNA Isolation**

Fibroblasts of 2- and 5-month-old *WT* and Neu1 gene knockout (*Neu1*<sup>-/-</sup>), Human fibroblast cell lines which were GM01718, GM01719, and GM02921 used for RNA isolation. For each cell sample, 500  $\mu$ l Trizol (Sigma) was added to the samples. These cell samples were first collected in the 15 mL falcons. To isolate RNA easily and also for the centrifuge conditions, each sample was transferred to the 2 mL Eppendorf tubes which are mice and human fibroblasts of each sample. Each cell sample was homogenized with pipetting to prevent any clump and prevent any efficiency of RNA isolation. After that, 100  $\mu$ l chloroform was added to each sample. After adding chloroform to each sample, samples were shaken vigorously for 10-15 seconds. Centrifuged for each sample at 15000xg and 4°C for 15 minutes for separation for phases to isolate RNA from DNA and cell debris. After the centrifugation finished, the colorless aqueous part of the sample remaining at the top of each tube was collected into the new 1.5 mL Eppendorf tubes. This aqueous part had an RNA and according to that, the same volume of 100%

isopropanol was added to this colorless aqueous part and 10 minutes of incubation at room temperature followed this step. After the 10 minutes of incubation at room temperature, RNA was precipitated, and this step was followed by the 10 minutes at 15000xg at 4°C centrifugation to collect RNAs—the form of pellet RNA after the centrifugation was obtained. The supernatant was removed and 1 ml of 70% ethanol was added to the RNA pellets in each Eppendorf tube. This step was followed because of the washing RNAs. After adding 70% ethanol to each sample, centrifugation was conducted at 15000xg and 4°C for 5 minutes. The supernatant of each sample was discarded with a pipette carefully. RNA pellets were dried with air-dry at 4°C for 5-10 minutes. 20-50 µl RNase-free water was added to each sample to dissolve RNAs. To dissolve each sample spatially, the samples were put into a bath of water(55°C) for 10-15 minutes. In the last step of the RNA isolation part, a Nanodrop Spectrophotometer (ND-1000) was used to obtain RNA concentrations.

### **2.6.2. cDNA Synthesis**

After the isolation of RNAs was conducted, the cDNA conversion part of the real-time PCR procedure was followed. For cDNA conversion processes, Bio-Rad cDNA Master (Bio-Rad), and specific instructions from the Bio-Rad were followed. The volume of the reaction mixture was 20 µl and the concentration of cDNA was synthesized at 50 ng/ µl for each sample. A mixture of cDNA synthesis contains 2 µl of 10X Enzyme Mix, 1X reaction buffer, water, and RNA. RNA amount was determined according to the nanodrop results. Conversion of cDNA was also followed with precise conditions. These were 15 minutes at 42°C; 5 minutes at 85°C, and 15 minutes at 65°C.

In the second part, after the conversion of cDNA occurred, PCR protocol was enforced to test whether all RNAs converted to cDNA or not. This PCR protocol was implemented for the GAPDH gene which is a housekeeping gene to test cDNAs. For This protocol of GAPDH, the mixture volume was 25 µl and it also contained 0.8 mM of GAPDH primers, 10 mM of each dNTP, 1X reaction buffer which contained MgCl<sub>2</sub>, 1.75 units DNA polymerase (GeneDireX), and 50 ng concentrated cDNA for each sample. For the GAPDH PCR, the following conditions were followed to proceed with this GAPDH PCR. 2 minutes at 95°C; 20 seconds at 95°C (30 seconds), 15 seconds at 65°C (30 seconds), 22 seconds at 72°C, and 3 minutes at 72°C. After the PCR was finished, agarose

gel was prepared at 1% concentration and each PCR sample was added to the gel of agarose and the samples were run for 30 minutes for 90 volts.

### 2.6.3. RT-PCR

RT-PCR protocols were followed according to RNA level and based on gene expression analysis results. Genes which are related to inflammation (CCL2, CCL3, CCL5, CXCL10) were analyzed. In this process, Roche LightCycler 480 SYBR Green I Master Mix was used, and Roche LightCycler® 96 System was used in the RT-PCR protocol.

Table 2.2. Primer of the forward and reverse of the inflammation marker genes.

Gene	Primer Sequences	Product
CXCL10 (Mouse)	F:5'-ACCATGAACCCAAGTGCTGCCGT-3' R:5'-AGGAGCCCTTTTAGACCTTTTTTG-3'	298 bp
CXCL10 (Human)	F:5'-TGAGCCTACAGCAGAGGAA-3' R:5'-TACTCCTTGAATGCCACTTAGA-3'	102 bp
CCL3 (Human)	F:5'TGCAGGTCTCCACTGCTGCCCTT-3' R:5'-GCACTCAGCTCCAGGTCGCTGAC-3'	275 bp
CCL3 (Mouse)	F:5'-TCTGTACCATGACACTCTGC- 3' R:5'- AATTGGCGTGGAATCTTCCG-3'	103 bp
CCL2 (Human)	F:5'-ATGAAAGTCTCTGCCGCCCTTCTGT3' R:5'-AGTCTTCGGAGTTTGGGTTTGCTT-3'	297 bp
CCL2 (Mouse)	F:5'-ATGCAGTTAATGCCCCACTC-3' R:5'-TTCCTTATTGGGGTCAGCAC-3'	167 bp
CCL5 (Human)	F:5'- CCTGCTGCTTTGCCTACATTGC-3' R:5'- ACACACTTGGCGGTTCTTTCGG-3'	125 bp

CCL5 (Mouse)	F:5'-AGTGCTCCAATCTTGCAGTC-3' R:5'-AGCTCATCTCCAAATAGTTG-3'	108 bp
GAPDH (Human)	F:5'-ACCCACTCCTCCACCTTTGA-3' R:5'-CTGTTGCTGTAGCCAAATTCGT-3'	101 bp
GAPDH (Mouse)	F:5'-CCCCTTCATTGACCTCAACTAC-3' R:5'-ATGCATTGCTGACAATCTTGAG-3'	347 bp

A mixture of reaction volume was 10  $\mu$ l and this mixture contains 50ng cDNA, 1X Roche LightCycler 480 SYBR Green I Master Mix, 0.4  $\mu$ M each primer for each volume of each gene. For the inflammation genes, reaction conditions were followed in an orderly; 10 minutes at 95°C; 20 seconds at 95°C (45 cycles), 15 seconds at 57°C, and 22 seconds at 72°C. For RT-PCR, according to the results, GAPDH as a housekeeping gene was used to normalize each result of each gene. RT-PCR experiments were repeated three times for each genotype and each cell line fibroblast sample for statistical analysis. The average of each sample was calculated and statistical analysis for each sample was conducted with two-way ANOVA on GraphPad Prism.

## 2.7. QPCR Array

RT<sup>2</sup> Profiler PCR Arrays were conducted to analyze 84 different gene expression levels for Cytokines & Chemokines for both human and mouse fibroblast cell line samples. These RT<sup>2</sup> Profiler PCR Arrays were Qiagen, Human Cytokines & Chemokines, PAHS-150ZF and Qiagen, Mouse Cytokines & Chemokines, and PAMM-150ZF. According to the figure, besides the 84 different genes for Cytokines & Chemokines for both humans and mice, there were 5 different housekeeping genes and 1 genomic DNA control sample, also 3 Reverse transcriptional controls and 3 positive PCR controls consisting of the 96-well plate.

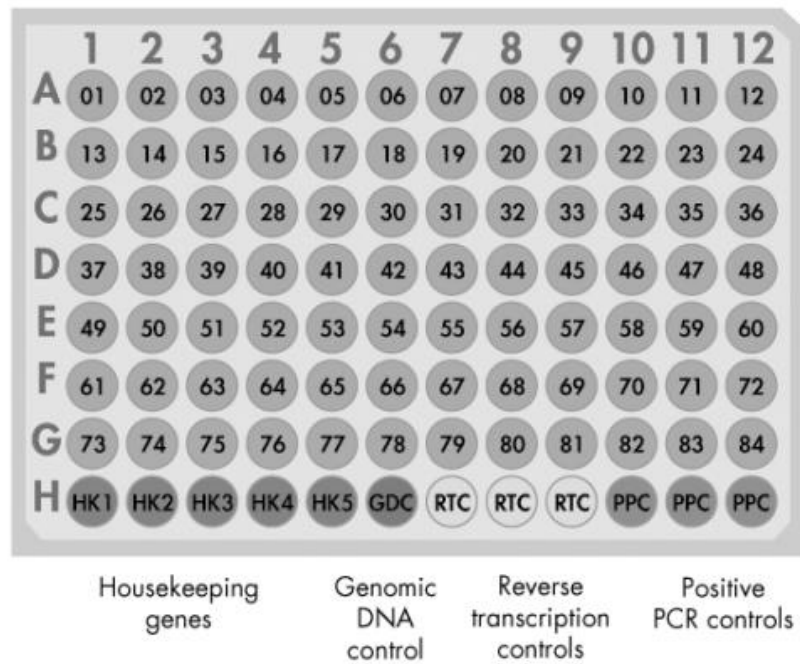


Figure 2.2. RT<sup>2</sup> profiler PCR Array Format

### 2.7.1. RNA Isolation with Qiagen RNase Plus Mini Kit

To obtain RNAs from both human and mice fibroblast samples, Qiagen RNase Plus Mini Kit (Catalog No:74134, Qiagen) was used to obtain pure RNA isolation results for the RT2 Profiler PCR Array of Chemokines and Cytokines PCR Array in both human and mouse. The kit for the RNA isolation was used because the RT2 Profiler PCR Array instruction suggested using this RNA isolation kit for each sample to obtain accurate and precise results. According to the procedure of the Qiagen RNase Plus Mini Kit, because our cells were grown in monolayer in the flask, cells were lysed directly with the trypsinization and collected as a cell pellet. To remove the completely supernatant from the cell samples, a 300 rpm 5-minute centrifuge was conducted and then, 10 to 1000 ratio  $\beta$ -mercaptoethanol added to the Buffer RLT mixture was added onto each sample. According to the procedure, 350  $\mu$ l Buffer RLT was enough for cell pellets. Cell pellets were flicked up and down for dividing homogenize in the tubes. Disrupting and homogenizing the starting sample was conducted with the 1-minute vortex. The lysate which is each sample was pipetted into a a QIAshredder spin column which was placed in a 2 ml collection tube after that centrifugation was conducted for 2 minutes at full speed which is 15000 rpm. After that part, the gDNA Eliminator spin column was placed in a 2

ml collection tube. The samples were transferred onto the gDNA Eliminator spin column. 1 volume of 70% ethanol was to the samples, mixture was pipetted and carefully stored. Samples were transferred to an RNeasy spin column placed in a 2 ml collection tube and their volumes were up to 700  $\mu$ l. The lid of each sample was closed and 15 second 11000 rpm centrifuge was conducted. The flow-through was discarded. Because my samples were up to 700  $\mu$ l, the centrifugation step was repeated. The lid of each tube was closed very carefully, and 15 seconds of 11000 rpm centrifugation was conducted. The flow-through was discarded. 700  $\mu$ l Buffer RW1 into the RNAeasy spin column was added. The lid of each tube was closed very carefully, and 15 seconds of 11000 rpm centrifugation was conducted. And The flow-through was discarded. 500  $\mu$ l Buffer RPE to the RNeasy spin column was added and again 15 seconds of 11000 rpm centrifuged was conducted. The flow-through was discarded. 500  $\mu$ l Buffer RPE to the spin column was added a second time for precise purification and this time centrifugation was conducted for 2 minutes at 11000 rpm. After all these steps, the RNAeasy spin column was cautiously removed from the 2 ml collection tube and this spin column was placed in a new 1.5 ml collection tube which came with the RNAeasy Mini Plus Kit. Onto this spin column membrane, 30-50  $\mu$ l Water was added directly and elucidation of RNA occurred. The lids of each tube were closed very gently and again centrifuge was conducted for 15 seconds at 11000 rpm to obtain RNA in water.

### **2.7.2. cDNA Conversion for Real-Time PCR Array**

For cDNA conversion processes, Bio-Rad cDNA Master (Bio-Rad), and specific instructions from the Bio-Rad were followed. The volume of the reaction mixture was 20  $\mu$ l and the concentration of cDNA was synthesized at 50 ng/  $\mu$ l for each sample. The details about the cDNA conversion step were explained in the previous cDNA conversion section under the Real-Time PCR chapter.

### **2.7.3. RT<sup>2</sup> Profiler PCR Array**

In the handbook of RT<sup>2</sup> Profiler PCR Array, for the successful results, 0.5  $\mu$ g total RNA for 96-well plate format was described. Because of that reason, according to the cDNA synthesize kit from Bio-Rad 1000  $\mu$ g cDNA was expressed in 20  $\mu$ l. For obtaining

0.5 µg total RNA, 10 µl of these cDNA mixtures were separated. 100 µl RNase-free water to each sample was added. So, we obtained a 110 µl cDNA component for one 96-well plate. 1350 µl SYBR Green Mastermix was added and also 1248 µl RNase-free water was added to the mixture. Components of PCR were mixed in the 15 ml falcon and after that, this mixture was poured to the loading reservoir. PCR components to each well of the RT<sup>2</sup> Profiler PCR Array were added 25 µl amount. An 8-channel pipettor was used while dividing this amount of mixture. RT<sup>2</sup> Profiler PCR Array with Optical Adhesive Film was tightly sealed. After the seal was prepared, the centrifugation step was conducted for 1 minute at 1000 g at room temperature to remove any remaining bubbles. While the PCR cycling program was prepared, the 96-well plate was preserved on the ice.

Table 2.3. PCR component mix

Array Format	96-well
RT <sup>2</sup> SYBR Green Mastermix	1350 µl
cDNA synthesis reaction	102 µl
RNase-free water	1248 µl
The total volume of the master mix	2700 µl

The conditions of cycling for Roche LightCycler 96 were prepared with 1 cycle at 10 minutes at 95°C. After that 45 cycles for 15 seconds at 95°C and 1 minute at 60°C were arranged in the RT-PCR machine from the instruction of Qiagen as we seen in the Table. Also, for the LightCycler 96 machine, the ramp rate was adjusted to the 1.5°C/s.

Table 2.4. Cycling conditions for Roche LightCycler 96

Cycles	Duration	Temperature
1	10 min	95°C
45	15s	95°C
	1 min	60°C

For the analysis of QPCR ARRAY results, Absolute Quantification data was obtained from the RT-PCR machine. After taking all raw data from the machine, 5 of the housekeeping gene's average was taken. After that, each of the gene reads was calculated with the normalization with the housekeeping gene average. Statistical analysis for each sample was conducted with two-way ANOVA on GraphPad Prism.

## **2.8. Western Blot**

Western Blot analysis was conducted to analyze the proteins of samples. First of all, each sample from each cell line from 2- and 5-month-old *WT* and Neu1 gene knockout (*Neu1*<sup>-/-</sup>) mice fibroblast and GM01718, GM01719, and GM02921 human fibroblast cell line sample's proteins were isolated. After that isolation step, the Bradford Assay system was used to monitor the concentration of protein levels. In the last part of the Western blot, SDS-PAGE gel electrophoresis was conducted. Three different mice cell lines for each genotype were used and three different samples for human cell lines were used for Western Blot analysis.

### **2.8.1. Protein Isolation**

The samples were collected from 10 mm<sup>2</sup> Flask with D-PBS and stored at -80°C. Protein isolation from each sample was conducted from 2- and 5-month-old *WT* and Neu1 gene knockout (*Neu1*<sup>-/-</sup>) mice fibroblast and GM01718, GM01719, and GM02921 human fibroblast cell line samples. Lysis of protein buffer contains 1% TritonX100, 50mM Hepes, 150 mM NaCl, 10% Glycerol, 50 mM Tris-Base, 1% PMSF, 1% protease inhibitor. This protein lysis buffer was used for mice and human cell samples. 100 µl of protein lysis buffer was added to each cell sample. The homogenization procedure was followed on ice and every 10 minutes, each sample was vortexed for 30 seconds to homogenize and lysate the samples. This process was followed on ice. After 1 hour of incubation and vortex to mix samples, a centrifugation step at 14000rpm (0°C) for 15 minutes was conducted and each Eppendorf tube supernatant was transferred to the new Eppendorf tubes to collect protein samples.

### **2.8.2. Bradford Assay and Protein Preparation**

Protein concentration of different samples was considered. Bradford Assay was chosen to determine the concentration of proteins in each sample. First, proteins that were isolated from each sample were diluted at 1:20 with distilled water (2 µl sample protein + 38 µl dH<sub>2</sub>O). Also, the Lysis buffer which was used in the protein isolation process was

diluted at 1:20 with distilled water. This diluted lysis buffer was used as a normalization point for each protein concentration for each sample. Also, Bovine Serum Albumin (BSA) solutions with different concentrations were used. These concentrations were (10, 20, 40, 80, and 100  $\mu\text{g/ml}$ ). These BSA concentrations were diluted with serial dilution from 100  $\mu\text{g/ml}$  and according to the processes standard curve was drawn from the BSA concentrations and was used for the calculation of the protein concentration of each sample.

10  $\mu\text{l}$  of each diluted sample and BSA solution was prepared and added onto the 96 well plate and 200  $\mu\text{l}$  Bradford reagent (SERVA Electrophoresis GmbH, Heidelberg, Germany) was added to each sample. After preparing 96 well plates, 10 minutes at room temperature incubation was conducted to homogenize the sample and Bradford. 595 nm with i-Mark Microplate Absorbance Reader (Bio-rad Laboratories, California, USA) was used for evaluation of each sample's absorbance ratio. Also, in 96 well plates, the reader gave us BSA concentrations with different absorbance levels and these different BSA concentration's absorbance levels were used to create a plot for drawing the standard curve. From the standard curve, protein concentration calculations were conducted and to create an equation, different BSA concentrations were used. The protein concentration of each sample was calculated from the equation of the plot and these calculations were followed to find the 20  $\mu\text{g}$  protein concentration of each sample.

The sample's protein values were calculated according to the calculation from the equation of the BSA plot and protein volume was calculated. Preparing for each sample to equal the 20- $\mu\text{g}$  protein amount was arranged. The amount of water and protein amounts was prepared and arranged in the Eppendorf tubes for each sample. After that, each sample was prepared to the 20- $\mu\text{g}$  protein with the proper amount of water, loading buffer was added. The loading buffer had a 4:1 ratio and it contained 240 mM Tris-HCl pH 6.8, 0.04% Bromophenol Blue, 40% Glycerol, 8% SDS, and 5%  $\beta$ -mercaptoethanol. After adding the loading buffer to each sample was boiled at 95°C for 10 minutes. After this boiling step, samples were ready for the next step. The next step of this experiment was SDS-PAGE gel electrophoresis for the Western Blotting experiment.

### 2.8.3. SDS-PAGE Gel Electrophoresis

In the SDS-PAGE Gel Electrophoresis, there were two types of gel for running proteins. At the bottom of the whole gel, a resolving gel was prepared. Resolving gel (10%) was contained 4 ml 30% Acrylamide-Bis (Bio-Rad), 5 ml dH<sub>2</sub>O, 3 ml pH 8.8, 1M Tris-HCl (Lower Buffer), 60 µl Ammonium persulfate, 60 µl SDS, 6 µl Tetramethyl ethylenediamine. All these ingredients were mixed and immediately poured into the setup. Proper and compatible thin and thick two different glass pieces were held together with plastic attachment and this setup was a baseline for SDS-PAGE Gel. The resolving gel mixture was poured into the gap between these two glasses and waited at room temperature for the polymerization of the resolving gel. After that, the stacking gel part was prepared before the last step. The stacking gel was containing 1.5 ml, 1M, pH 6.8 Tris-HCl, it was called upper buffer, 1 ml 30% Acrylamide-Bis (Bio-Rad), 3.5 ml Water, 60 µl Ammonium persulfate, 60 µl SDS, 6 µl Tetramethyl ethylenediamine. Same as the resolving gel, stacking gel ingredients were mixed and poured immediately to prevent any freezing, and the gel was homogenized. After that, a proper comb for loading the sample of proteins was added to the stacking gel part. After that again for polymerization, at room temperature, incubation for at least 20 minutes was conducted. After the gel was completely polymerized, the proper comb was removed carefully, and the glass setup was removed from the plastic system. The gel-containing glass was placed on the proper running cassette. This cassette was also placed in the tank of the running process. According to the initiate running, a proper running buffer was produced. The running buffer contained 1.92M Glycine, 1% SDS, and 0.25M Tris-Base. Running Buffer was poured into both tank and cassette which contain gel to load proteins. The running procedure was repeated for 1-1.5 hours at least for proper separation of running proteins from each other. The running process was conducted under constant 120V conditions. After the running step was conducted, the Transfer step was continued. Transferring the gel to the membrane process was acquired in this step. To transfer the gel to the nitrocellulose membrane (Bio-Rad), a Transfer cassette is required. The transfer cassette was like a sandwich to prepare the correct order for an accurate and precise transfer method. Proteins were run again for the transfer period and the Transfer buffer contained glycine (39 mM), methanol (20%), and Tris Base (48 mM) also the 9.2 pH was adjusted. The transfer step was monitored on ice to prevent any degradation because of the heat from the transferring electricity and this process continued for 75 minutes. After 75

minutes, the transferring process was finished and the transferring of proteins from gel to membrane occurred. Continuing to this step, blocking for preventing any nonspecific antibody binding was proceeded. To block the membranes which are called blots, a blocking solution was prepared. The blocking solution contained powder of milk which is 5% and it was dissolved in 1X PBS-T which was containing 0.005% Tween20 solution in Phosphate Buffered Saline. The blocking solution was poured onto the membrane which is inside the plastic cap. The blocking process proceeded for 60 minutes. After the membrane was blocked with the blocking solution, blots were prepared for washing 3 times and at least 5 minutes with 1X PBS for each time to get rid of the blocking solution from the top of the membrane.

After that part, membranes were ready to incubate overnight at +4°C with the primary antibodies. Primary antibodies were prepared with the dilution processes according to the instructions from the company that we bought. The antibodies were anti-I $\kappa$ B- $\alpha$  (1:1000, Cell Signaling Technology, 9242), NF- $\kappa$ B (1:1000, Cell Signaling Technology, D14E12), and  $\beta$ -actin (1:1000, Cell Signaling Technology, 13E5).  $\beta$ -actin was used because it is a housekeeping gene, and it was used as a control while calculating the other protein amounts.  $\beta$ -actin primary antibody was incubated onto the blot for at least 1 hour from the manufacturer's instructions. These primary antibodies were solved in the Red Solution and Red Solution consisting of 0.02% NaAzide, 0.04% Phenol Red, and 5%BSA, and these ingredients were solved in PBS-T which also had a 7.5 pH. After all membranes were incubated with the primary antibodies, to get a response from the blots with the antibody enhancing, secondary antibodies were conducted. Before the secondary antibody application to the membranes, 3 times and each time 5-minute washing process was repeated to clean blots from the primary antibodies. The remaining primary antibodies were stored at +4°C in a fridge and these primary antibodies were used repeatedly at least 5 times. A secondary antibody application was prepared in the blocking solution, and it was diluted to a 1:10000 ratio. HRP-conjugated secondary antibodies (Jackson ImmunoResearch Lab) were used in the secondary antibody application processes. A secondary antibody was poured onto the membrane and 1-hour incubation was conducted to attach primary and secondary antibodies to the reaction. After that, Secondary antibodies in the blocking solution were collected from the membrane, and the membrane was washed 3 times each time for 5 minutes. To visualize proteins under the imaging system which is a computational imaging system (Fusion SL, Vilber Lourmat), Luminata<sup>TM</sup> Forte Western HRP Substrate (Millipore) was used for

visualization of blots. Protein band intensities were calculated and monitored the amounts with the ImageJ program and statistical analysis was conducted with the two-way ANOVA method on GraphPad Prism.

## **2.9. Lipidome Analysis**

Lipidome analysis called a mass spectrometer analysis requires specific sample preparation which was instructed by the manufacturer and proceeded with our sample analysis. Samples were considered according to the instructions and the following procedures were followed and detail explained in the next section.

### **2.9.1. Preparing Samples for Shotgun Lipidome Analysis**

The samples were handled to ensure the purity and preservation of their lipid compositions. Cell samples which are both human and mouse fibroblast cell lines were prepared on the Eppendorf tubes (cat# 0030120086). To obtain cell samples for lipidome analysis, cells were counted with the Trypan Blue Solution (cat#P08-34100, 0.4%, PAN Biotech) method. In the manufacturer's procedure, cell samples were required to reach their volume to the concentration of 3000 cells/ $\mu$ L. The cells were counted for each sample and calculations were conducted for each sample separately to monitor and obtain the concentration of 3000 cells/ $\mu$ L and each sample was prepared according to this calculation of volume. These cells were homogenized in the D-PBS without Mg, and Ca, after that concentration was reached, at least 300  $\mu$ L of cell suspension to a fresh Eppendorf tube was transferred. All collected samples were homogenous for lipidome analysis. For the analysis of the whole cell lipidome, centrifuging samples were not conducted after cell lysis. Lipid Data which came from the manufacture of the mass spectrometer, were analyzed on GraphPad Prism. The amount of lipids pmol was placed onto the graphs. One-way ANOVA analysis was conducted for lipidome analysis.

## CHAPTER 3

### RESULTS

#### 3.1. Genotyping of Mice for Neu1

Genotyping of mice was conducted via Polymerase Chain Reaction (PCR). According to monitor the wild-type and mutant alleles. Wild-type (*Neu1*<sup>+/+</sup>) and mutant (*Neu1*<sup>-/-</sup>) were determined according to the amplified PCR products.

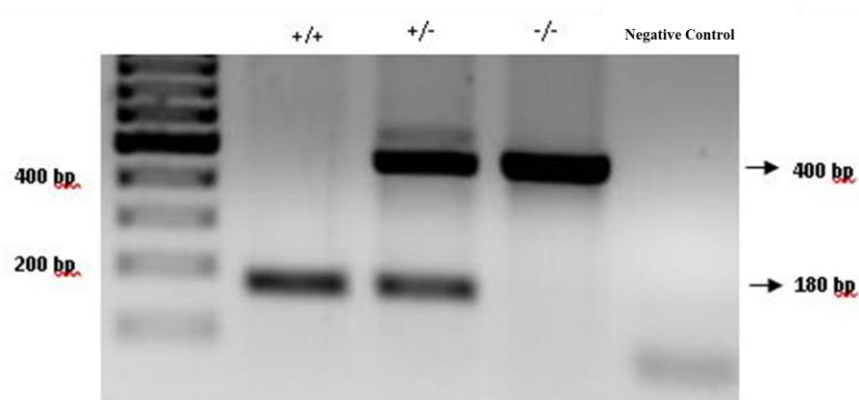


Figure 3.1. Neu1 gene alleles genotyping which is coming from the tails of mice by conducting PCR protocols. Amplification of the mutant allele was monitored in 180 bp and wild type allele was monitored in 400 bp.

PCR of the Neu1 reaction was conducted with the specific primers of the Neu1 gene. These primers are MNTG-1, MNTG-2, and LacZ primers. Base pair of each allele of the gene orderly 180 bp and 400 bp which are *WT* and alleles of the gene Neu1, respectively (Figure 3.1).

#### 3.2. Lipidome Analysis

Lipidome analysis was conducted for both 2-month-old and 5-month-old mice fibroblast cell lines. It is shown in Figure 3.2. In compared 2-month-old *WT* and 2-month-old Neu1 mice sample amount of the Glycerophospholipid, PC, and PC O- was significantly decreased compared to the 2-month-old *WT* mice fibroblast in Figure 3.2A,

also LPI, LPG, and LPS lipids were monitored slightly decreased in *Neu1* samples compare to the *WT* samples in 2-month-old mice fibroblast in Figure 3.2C.

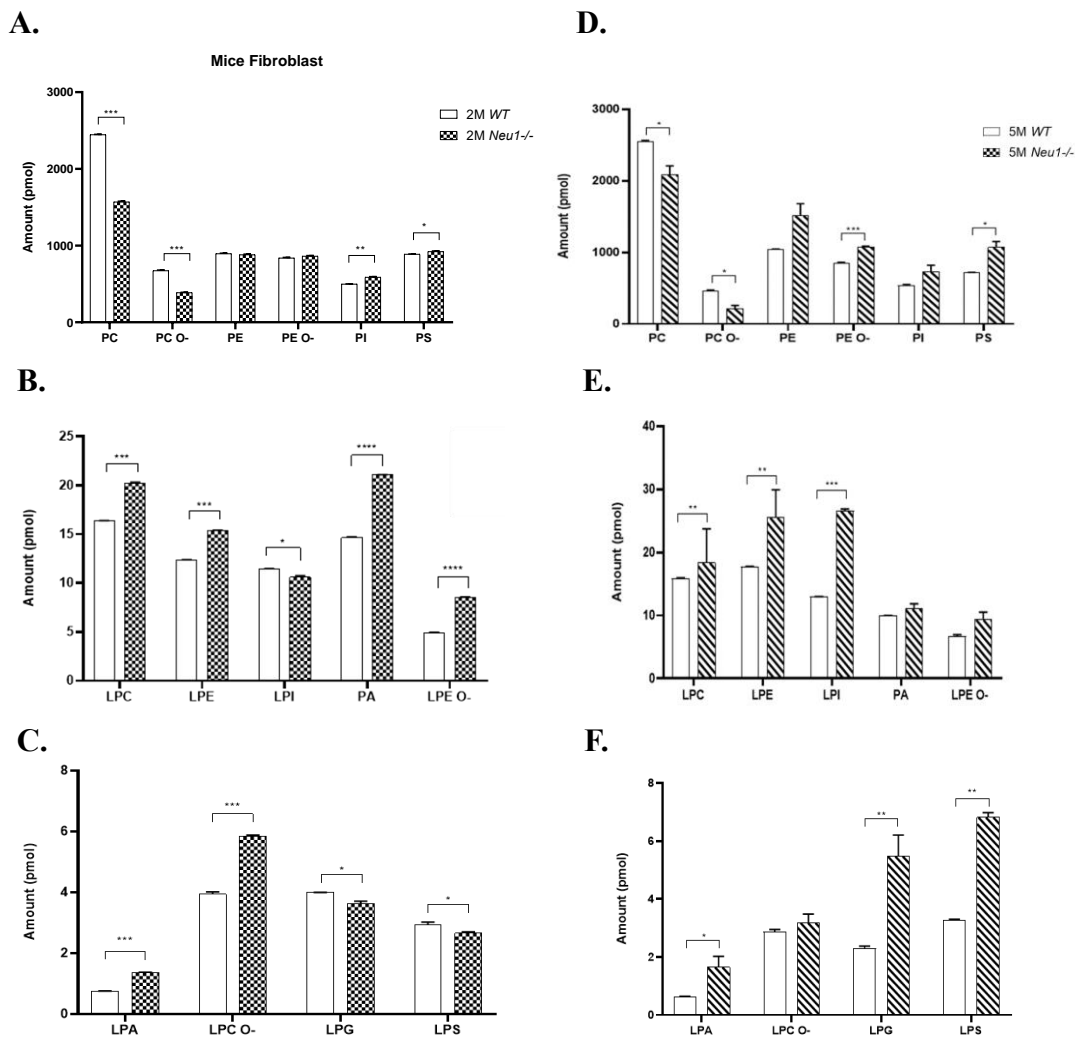


Figure 3.2. Glycerophospholipid lipidome assays from 2-month-old *WT* and *Neu1*<sup>-/-</sup> mice (A, B, and C) and 5-month-old *WT* and *Neu1*<sup>-/-</sup> mouse fibroblasts (D, E, and F) were shown in Figure 3.2. The comparison between *WT* and *Neu1*<sup>-/-</sup> was determined with the GraphPad analysis and the One-way ANOVA test was conducted. In each sample was conducted with n=3.

On the other hand, some lipids are significantly increased in *Neu1* samples compared to *WT* samples in 2-month-old mice fibroblast results. PI, LPC, LPE, PA, LPE O-, LPA, and LPC O- were significantly increased compared to the *WT* samples in Figure 3.2A, Figure 3.2B, and Figure 3.2C. PS slightly increased compared to *WT* in Figure 3.2A and PE and PE O- were not monitored for any significant alteration compared to *WT* and *Neu1* samples in the results of Figure 3.2A.

In Figure 3.2D, E, and F was the amount of 5-month-old mice fibroblast cell line Glycerophospholipid results of *WT* and *Neu1*<sup>-/-</sup> samples. In Figure 3.2D, PC and PC O-*Neu1* sample results of these lipids were slightly decreased compared to *WT* results. On the other hand, PE O-, LPC, LPE, LPI, LPG, and LPS were significantly increased in *Neu1* samples compared to *WT* samples in the results of Figure 3.2D, E, and F. Also, PS and LPA were slightly increased. However, in 5-month-old mice fibroblast results of PA, PI, LPE O-, and LPC O-, there was no significant change between the *WT* and *Neu1* results in Figure 3.2D, E, and F.

In Figure 3.3, Glycerophospholipid lipidome assays from human fibroblast cell lines were monitored. Each patient sample was compared with the *WT* sample of the human fibroblast cell results of each lipid amount in Figure 3.3A, B, and C. Compared to the *WT* samples, in human sialidosis patients results of these lipids significantly increased. These are PC O-, CL, LPC, LPE, LPI, PA and LPE O-, LPA and LPC O-. Also, some of both patient samples decreased compared to the control fibroblast cell line which are PC and PI. Moreover, in some of the lipids for the comparison between the *WT* and sialidosis patient's fibroblast cell line samples, there was no significant difference in these lipids which are PS, LPG, and LPS.

In Figure 3.4, Glycerolipid lipidome assays from 2-month-old *WT* and *Neu1*<sup>-/-</sup> mouse (3.4A) and 5-month-old *WT* and *Neu1*<sup>-/-</sup> mouse fibroblast cell line samples (3.4B) were monitored. Also, in Figure 3.4C, Glycerolipid lipidome assays from human fibroblast cell lines samples compared to the *WT* human fibroblast of two different patients' fibroblast was monitored. In this figure, some of the lipids were altered in the *Neu1* samples compared to the *WT* samples. For mouse 2-month-old mice fibroblast *Neu1*<sup>-/-</sup> samples, HexCer and Cer lipids were significantly increased according to the *WT* in 2-month-old Mice Fibroblast results in Figure 3.4A.

On the other hand, TAG lipid amount was significantly decreased compared to *WT* for the 2-month-old *Neu1*<sup>-/-</sup> sample of mice results in 3.4A. Also, for SM and DAG lipid samples, the alteration was not detected for these lipid samples. For Figure 3.4B, 5-month-old mice fibroblast samples of *WT* and *Neu1*<sup>-/-</sup> were monitored. For 5-month-old mice fibroblast samples, there was a significant increase in SM and Cer lipid samples, however, there was a significant decrease in TAG lipid amount compared to *WT* in 5-month-old *Neu1*<sup>-/-</sup> mice fibroblast sample. Also, there was no significant change in the DAG and HexCer lipid group.

For the human glycerolipid sample results in Figure 3.4C, HexCer and TAG were detected for a significant increase in the Neu1 sample of human fibroblast compared to the *WT* fibroblast sample amount. Also, for the DAG lipid, one of the patient samples was decreased compared to the *WT* but the severe patient's result showed very significant increases in Neu1 results compared to WT.

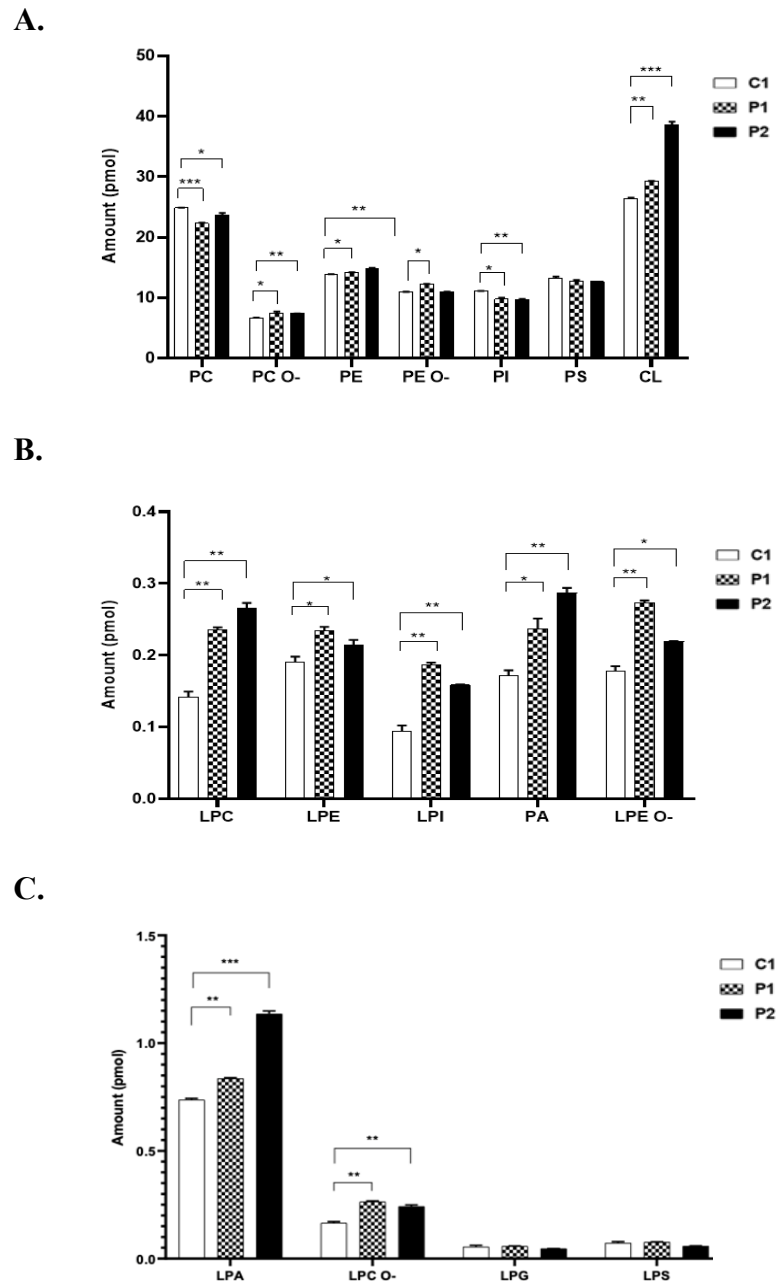


Figure 3.3. Glycerophospholipid lipidome assays from human fibroblast cell lines. Orderly, GM01719, GM02921, and GM01718 are human fibroblast cell lines. GM01719 is called C1, control 1. GM02921 is counted as a P1, patient 1. GM01718 is counted as P2, patient 2. The analysis was conducted according to the comparison between *WT* and *Neu1*<sup>-/-</sup> was determined with

the GraphPad analysis and a One-way ANOVA test was conducted. In each sample was conducted with n=3.

In Figure 3.4C one of the patient's samples which had %8 enzyme activity, GM02921 showed a slight decrease in the amount of Cer compared to the *WT* however, there is no alteration detected for other patients compared to the *WT* sample amount. Lastly, for SM lipid, there was no significant change detected for both patients' samples compared to WT.

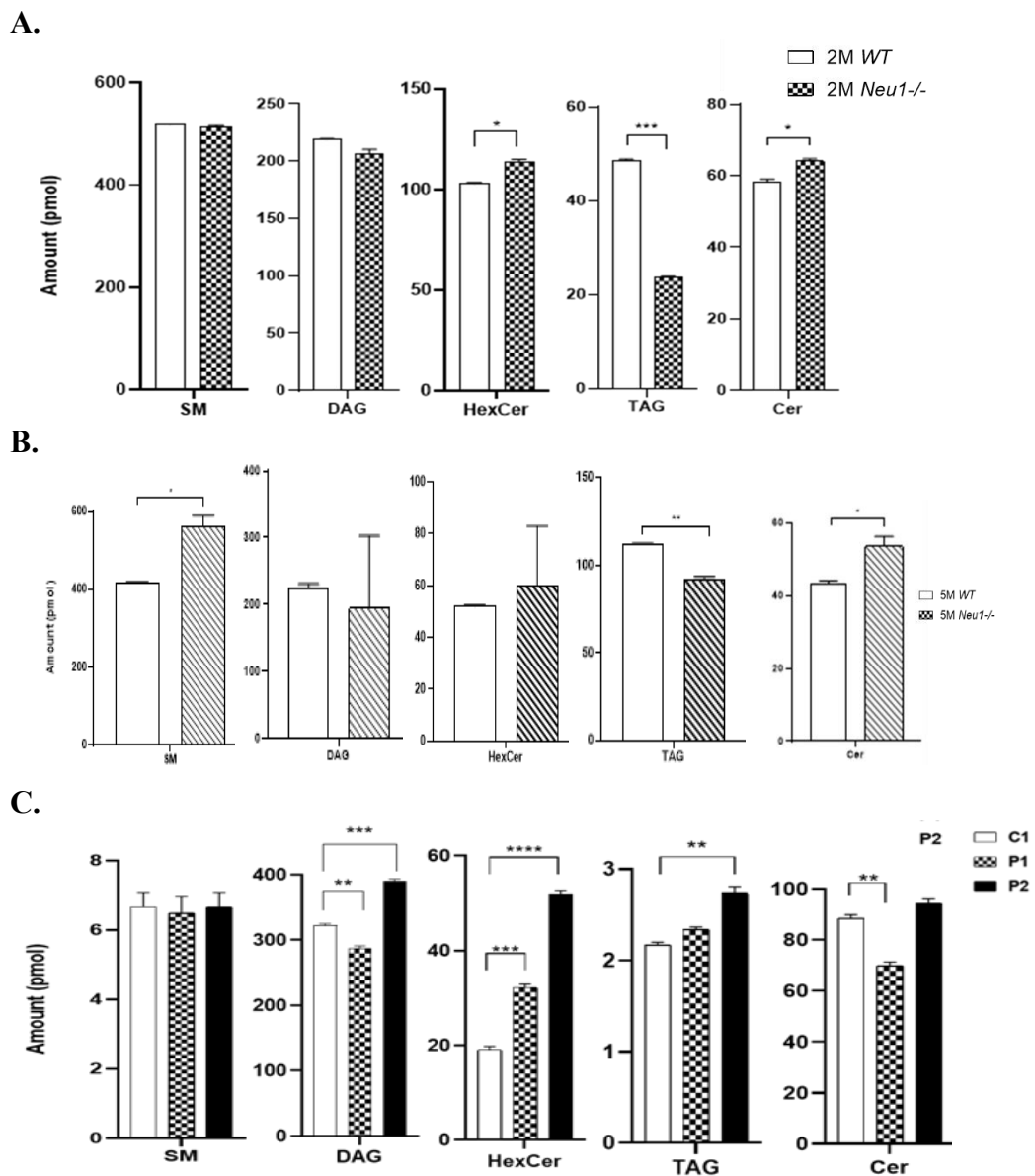


Figure 3.4. Glycerolipid lipidome assays from 2-month-old *WT* and *Neu1*<sup>-/-</sup> mouse (A) and 5-month-old *WT* and *Neu1*<sup>-/-</sup> mouse fibroblast cell line samples (B), and human fibroblast cell lines (C). Orderly, GM01719, GM02921, and GM01718 are human fibroblast cell lines. GM01719 is called C1, control 1.

GM02921 is counted as a P1, patient 1. GM01718 is counted as P2, patient 2. The amount of each lipid was added, and a one-way-ANOVA analysis was used to determine p-values by using GraphPad. Data were reported as means SEM (n=3, \*p<0,05, \*\*p<0,01, \*\*\*p<0,001). In each sample was conducted with n=3.

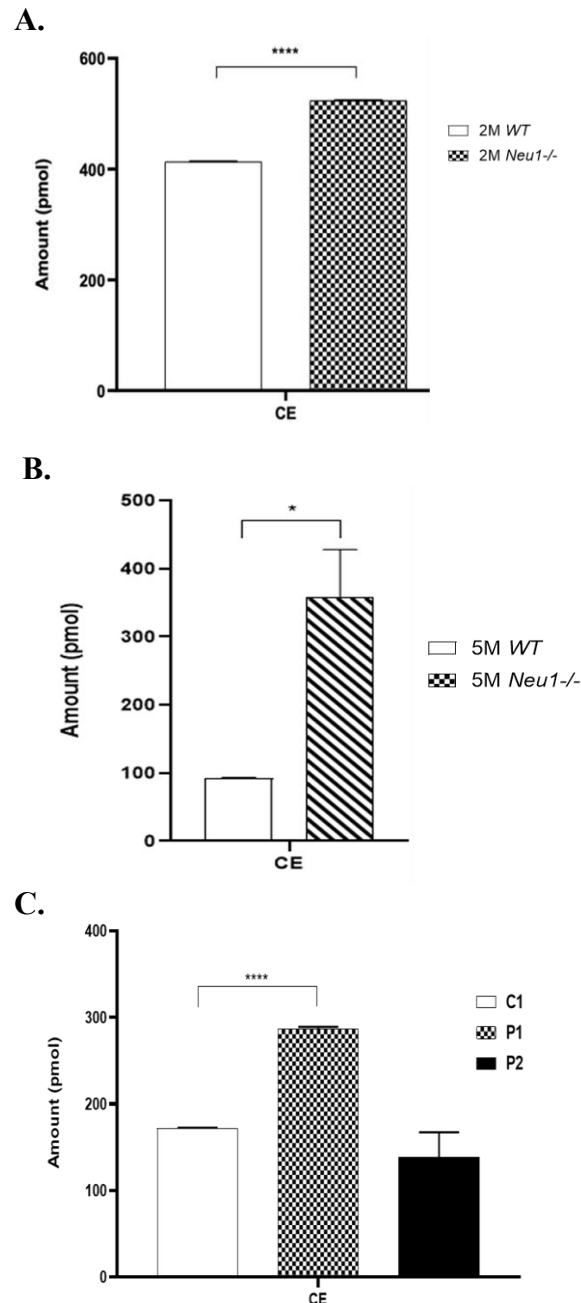


Figure 3.5. Sterol lipids lipidome assays from 2-month-old *WT* and *Neu1*<sup>-/-</sup> mouse (A) and 5-month-old *WT* and *Neu1*<sup>-/-</sup> mouse fibroblast cell line samples (B), and human fibroblast cell lines (C). Orderly, GM01719, GM02921, and GM01718 which are human fibroblast cell lines. GM01719 is called C1, control 1. GM02921 is counted as a P1, patient 1. GM01718 is counted as P2, patient 2. The amount of each lipid was added, and a 2-way ANOVA analysis was used to determine p-values by using GraphPad. Data were reported as

means SEM (n=3, \*p<0,05, \*\*p<0,01, \*\*\*p<0,001). In each sample was conducted with n=3.

In Figure 3.5 there is a sterol lipid expression level for 2-month-old, and 5-month-old mice fibroblast results were shown in 3.5A and 3.5B. Also, in Figure 3.5C there is a Cholesterol Ester (CE) level in both human patients, and one of the controls of human fibroblast results of sterol lipid was monitored. In Figure 3.5A, 2-month-old mice fibroblast results compared to *WT* fibroblast were determined and significantly increased in *Neu1*<sup>-/-</sup>. Also, in Figure 3.5B, there is a result of 5-month-old mice fibroblast compared to *WT*, there is also found a slight increase in *Neu1*<sup>-/-</sup> sample of results compared to *WT*. In Figure 3.5C, there are human fibroblast results shown. Compared to the *WT* and sialidosis patients, one of the sialidosis patients (P1) results compared with *WT* are significantly increased in comparison with the other patient and *WT* human fibroblast results of the sterol lipid level.

### 3.3. RT-PCR

Real-time PCR was conducted with the QPCR Array of Chemokines and Cytokines and to obtain precise and accurate results, manually selected genes were monitored. For Array RT-PCR, 84 different genes were observed and investigated with the Array. Also, manually selected genes were *Ccl2*, *Ccl3*, *Ccl5*, and *Cxcl10* for mice and human fibroblasts in both *WT* and *Neu1*<sup>-/-</sup>.

#### 3.3.1 Array Results

According to Figure 3.6, RT-PCR Qiagen Chemokine and Cytokine Array results were observed for 2-month-old mouse fibroblasts, 5-month-old mouse fibroblasts, and human fibroblasts. In Figure 3.6A 2-month-old *WT* and 2-month-old *Neu1*<sup>-/-</sup> mice fibroblast expression ratios according to the housekeeping genes were compared. Moreover, *Ccl11*, *Ccl5*, *Cxcl11*, and *Cxcl16* were significantly increased compared to the *WT* in 2-month-old *Neu1*<sup>-/-</sup> results of mouse fibroblasts. Also, compared to the *WT* results of expression ratios in 2-month-old mouse fibroblasts, some of which are *Ccl17*, *Ccl19*, *Ccl20*, *Ccl22*, *Ccl24*, *Cx3c11*, *Cxcl10*, *Cxcl11*, *Cxcl13*, *Cxcl9*, *Ppbbp*, *Xcl1* significantly

decreased. Also, some of the gene expression ratios for 2-month-old mouse fibroblasts were not detected in any significant change which are Ccl1 and Ccl3.

In Figure 3.6B, 5-month-old *WT* and 5-month-old *Neu1*<sup>-/-</sup> mice fibroblast expression ratios according to the housekeeping genes were compared. Moreover, Ccl11, Ccl19, Ccl20, Ccl24, Ccl3, Ccl5, Cxcl1, Cxcl11, Cxcl16, Pbbp, was significantly increased compared to the *WT* in 5-month-old *Neu1*<sup>-/-</sup> results of mouse fibroblasts. Also, some of the gene expression ratios for 5-month-old mouse fibroblasts were not detected in any significant change, which is Cx3cl1.

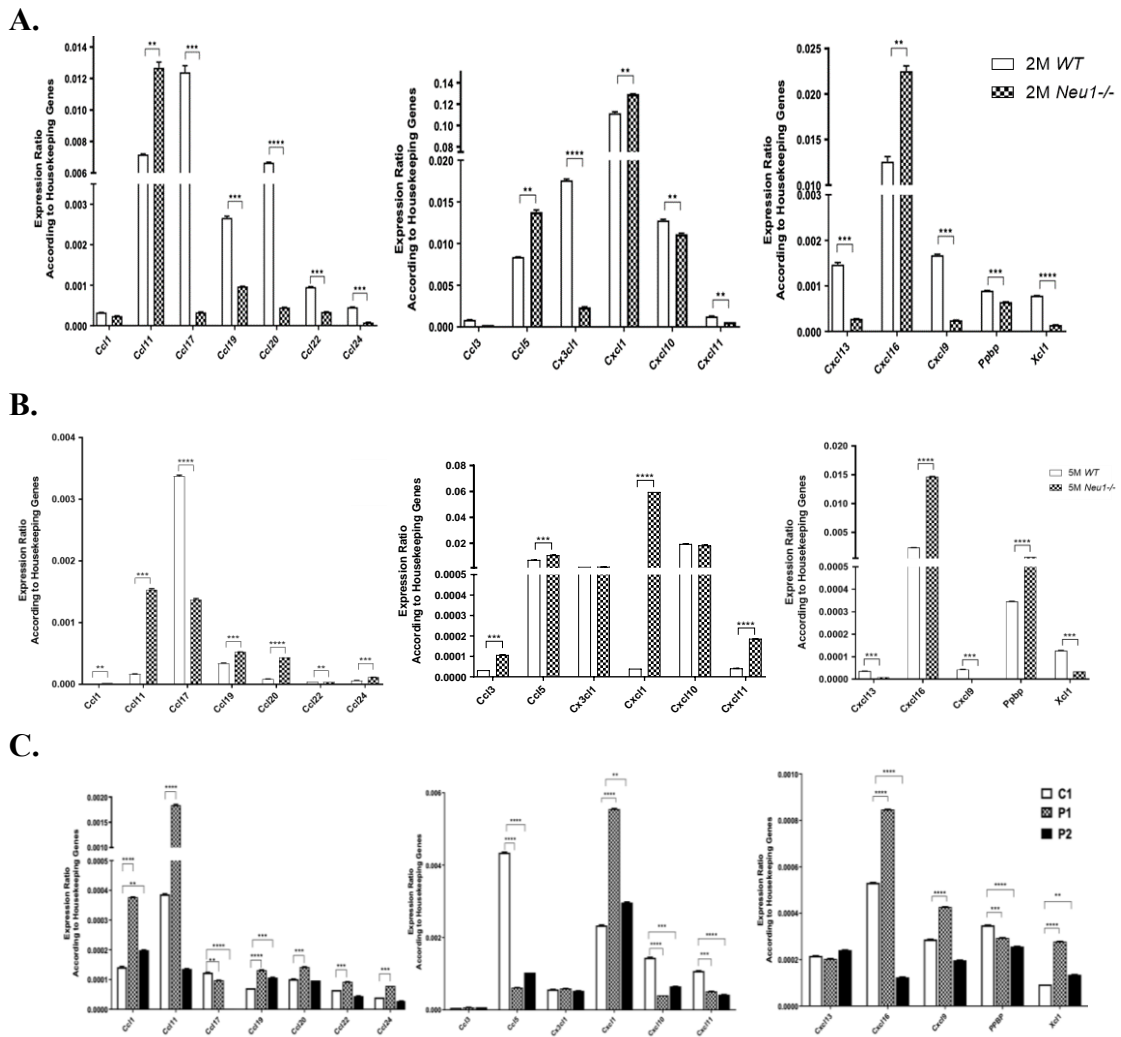


Figure 3.6. Gene expression ratio of chemokines in 2-month-old *WT* and *Neu1*<sup>-/-</sup> mouse fibroblasts (A) and 5-month-old *WT* and *Neu1*<sup>-/-</sup> mouse fibroblasts (B) also Orderly, GM01719, GM02921 and GM01718 which are human fibroblast cell lines. GM01719 is called C1, control 1. GM02921 is counted as a P1, patient 1. GM01718 is counted as P2, patient 2 (C). Expression ratios were calculated with  $\Delta$ CT method and 2-way-ANOVA analysis was used to

determine p-values by using GraphPad. Data were reported as means SEM (n=3, \*p<0,05, \*\*p<0,01, \*\*\*p<0,001).

In Figure 3.6C, the Gene expression ratio of chemokines in orderly, GM01719, GM02921, and GM01718 which are human fibroblast cell lines. GM01719 is called C1, control 1. GM02921 is counted as a P1, patient 1. GM01718 is counted as P2, patient 2 was monitored. In human fibroblasts gene expression ratio of chemokine, results showed that some of the genes are significantly increased for both patients' samples compared to the *WT* results which are *Ccl1*, *Ccl19*, *Cxcl1*, and *Xcl1*. Also, some of the gene expression ratios for human patients' fibroblasts compared to the *WT* only were detected with P1 for increasing, and no significant alteration was observed within *WT* and P2 expression ratio results. These genes are *Ccl20*, *Ccl22*, *Ccl24*, *Cxcl9*. On the other hand, some of both patients' samples compared to the *WT* results were significantly decreased and these genes are *Ccl17*, *Cxcl10*, *Cxcl11*, and *Ppbb*. Moreover, for some of the genes from the human fibroblasts, there is no alteration was monitored. These genes are *Ccl3*, *Cx3cl1*, *Cxcl13*.

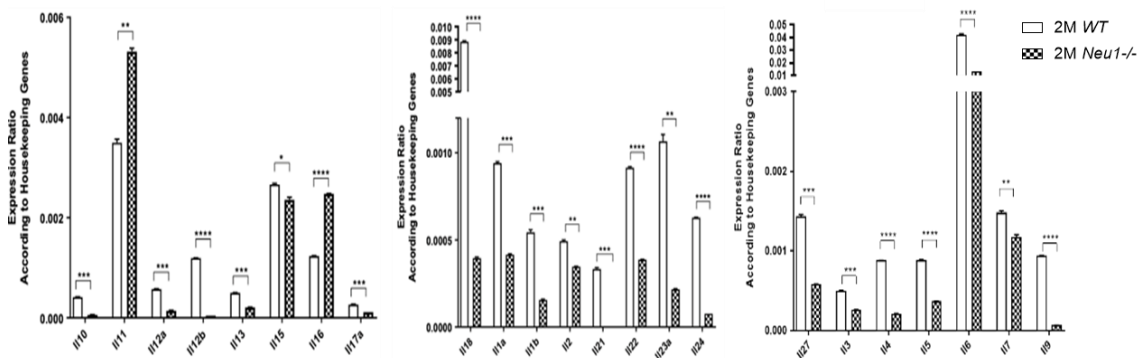
In Figure 3.7 gene expression ratio of interleukins in 2-month-old *WT* and *Neu1*<sup>-/-</sup> mouse fibroblasts and 5-month-old *WT* and *Neu1*<sup>-/-</sup> mouse fibroblasts and human fibroblasts samples was monitored. According to the results of interleukins, in Figure 3.7A 2-month-old *WT* and 2-month-old *Neu1*<sup>-/-</sup> mice fibroblast expression ratios according to the housekeeping genes were compared. Some genes were detected as significantly increased in 2-month-old *Neu1*<sup>-/-</sup> sample results compared to the 2-month-old *WT* sample results. These genes are *Il11* and *Il16*. Also, some of the genes are significantly decreased in 2-month-old *Neu1*<sup>-/-</sup> sample results compared to the 2-month-old *WT* sample results. These genes are *Il10*, *Il12a*, *Il12b*, *Il13*, *Il17a*, *Il18*, *Il1a*, *Il1b*, *Il21*, *Il22*, *Il24*, *Il27*, *Il3*, *Il4*, *Il5*, *Il6*, *Il9*. Also, some of the genes are slightly different than *WT* samples which are *Il15*, *Il2*, *Il23a*, and *Il7*.

In Figure 3.7B, 5-month-old *WT* and 5-month-old *Neu1*<sup>-/-</sup> mice fibroblast expression ratios according to the housekeeping genes were compared and interleukin genes were monitored. Some genes were detected as a significantly increased in 5-month-old *Neu1*<sup>-/-</sup> sample results compared to the 5-month-old *WT* sample results which are *Il10*, *Il11*, *Il12a*, *Il16*, *Il18*, *Il1a*, *Il1b*, *Il22*, *Il24*, *Il6* and *Il7*. Also, some of the gene expression ratios were detected as slightly increased compared to the *WT* in *Neu1*<sup>-/-</sup> samples of 5-month-old results, these genes are *Il27*, *Il3*, and *Il5*. Moreover, in Figure 3.7B some of the 5-month-old mice fibroblast samples were detected as a significant

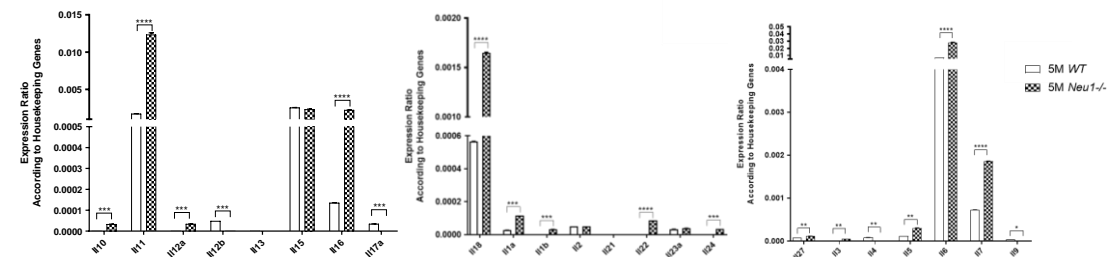
decrease in *Neu1*<sup>-/-</sup> samples compared to WT. These genes are Il12b and Il17a. Also, for some of the genes, no alteration is detected in any significance which are Il13, Il2, Il21, Il23a, and Il9.

In Figure 3.7C, human fibroblast cell lines were used to detect interleukin genes. GM01719 is called C1, control 1. GM02921 is counted as a P1, patient 1. GM01718 is counted as P2, patient 2. There was detected significant elevation in the Patient's sample compared to the *WT* sample of human fibroblasts in interleukin genes. These genes are Il10, Il11, Il18, Il1a, Il1b, Il23a, Il24, Il27 and Il3. Also, some of the genes were detected which were significantly decreased in both patients' results compared to *WT* of human fibroblast results. These significant decreased genes are Il12b, Il15, Il16, Il17a, Il21, Il4, Il5 and Il6. For other genes in Figure 3.7, alterations were only detected within only patient or the patient. Only the results were selected as significant if the results were both altered in patient1 and patient2 compared with *WT* of human fibroblasts.

**A.**



**B.**



**C.**

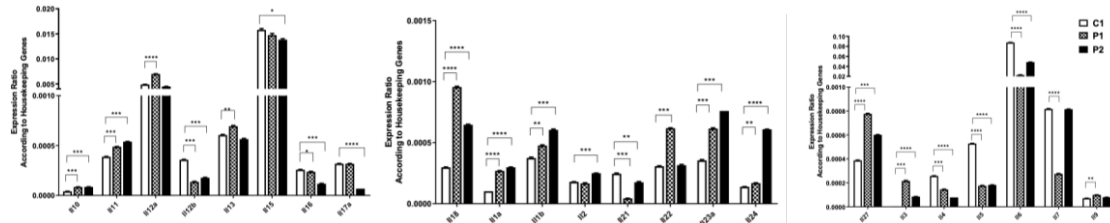


Figure 3.7. Gene expression ratio of interleukins in 2-month-old *WT* and *Neu1*<sup>-/-</sup> mouse fibroblasts (A) and 5-month-old *WT* and *Neu1*<sup>-/-</sup> mouse fibroblasts (B) also orderly, GM01719, GM02921, and GM01718 which are human fibroblast cell lines. GM01719 is called C1, control 1. GM02921 is counted as a P1, patient 1. GM01718 is counted as P2, patient 2 (C). Expression ratios were calculated with  $\Delta$ CT method and 2-way-ANOVA analysis was used to determine p-values by using GraphPad. Data were reported as means SEM (n=3, \*p<0,05, \*\*p<0,01, \*\*\*p<0,001).

In Figure 3.8 gene expression ratio of interferons and TNF Receptor Family Members in 2-month-old *WT* and *Neu1*<sup>-/-</sup> mouse fibroblasts (Figure 3.8A and B) and 5-month-old *WT* and *Neu1*<sup>-/-</sup> mouse fibroblasts (Figure 3.8C and D) also orderly, GM01719, GM02921 and GM01718 which are human fibroblast cell lines was monitored (Figure 3.8E and F). There was detected significant decrease in all gene expression ratios for 2-month-old *Neu1*<sup>-/-</sup> samples compared to 2-month-old *WT* in mouse fibroblasts (Figure 3.1A and B) for interferons and TNF receptor family member genes. Which are *Ifna2*, and *Ifng* for interferons and for TNF family members *Cd40lg*, *Fasl*, *Lta*, *Tnfrsf11b*, *Tnfsf10*, *Tnfsf11*, and *Tnfsf13b* are significantly decreased in 2-month-old *Neu1*<sup>-/-</sup> samples compared to 2-month-old *WT* fibroblast mice samples. Moreover, only the TNF gene was increased in 2-month-old *Neu1*<sup>-/-</sup> samples compared to 2-month-old *WT* fibroblast mice samples. On the other hand, 5-month-old *WT* and *Neu1*<sup>-/-</sup> mouse fibroblasts were detected in Figure 3.8C and D. Significantly increased 5-month-old *Neu1*<sup>-/-</sup> sample results compared to 5-month-old *WT* results were shown within the genes which are significantly increased for 5-month-old *Neu1*<sup>-/-</sup> mice fibroblast samples are *Ifna2*, *Ifng* for interferons, *Fasl*, *Tnf*, *Tnfrsf11b*, *Tnfsf10* and *Tnfsf13b* for TNF receptor family members. However, *Cd40lg*, *Lta*, and *Tnfsf11* are significantly decreased in 5-month-old *Neu1*<sup>-/-</sup> mice fibroblast samples according to the comparison with 5-month-old *WT* mice sample results.

In Figures 3.8E and F, human fibroblast cell lines were used to detect interferons and TNF Receptor Family Members. GM01719 is called C1, control 1. GM02921 is counted as a P1, patient 1. GM01718 is counted as P2, patient 2. There was detected significant decrease in both Patients' samples compared to the *WT* sample of human fibroblasts in interferon genes. These decreased interferon genes are *Ifna2* and *Ifng*. Also, TNF receptor family members were detected and compared with each other. A significant decrease in both patient's samples compared with *WT* human fibroblast was detected for some of the TNF family member genes and these genes are *Tnf*, *Tnfrsf11b*, *Tnfsf10*,

Tnfsf11 and Tnfsf13b. On the other hand, significant increases were also detected in both patients' fibroblast expression ratio results compared to *WT* human fibroblast expression ratio results. These elevated genes are Faslg and Lta.

In Figure 3.9, the gene expression ratio of Growth Factors in 2-month-old *WT* and *Neu1*<sup>-/-</sup> mouse fibroblasts (Figure 3.9A) and 5-month-old *WT* and *Neu1*<sup>-/-</sup> mouse fibroblasts (Figure 3.9B) also orderly, GM01719, GM02921 and GM01718 which are human fibroblast cell lines (Figure 3.9C). GM01719 is called C1, control 1. GM02921 is counted as a P1, patient 1. GM01718 is counted as P2, patient 2 (C) was monitored.

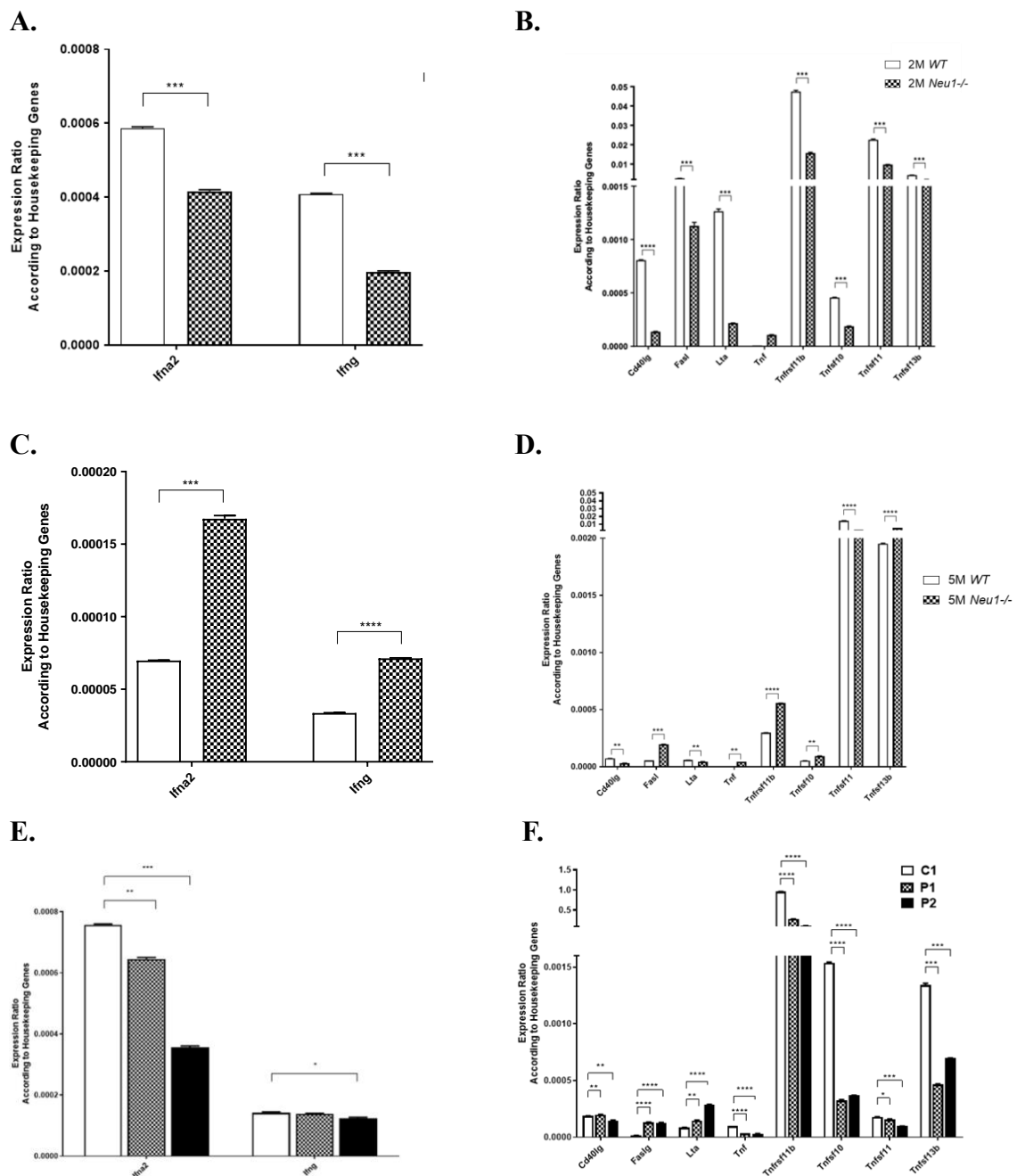


Figure 3.8. Gene expression ratio of interferons and TNF Receptor Family Members in 2-month-old *WT* and *Neu1*<sup>-/-</sup> mouse fibroblasts (A and B) and 5-month-old *WT* and *Neu1*<sup>-/-</sup> mouse fibroblasts (C and D) also Orderly, GM01719, GM02921 and GM01718 which are human fibroblast cell lines. GM01719 is called C1, control 1. GM02921 is counted as a P1, patient 1. GM01718 is counted as P2, patient 2 (E and F). Expression ratios were calculated with  $\Delta$ CT method and 2-way-ANOVA analysis was used to determine p-values by using GraphPad. Data were reported as means SEM (n=3, \*p<0,05, \*\*p<0,01, \*\*\*p<0,001).

For 2-month-old mice fibroblast cell line results, some of the growth factor genes were detected as a significant decrease in 2-month-old *Neu1*<sup>-/-</sup> samples of mouse fibroblasts compared to *WT* of 2-month-old mice fibroblast results. These expression ratios significantly decreased genes are *Bmp2*, *Bmp4*, *Bmp6*, *Bmp7*, *Cntf*, *Csf2*, *Mstn*, *Osm* and *Thpo*. Also, some of the genes are slightly decreased compared to 2-month-old *WT* mice fibroblast results in Figure 3.9A. These slightly decreased genes are *Csf3*, *Lif*, and *Nodal*. For 5-month-old mice fibroblast cell line results, some of the growth factor genes were detected as a significant decrease in 5-month-old *Neu1*<sup>-/-</sup> mice fibroblast samples compared to *WT* of 5-month-old mice fibroblast results. These expression ratios significantly decreased genes for 5-month-old *Neu1*<sup>-/-</sup> of the mice fibroblast results are *Bmp2*, *Lif*, and *Osm*. Also, for 5-month-old mice fibroblast cell line results, some of the growth factor genes were detected as a significant increase in *Neu1*<sup>-/-</sup> samples compared to *WT* of 5-month-old results (Figure 3.9B). These expression ratios are significantly elevated genes are *Bmp4*, *Bmp6*, *Csf2*, *Mstn*, *Nodal*, and *Thpo*. For 5-month-old mice, fibroblast cell line results, *Bmp7*, and *Cntf* genes were not detected in any significant alteration compared to 5-month-old *WT* samples.

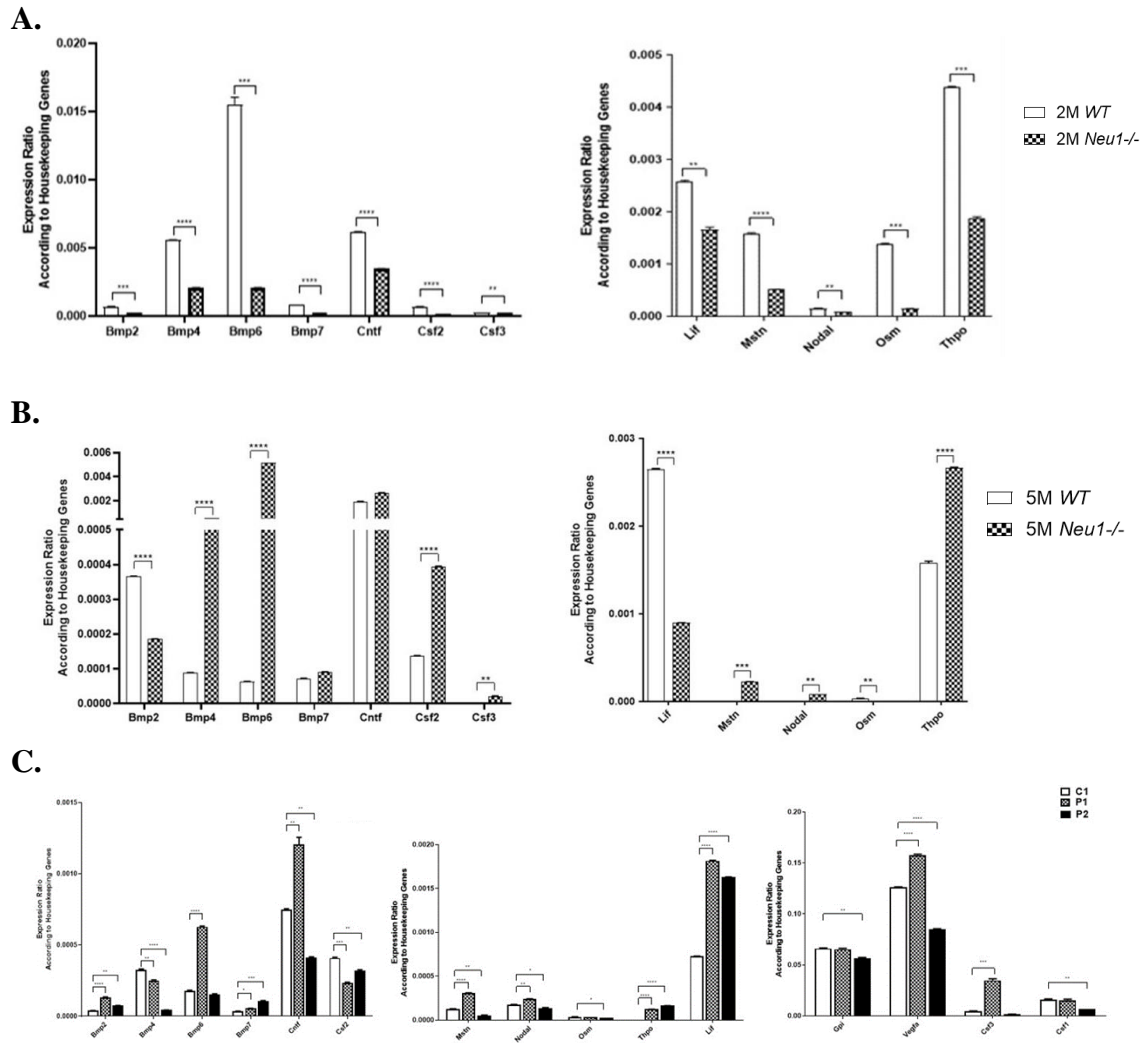


Figure 3.9. Gene expression ratio of Growth Factors in 2-month-old *WT* and *Neu1*<sup>-/-</sup> mouse fibroblasts (A) and 5-month-old *WT* and *Neu1*<sup>-/-</sup> mouse fibroblasts (B) also orderly, GM01719, GM02921, and GM01718 which are human fibroblast cell lines. GM01719 is called C1, control 1. GM02921 is counted as a P1, patient 1. GM01718 is counted as P2, patient 2 (C). Expression ratios were calculated with  $\Delta$ CT method and 2-way-ANOVA analysis was used to determine p-values by using GraphPad. Data were reported as means SEM (n=3, \*p<0,05, \*\*p<0,01, \*\*\*p<0,001).

In human fibroblast sample results of the Array, Growth factors were also detected. For Figure 3.9C, some of the growth factor genes were detected with a significant decrease in *Neu1*<sup>-/-</sup> patient samples compared to *WT* of human fibroblast results. These genes are Bmp4, Csf2, Osm, Gpi and Csf1. On the other hand, some of the growth factor genes were detected with a significant increase in *Neu1*<sup>-/-</sup> patient samples compared to *WT* of human fibroblast results. These genes are Bmp2, Bmp6, Bmp7, Mstn, Nodal, Thpo, Lif and Csf3.

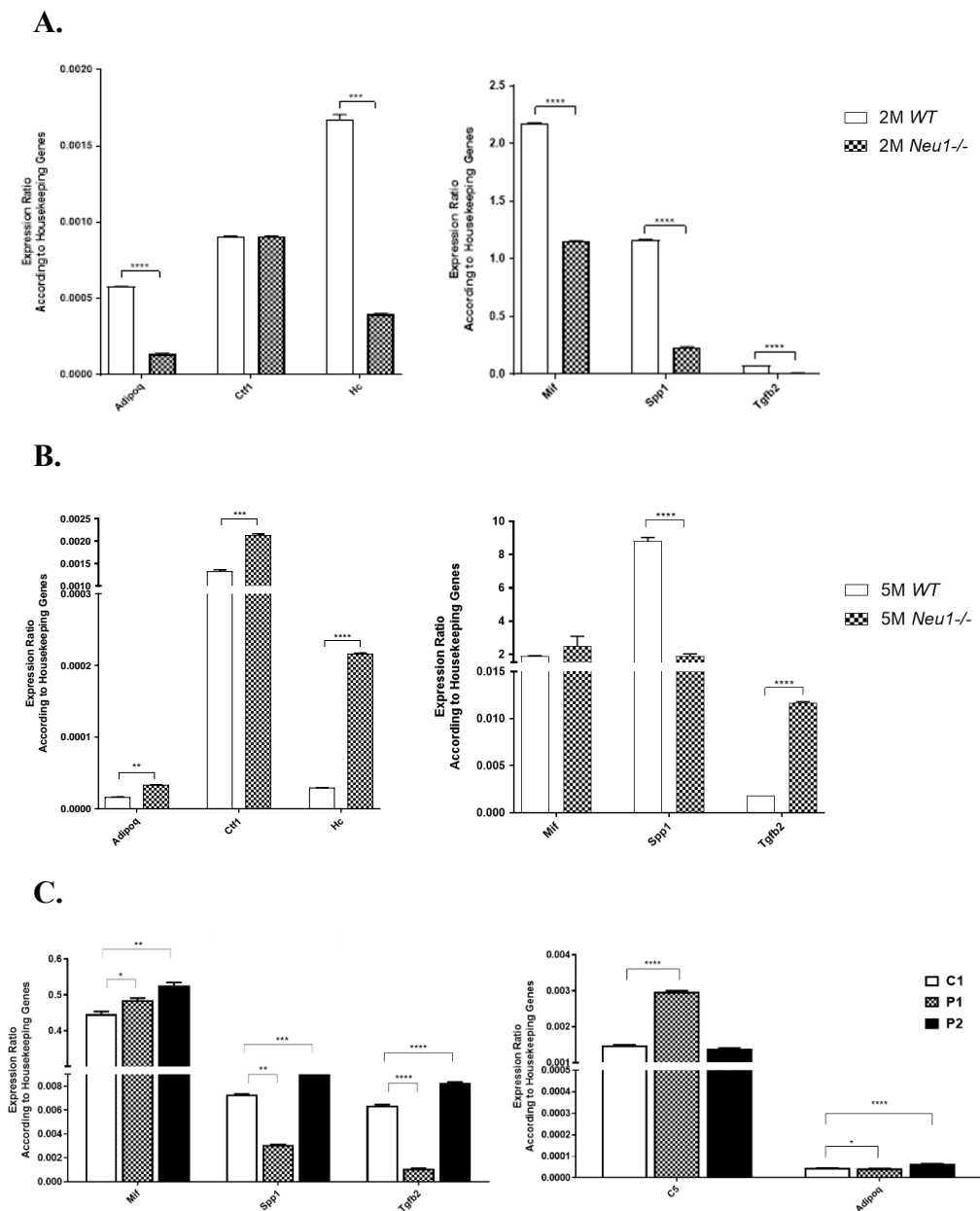


Figure 3.10. Gene expression ratio of Other Cytokines in 2-month-old *WT* and *Neu1*<sup>-/-</sup> mouse fibroblasts (A) and 5-month-old *WT* and *Neu1*<sup>-/-</sup> mouse fibroblasts (B) also Orderly, GM01719, GM02921 and GM01718 which are human fibroblast cell lines. GM01719 is called C1, control 1. GM02921 is counted as a P1, patient 1. GM01718 is counted as P2, patient 2 (C). Expression ratios were calculated with  $\Delta$ CT method and 2-way-ANOVA analysis was used to determine p-values by using GraphPad. Data were reported as means SEM (n=3, \*p<0,05, \*\*p<0,01, \*\*\*p<0,001).

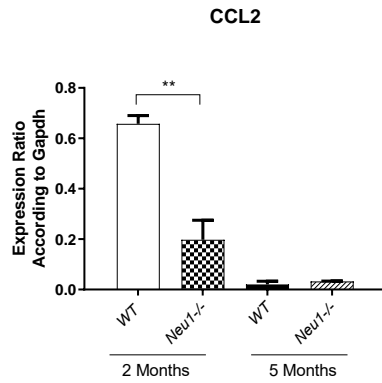
In Figure 3.10, the gene expression ratio of other cytokines in 2-month-old *WT* and *Neu1*<sup>-/-</sup> mouse fibroblasts (3.10A) and 5-month-old *WT* and *Neu1*<sup>-/-</sup> mouse fibroblasts (3.10B) and human fibroblasts (3.10C) was monitored. For 2-month-old mice

fibroblast cell line results, some of the other cytokine genes were detected as a significant decrease in *Neu1*<sup>-/-</sup> samples compared to *WT* of 2-month-old results. These expression ratios significantly decreased other cytokines are Adipoq, Hc, Mif, Spp1, and Tgfb2. Also, for the Ctf1 gene, no alteration was detected compared to the 2-month-old *WT* results of the samples. Moreover, in Figure 3.10B, for 5-month-old mice fibroblast cell line results, some of the other cytokine genes were detected as a significant increase in *Neu1*<sup>-/-</sup> samples compared to *WT* of 5-month-old results. These expression ratios significantly increased other cytokines such as Adipoq, Ctf1, Hc, and Tgfb2. On the other hand, only Spp1 was detected with a significant decrease in *Neu1*<sup>-/-</sup> of the 5-month-old mice fibroblast results compared to *WT* of 5-month-old mice fibroblast results. Also, For the Mif gene, there is no alteration detected for 5-month-old mice fibroblast sample results.

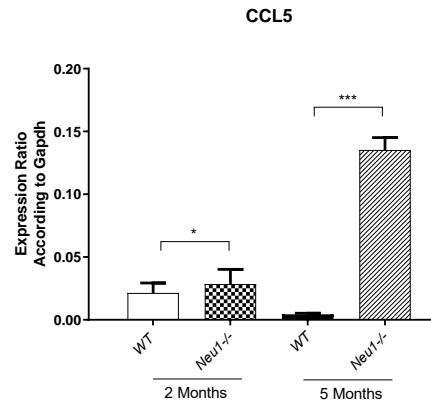
In human fibroblast sample results of the Array, other cytokines were also detected. For Figure 3.10C, some of the growth factor genes were detected with a significant increase in *Neu1*<sup>-/-</sup> patient samples compared to *WT* of human fibroblast results. These genes are Mif, C5, and Adipoq. Also, for some of the genes which are Spp1 and Tgfb2, compared to the *WT* of the human fibroblast samples, patient's 1 results were significantly decreased compared to *WT* however, Patient's 2 results were significantly increased compared to *WT* of the human fibroblast results for these 2 genes of the growth factor.

### 3.3.2. qPCR Results

A.



B.



C.

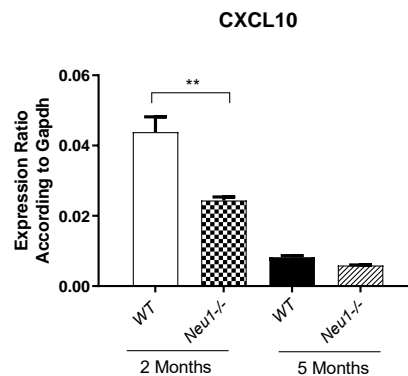


Figure 3.11. Gene expression ratio of *Ccl2*, *Ccl5*, and *Cxcl10* in 2-month-old *WT* and *Neu1*<sup>-/-</sup> mouse fibroblasts and 5-month-old *WT* and *Neu1*<sup>-/-</sup> mouse fibroblasts was shown orderly in A, B, and C part of the figure. Expression ratios were calculated with  $\Delta$ CT method and 2-way-ANOVA analysis was used to determine p-values by using GraphPad. Data were reported as means SEM (n=3, \*p<0,05, \*\*p<0,01, \*\*\*p<0,001).

In Figure 3.11, compared to the Array qPCR results from 3.6 to 3.10, some of the genes were selected and tested to prove and check the result's precision and accuracy. Gene expression ratio of *Ccl2*, *Ccl5*, and *Cxcl10* in 2-month-old *WT* and *Neu1*<sup>-/-</sup> mouse fibroblasts and 5-month-old *WT* and *Neu1*<sup>-/-</sup> mouse fibroblasts was monitored in Figure 3.11. According to the results, the *Ccl2* gene was decreased in the 2-month-old *Neu1*<sup>-/-</sup> sample of mice fibroblast compared to 2-month-old *WT* mice fibroblast and there is no significant alteration was detected between 5-month-old *WT* and 5-month-old *Neu1*<sup>-/-</sup> of the mouse fibroblasts (Figure 3.11A). Also, the expression ratio of the *Ccl5* gene,

according to the Gapdh which is a housekeeping gene, was monitored (Figure 3.11B). According to the results, the Ccl5 gene was elevated in a 2-month-old *Neu1*<sup>-/-</sup> sample of mice fibroblast compared to 2-month-old *WT* mice fibroblast and there is also a significant elevation of expression ratio in 5-month-old *Neu1*<sup>-/-</sup> compared to 5-month-old *WT* mouse fibroblasts. Moreover, Cxcl10 gene expression ratio was determined (Figure 3.11C). According to the results, the Cxcl10 gene was decreased in the 2-month-old *Neu1*<sup>-/-</sup> sample of mice fibroblast compared to 2-month-old *WT* mice fibroblast and there is no significant alteration was detected between 5-month-old *WT* and 5-month-old *Neu1*<sup>-/-</sup> of the mouse fibroblasts.

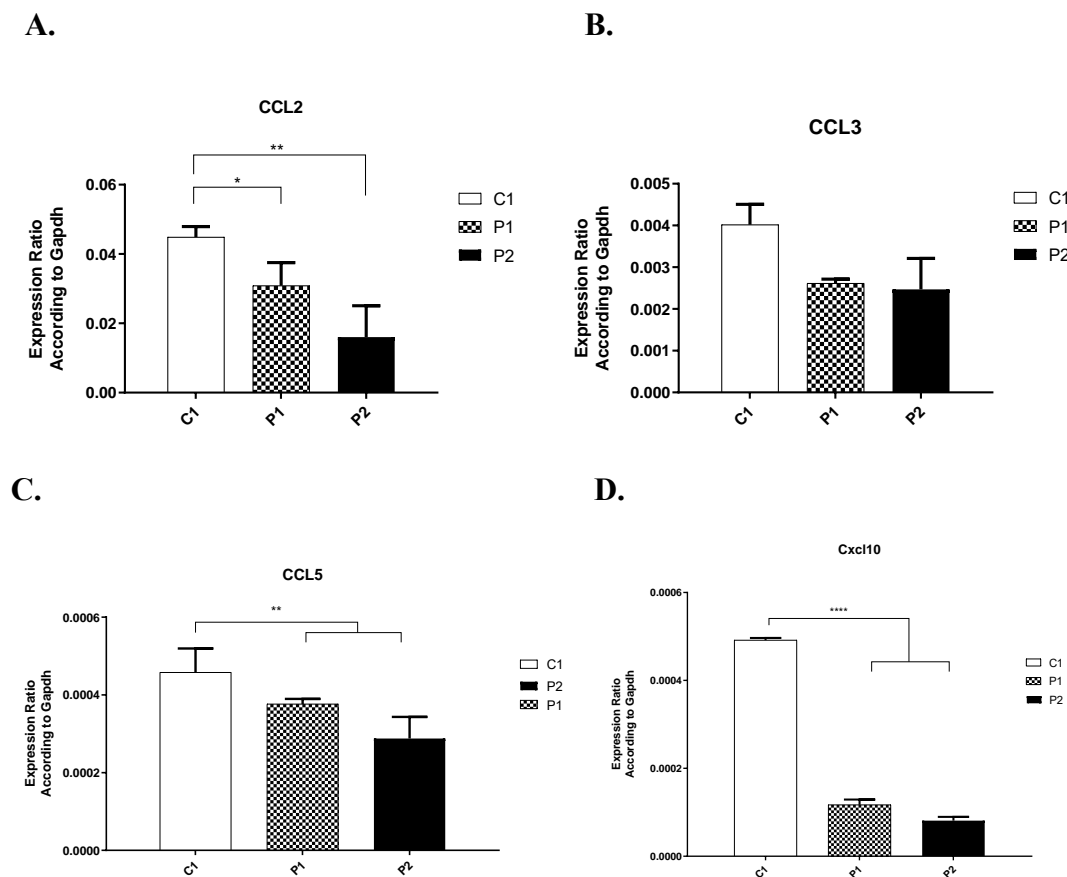


Figure 3.12. Gene expression ratio of Ccl2, Ccl3, Ccl5, and Cxcl10 in GM01719, GM02921, and GM01718 which are human fibroblast cell lines. GM01719 is called C1, control 1. GM02921 is counted as a P1, patient 1. GM01718 is counted as P2, patient 2 (C). Expression ratios were calculated with  $\Delta$ CT method and 2-way-ANOVA analysis was used to determine p-values by using GraphPad. Data were reported as means SEM (n=3, \*p<0,05, \*\*p<0,01, \*\*\*p<0,001).

In Figure 3.12, the Gene expression ratio of Ccl2, Ccl3, Ccl5, and Cxcl10 in GM01719, GM02921, and GM01718 which are human fibroblast cell lines was

determined and monitored. The expression ratio of *Ccl2* was significantly decreased for both *Neu1*<sup>-/-</sup> patient human fibroblasts compared to *WT* of human fibroblast results (Figure 3.12A). Also, the expression ratio of the *Ccl3* gene was monitored and no significant alteration was found in both patients' results in comparison with *WT* human fibroblast. Expression ratio according to the *Gapdh* was calculated for *CCL5* and there were significantly decreased *Ccl5* expression ratios in both *Neu1*<sup>-/-</sup> patient human fibroblasts compared to *WT* of human fibroblast results (Figure 3.12C). Lastly, the Expression ratio of *Cxcl10* was significantly decreased for both *Neu1*<sup>-/-</sup> patient human fibroblasts compared to *WT* of human fibroblast results (Figure 3.12D).

### 3.4. Western Blot

Western Blot analysis for inflammatory markers which are I $\kappa$ B- $\alpha$  and NF- $\kappa$ B were conducted to observe alterations in *Neu1*<sup>-/-</sup> and *WT* mouse fibroblasts and *Neu1*<sup>-/-</sup> patient and *WT* human fibroblasts. In Figure 3.13C, the antibody which is anti-I $\kappa$ B- $\alpha$  (1:1000, Cell Signaling Technology, 9242) was used with the anti- $\beta$ -actin (1:1000, Cell Signaling Technology, 13E5) to measure the I $\kappa$ B- $\alpha$  protein level in both 2-month-old and 5-month-old mouse fibroblasts of the *WT* and *Neu1*<sup>-/-</sup> (Figure 3.13C). In Figure 3.13D, NF- $\kappa$ B (1:1000, Cell Signaling Technology, D14E12) and anti- $\beta$ -actin (1:1000, Cell Signaling Technology, 13E5) were used to monitor alterations in 2-month-old and 5-month-old mice *WT* and *Neu1*<sup>-/-</sup> fibroblasts.  $\beta$ -actin was used as a housekeeping gene in both antibody measurements (Figure 3.13C and 3.13D). In Figure 3.13C, 2-month-old mouse fibroblasts I $\kappa$ B- $\alpha$  measurement did not change significantly compared to the *WT* however in 5-month-old *Neu1*<sup>-/-</sup> mouse fibroblasts were observed to significantly decreasing compared to 5-month-old *WT* in mouse fibroblasts (Figure 3.13C). Also, NF- $\kappa$ B and  $\beta$ -actin ratio was calculated, and the figure was monitored in Figure 3.13D. NF- $\kappa$ B expression ratio was significantly increased in 2-month-old *Neu1*<sup>-/-</sup> mouse fibroblasts compared to 2-month-old *WT* mouse fibroblasts, although there is no significant alteration was detected in between the 5-month-old *Neu1*<sup>-/-</sup> mouse fibroblasts and 5-month-old *WT* mouse fibroblasts for NF- $\kappa$ B expression ratio (Figure 3.13D). The representative Western Blot analysis for inflammatory detection orderly, GM01719, GM02921, and GM01718 which are human fibroblast cell lines was monitored in Figure 3.14. intensity of I $\kappa$ B- $\alpha$  for human *WT* and *Neu1*<sup>-/-</sup> fibroblast cells was analyzed and analysis of the intensity of NF-

$\kappa$ B for human *WT* and *Neu1*<sup>-/-</sup> fibroblast cells was also investigated in Figure 3.14C and Figure 3.14D. Intensity of I $\kappa$ B- $\alpha$  was determined as a significant decrease in patient 1 human fibroblast result compared to Control 1 of human fibroblast. However, no significant alteration was detected between Control 1 and Patient 2 human fibroblasts for the Intensity of I $\kappa$ B- $\alpha$  analysis. Moreover, analysis of the intensity of NF- $\kappa$ B for human *WT* and *Neu1*<sup>-/-</sup> fibroblast cells was determined as a significant elevation in P2 compared to Control1 human fibroblast cells. However, Patient 1 was not determined as a significant elevation or decrease compared to Control 1 human fibroblast. No alteration was detected between the C1 and P1 human fibroblasts (Figure 3.14D).

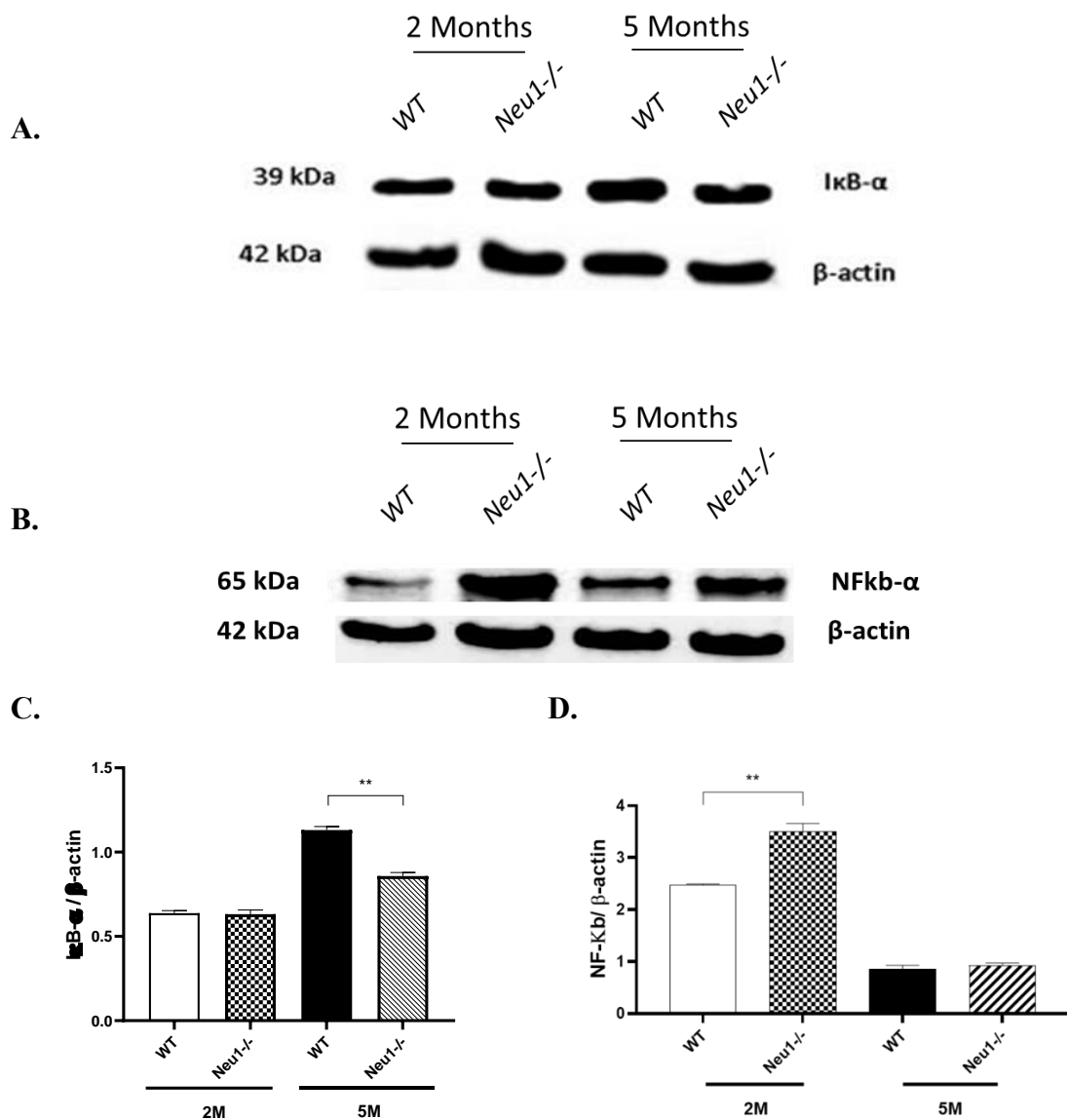


Figure 3.13. The representative Western Blot analysis for inflammatory detection of 2- and 5-month-old *WT* and *Neu1*<sup>-/-</sup> mice fibroblast cells. Analyses of immunoblot were monitored in Figure 3.12A for I $\kappa$ B- $\alpha$  and  $\beta$ -actin (A).

Analyses of immunoblot were monitored in Figure 3.12B for NF- $\kappa$ B and  $\beta$ -actin (B). Analysis of the intensity of I $\kappa$ B- $\alpha$  for 2- and 5-month-old *WT* and *Neu1*<sup>-/-</sup> mice fibroblast cells (C). Analysis of the intensity of NF- $\kappa$ B for 2-month (2M) and 5-month-old (5M) *WT* and *Neu1*<sup>-/-</sup> mice fibroblast cells (D).  $\beta$ -actin was used as a control. The intensity of each band was detected by using ImageJ and normalized to  $\beta$ -actin intensity. 2-way ANOVA analysis was used to determine p-values via GraphPad. Data were reported as means SE (n=3, \*p<0,05).

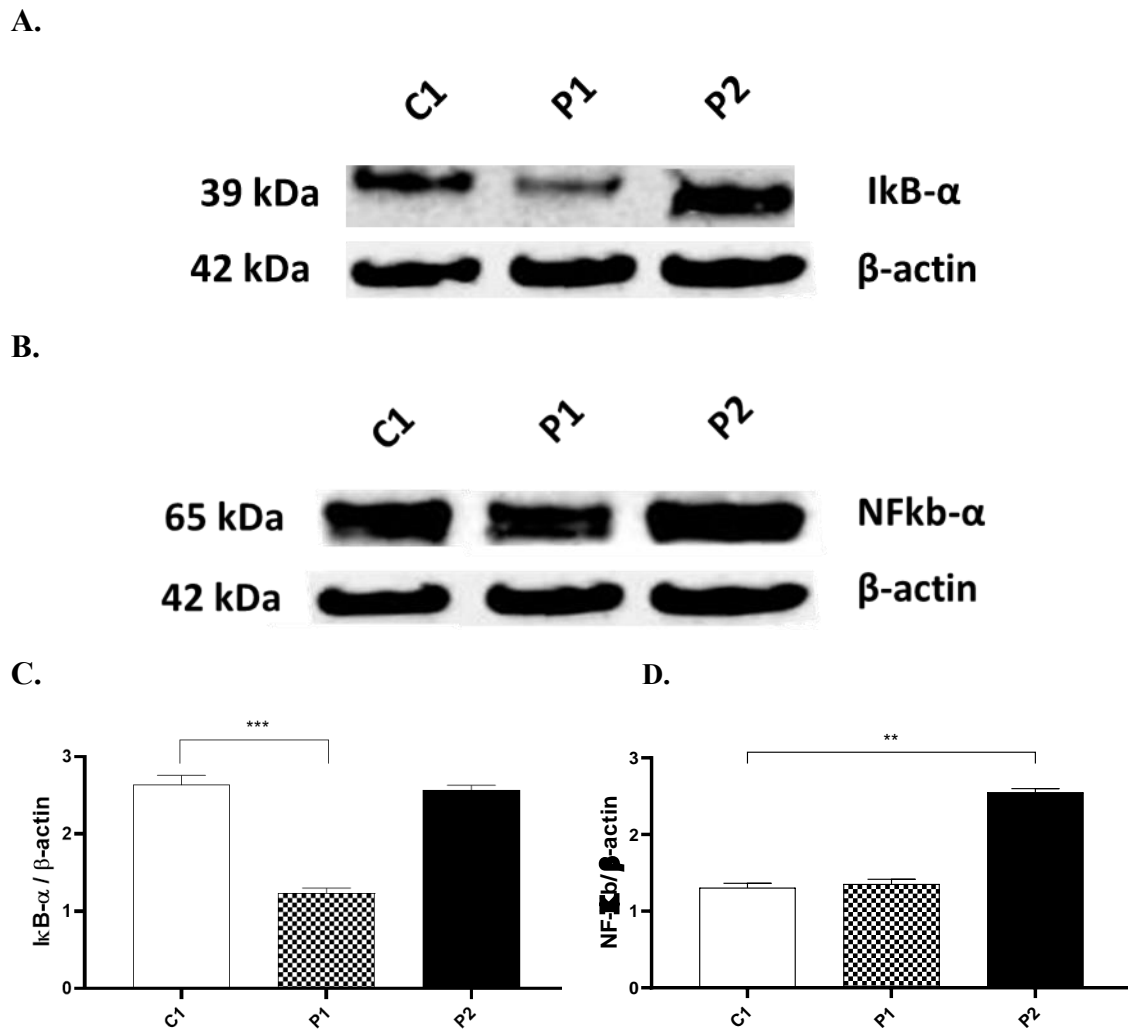


Figure 3.14. The representative Western Blot analysis for inflammatory detection of orderly, GM01719, GM02921, and GM01718 which are human fibroblast cell lines. One of the *WT* controls of the human fibroblast cell line from our laboratory used GM01719 is called C1, control 1. GM02921 is counted as a P1, patient 1. GM01718 is counted as P2, patient 2, these are human fibroblast cells. Analyses of immunoblot were monitored in Figure 3.13A for I $\kappa$ B- $\alpha$  and  $\beta$ -actin (A). Analyses of immunoblot were monitored in Figure 3.13B for NF- $\kappa$ B and  $\beta$ -actin (B). Analysis of the intensity of I $\kappa$ B- $\alpha$  for human *WT* and *Neu1*<sup>-/-</sup> fibroblast cells (C). Analysis of the intensity of NF- $\kappa$ B for human *WT* and *Neu1*<sup>-/-</sup> fibroblast cells (D).  $\beta$ -actin was used as a control. The intensity of each band was detected by using ImageJ and

normalized to  $\beta$ -actin intensity. 2-way ANOVA analysis was used to determine p-values via GraphPad. Data were reported as means SE (n=3, \*p<0,05).

### **3.5. Histological Analysis**

Histological analyses were conducted in mice and human fibroblasts to observe how lipids and oligosaccharides are altered in fibroblasts.

#### **3.5.1. Oil-Red-O Staining**

Oil-Red-O Staining was used to detect neutral lipids, lipoproteins, and cholesteryl esters. The staining method of Oil-Red-O has been used to monitor lipids of intracellular staining and staining of tissue because the dye has a permeability of cells, triglycerides, and neutral fats. The dye was observed after the staining with an orange-red tint.

There was an accumulation of neutral fats in 2-month *Neu1*<sup>-/-</sup> mouse fibroblasts compared to 2-month *WT* mouse fibroblasts and the accumulation of neutral fats was monitored in 5-month *Neu1*<sup>-/-</sup> mouse fibroblasts compared to 5-month *WT* mouse fibroblasts (Figure 3.15.). The accumulation of neutral fats according to the Oil-Red-O staining was observed in the sialidosis patient's fibroblasts compared to the Control 1 group in Figure 3.16. There is a slight increase in patient 1 and patient 2 human fibroblasts were monitored in comparison to Control 2 which is another control however it is a heterozygous of the *Neu1* sample.

#### **3.5.2. Periodic acid – Schiff Stain (PAS) Staining**

Periodic acid–acid–Schiff stain (PAS) staining was conducted to monitor the accumulation of Glycosphingolipid. To monitor the metabolism of glycolipid alterations in 2-month-old (2M) and 5-month-old (5M) *WT*, *Neu1*<sup>-/-</sup> mouse fibroblasts and *WT* and patient sialidosis human fibroblasts Periodic acid – Schiff Stain (PAS) staining was conducted.

There was an accumulation of glycoconjugates which are oligosaccharides in 2-month-old *Neu1*<sup>-/-</sup> mouse fibroblasts compared to 2-month-old *WT*, and this accumulation was detected and monitored in 5-month-old *Neu1*<sup>-/-</sup> mouse fibroblasts

compared to 5-month-old *WT* mouse fibroblasts. Glycoconjugate accumulation was monitored in some regions of both mice *Neu1*<sup>-/-</sup> cells (Figure 3.15). Periodic acid - Schiff Stain (PAS) staining in human fibroblast samples which are orderly, one of the human control fibroblasts from our laboratory as a Control 1, also GM01719, GM02921, and GM01718 which are human fibroblast cell lines. There was an accumulation of glycoconjugates which are oligosaccharides was monitored more intensely in human patient's fibroblast cell lines compared to Control of the human fibroblast cell samples (Figure 3.16).

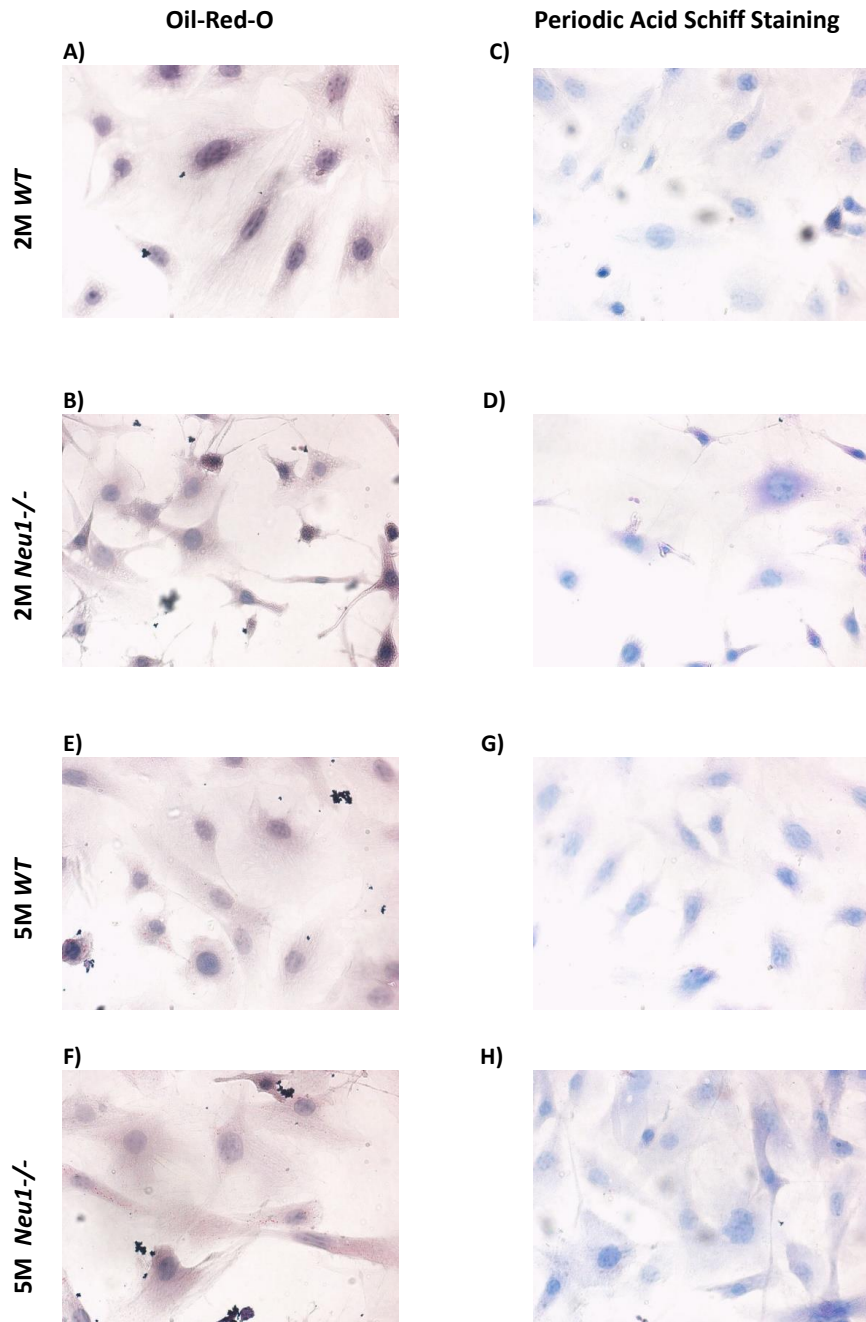


Figure 3.15. Oil-Red-O staining and Periodic acid-Schiff stain (PAS) staining in 2-month-old WT, *Neu1*<sup>-/-</sup> mice fibroblast samples (Figure 3.15A, B, C and D), and 5-month-old WT, *Neu1*<sup>-/-</sup> mice fibroblast samples (Figure 3.15E, F, G and H). Images were taken at 40X magnification by Olympus light microscope.

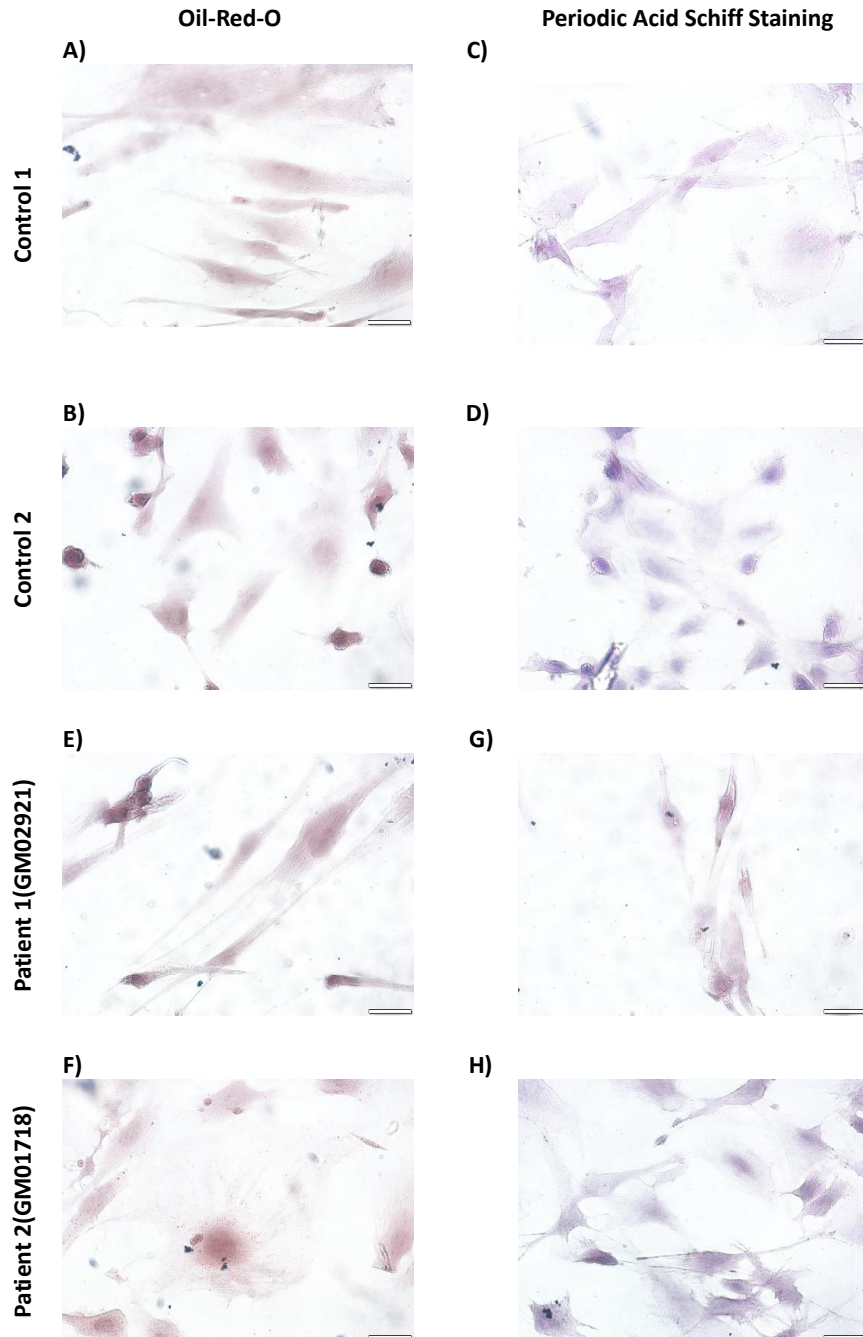


Figure 3.16. Oil-Red-O staining and Periodic acid - Schiff Stain (PAS) staining in human fibroblast samples which are orderly, one of the human control fibroblasts from our laboratory as a Control 1, also GM01719, GM02921, and GM01718 which are human fibroblast cell lines. One of the *WT* controls of the human fibroblast cell line from our laboratory used GM01719 is called C2, control 2. GM02921 is counted as a P1, patient 1. GM01718 is counted as P2, patient 2, these are human fibroblast cells (Figure 3.15A, B, C, D, E, F, G, and H). Images were taken at 40X magnification by Olympus light microscope.

## CHAPTER 4

### DISCUSSION

Terminal sialic acids from gangliosides were removed by Neuraminidases. Gangliosides can be described as one or more sialic acids containing the chain of glycan within glycosphingolipids. These molecules are crucially important for some biological processes in the membrane of cell plasma (Komura et al. 2017). Neu1 sialidase in lysosomes has a mission to degradation of sialoglycoconjugates and their catabolism (Frisch and Neufeld 1979). Sialidase of Neu1 generally was targeted to the oligosaccharides and glycopeptides for substrate and it has an important impact on glycolipid catabolism (Smutova et al. 2014). Neu1 sialidase is formed with two other lysosomal molecules which are lysosomal protective protein Cathepsin A (PPCA) and  $\beta$ galactosidase ( $\beta$ -Gal) (Van der Horst et al. 1989). Stabilization of glycosidase is supported by lysosomal protective protein Cathepsin A (PPCA). Galactosialidosis which is another lysosomal storage disorder because of the lack of protective protein Cathepsin A was investigated (Zammarchi et al. 1996). Because of the mutations in the genes, lysosomal storage disorders (LSDs) have occurred, and these rare diseases are also counted as metabolic hereditary diseases (R. Y. Wang et al. 2011). Deficiency of lysosomal enzymes such as hydrolases or protein of activator or transporter in the lysosome can cause the specific accumulations which are glycoproteins, glycosaminoglycans, glycosphingolipids and other lipids in lysosomes (Ferreira and Gahl 2017). Moreover, Sialidosis can be described as a lysosomal storage disorder which is caused by the Neu1 Sialidase deficiency. There are types of variants observed for sialidosis. These are Type I and Type II variants which are differentiated linking to the age of onset and the severity of the diseases (Seyrantepe et al. 2003). Sialidosis is described as a systematic disorder and there has not been any absolute therapy for sialidosis patients. One of the most detectable parts of sialidosis is the described accumulation of oligosaccharides which are sialylated in tissues. Also, sialylated oligosaccharides which are accumulated substances can be found in the urines or body fluids (VAN PELT et al. 1988). The model of the sialidosis disorder in mice was first created by d'Azur et al. 2002 to support the role of the Neu1 gene in physiological and

cellular mechanisms. The *Neu1* deficient mice which are nullizygous for the *Neu1* locus demonstrated very similar symptoms which are monitored also in sialidosis patients. This model of the mice is like the early onset of sialidosis which is Type II sialidosis. This model of sialidosis has nephropathy, edema, enlargement of the spleen, impairment of the neurological system, oligosaccharides in the extraction of urinary, hematopoiesis, and spine impairment were monitored as same as sialidosis patients and *Neu1* deficient mice model (Pedersen et al. 2002). Moreover, the accumulation of oligosaccharides can be linked to the accumulation of secondary lipid metabolism. Because sialic acid is linked to the glycolipid and glycoproteins (Mohammad et al. 2018). However, the role of the secondary lipid accumulations in sialidosis and the link between the secondary lipid accumulations and inflammation has not been elucidated in sialidosis in vitro research and fibroblasts. Within the whole picture of this thesis study, an investigation of biomarkers using lipidome-based research analysis was conducted to observe the link between secondary lipid accumulation and inflammation in sialidosis. Mice models and human sialidosis patients' fibroblasts were used to monitor any alterations in these inflammation-related biomarkers. In correlation with this purpose, all samples of the fibroblasts were analyzed in shotgun lipidome analysis, and different secondary lipid alterations were detected (A. Wang et al. 2023). In this thesis study, two groups of age mice which are 2- and 5-month-old *Neu1*<sup>-/-</sup> samples were used, and three different human fibroblast samples were used. Both mice and human fibroblast samples were investigated to comprehend whether the link between the inflammatory markers and secondary lipid alterations is related to also age of the patients in the physiological and cellular mechanisms of sialidosis.

Accumulation of sialylated oligosaccharides in the cells of the sialidosis patient cannot be digested and the response of the inflammation can occur as a chronic inflammation and is continued because of this accumulation and deposition of substrates. For comprehending each lysosomal storage disease, the connection between the pathogenesis of disease and secondary lipid accumulations plays a critical role in the understanding of all aspects of the disorders (Steven U. Walkley and Vanier 2009).

According to the lipid results in both mice and human fibroblasts, Lysophosphatidylcholine (LPC) and lysophosphatidic acid (LPA) which are lysophospholipids were found to a significantly elevated in *Neu1*<sup>-/-</sup> samples compared to the *WT* samples (Figure 3.2 and Figure 3.3). This was supported by the literature that the two most common lysoglycerophospholipids, lysophosphatidylcholine (LPC) and

lysophosphatidic acid (LPA), are beginning to emerge as a new class of inflammatory lipids (Sevastou et al. 2013). Membrane-derived phospholipids known as lysophospholipids can be monitored from either homeostatic lipid metabolism or from cellular activation triggered by stimuli. These lipids are conducted with the lack of one of the two fatty acid chains that are connected to the backbone of glycerol to shape a phospholipid. They possess' specific importance because they reflect their role as a messenger molecule to create cellular responses(Moolenaar and Hla 2012). LPA has been monitored to see that it has a tremendous impact on the survival of cells, cell proliferation, pain, cancer, metabolic syndromes, or inflammation.

The level of Lysophosphatidylinositol (LPI) is related to inflammatory responses such as activation of macrophages and inflammation because LPI is counted also as a bioactive lipid which is monitored in several cellular and physiological mechanisms and pathways such as migration, tumorigenesis, and proliferation of cells or another role of LPI is monitored in such disorders related to obesity and metabolism(Masquelier et al. 2018). According to the literature and lipidome results, LPI results of the thesis showed that LPI is related to inflammation because LPI is elevated in both human and mouse fibroblasts compared to *WT* samples (Figure 3.2 and Figure 3.3).

The level of Lysophosphatidylethanolamines (LPE) was detected as increased compared to the *WT* of both mice and human fibroblast samples (Figure 3.2 and Figure 3.3) and LPE is related to the differentiation of cellular processes, cellular migration of the neuronal cells, and LPE is related to the different cell of cancers(J. Wu et al. 2022).

Hexosylceramides are contained in the group of cerebrosides within the sphingolipids. They are involved in the complex glycosphingolipid biosynthesis such as gangliosides. Moreover, HexCer has different important roles in cellular function such as integrated into the membrane of cells or lipid rafts. The level of glycerolipids was also analyzed (Figure 3.4). It was demonstrated that HexCer levels in 2-month-old mice fibroblast and human fibroblast *Neu1* samples were elevated compared to the *WT* samples however for 5-month-old mice fibroblast samples, there is no alteration between the *Neu1*<sup>-/-</sup> and *WT* sample detected. Some of the lipids such as HexCer correlated with some of the alterations in inflammatory markers(A. Wang et al. 2023).

Cholesteryl esters (CE) are the members of the group of cholesterol lipids which also belong to the sterol lipids. The structure of the CE possesses cholesterol which is connected to the steroid structure and fatty acid. They have a role as a pool for storing cholesterol in cells in lipid droplets to synthesize hormones. It was demonstrated that

Cholesteryl esters (CE) which is sterol lipid was elevated in *Neu1* samples of 2-month-old and 5-month-old mice fibroblast results compared to *WT* of mice results. Also, one of the human patient results was monitored as an increase compared to the Control of the human sample for CE (Figure 3.5). In a nutshell, secondary lipid alterations are related to the inflammatory markers in sialidosis.

Real-time PCR with the QPCR array of chemokines and cytokines was performed to monitor whether the link between the expression ratio of cytokines and chemokines is related to the secondary lipid alterations in sialidosis. According to the lipidome profile of mice and human fibroblast samples, glycerophospholipid, glycerolipid, and sterol lipid accumulations were reported. Continued and linked to these results, the QPCR array of chemokines and cytokines showed that there is a link between the alteration of inflammatory markers and secondary lipid alterations. Our study is also supported by literature in which Gaucher disease is one of the lysosomal storage disorders linked to inflammation (Simonaro 2016). Our study demonstrated the expression of chemokines, interleukins, TNF receptor family members, interferons, growth factors, and other cytokines in both mice and human fibroblasts. Moreover, to support this QPCR array of chemokines and cytokines data, a Real-Time PCR experiment was conducted with some of the gene's primers. These genes are *Ccl2*, *Ccl5*, and *Cxcl10* for 2-month-old and 5-month-old *WT* and *Neu1*<sup>-/-</sup> mouse fibroblasts samples, and *Ccl2*, *Ccl3*, *Ccl5*, and *Cxcl10* gene primers were used to investigate expression ratio of these genes in human fibroblast samples which are orderly, GM01719, GM02921 and GM01718 which are human fibroblast cell lines. GM01719 is called C1, control 1. GM02921 is counted as a P1, patient 1. GM01718 is counted as P2, patient 2. In this thesis study, it was monitored that in Figure 3.6 2- and 5-month-old *WT* and 2- and 5-month-old *Neu1*<sup>-/-</sup> mice fibroblast expression ratios according to the housekeeping genes were compared. Moreover, *Ccl11*, *Ccl5*, *Cxcl11*, *Cxcl16* was significantly increased in both 2-month-old and 5-month-old *Neu1*<sup>-/-</sup> results compared to the *WT* of each 2-month-old and 5-month-old *Neu1*<sup>-/-</sup> results of mouse fibroblasts. *Ccl11* plays a crucial role in pro-inflammatory pathways especially because it supports and promotes the senescence of cellular mechanisms in humans and aging (Ivanovska et al. 2020). *Ccl5* has a tremendous impact on cellular homeostasis, proliferation of oligodendrocytes, neuronal and glial communication of cells and it is counted as an inflammatory cytokine (Lanfranco et al. 2018). *Cxcl11* also plays an important role in regulating immune response and inflammatory responses. The chemokine (C-X-C motif) ligand 1 can be described as a chemoattractant for different

types of immune cells, specifically neutrophils(Jerva, Sullivan, and Lolis 1997). Cxcl16 can be moved with its receptor which is Cxcr6. Cells that produce Cxcl16 containing dendritic cells which are also found in the T-cell of lymphoid organs and these cells can be detected in the spleen(Matloubian et al. 2000). Also, the correlation between the Cxcr6 and Cxcl16 has a tremendous impact on NKT cell activation and its homeostasis, this correlation also supports inflammation and fibrosis of liver(Wehr et al. 2013). Cxcl16 plays a critical role in supporting to take of different kinds of chemotaxis and pathogens of NKT and T cells by representing these cells directly to its domain of chemokines. According to the human fibroblast chemokine results, elevation was detected in Ccl11, Cxcl11, and Cxcl16 gene expression levels in both human and mice 2-month-old and 5-month-old fibroblast compared to healthy fibroblasts. In human samples, patient 1 and patient 2 results of chemokines were reported differently in some gene expression levels. The reason can be described in each patient's gene and environmental conditions history can vary this differentiation of chemokine and cytokine gene expressions. It was affected from patient to patient because inflammation can depend on different parameters such as environmental factors(Bachmann et al. 2020). On the other hand, interestingly Ccl17 gene expression ratio was decreased in both 2- and 5-month-old mice and human patient fibroblast results compared *WT* of each sample. Ccl17 was found in the literature to be a requirement for inducing intestinal inflammation(Eraza et al. 2021). This data can be explained as a sample used in this experiment, fibroblast samples were conducted, and the chemokine and cytokine ratio can vary compared to in vivo experiments. Because of that reason, some of the chemokine variation can be explained by using fibroblasts in vitro experiments.

The interleukins expression ratio of both mice and human fibroblasts was demonstrated in Figure 3.7. The role of interleukins in inflammation can be described as a modulation of growth, activation, and differentiation responses of immunity. Interleukins contain huge amounts of proteins that can provide and support many interactions in cells and tissues side by side while affecting cell surface receptor binding affinity. Interleukins have a tremendous impact on immune cell differentiation and activation and adhesion, proliferation, migration, and maturation(Brocker et al. 2010). According to both mice and human fibroblast Real-Time PCR array results, only IL11 was significantly increased in *Neu1*<sup>-/-</sup> samples compared to the WT. In the literature, it was demonstrated that an increased level of IL-11 expression is linked with the pathology of different types of diseases. IL-11 can be monitored in some inflammatory diseases such

as Asthma, Inflammatory Bowel Disease (IBD), Arthritis, and Multiple sclerosis (Fung et al. 2022). The apparent or prominent role of IL-11 was demonstrated in inflammatory diseases through literature. On the other hand, IL12b, IL17a, and IL4 gene expression ratios interestingly and significantly decreased in *Neu1*<sup>-/-</sup> samples in both mice and human fibroblasts compared to *WT* of each other. IL12b was produced because of microbial or bacterial infections. Early stage of these infections, IL12b is used to proliferate NK and T cells of IFN- $\gamma$  which supports to activation of phagocytic cells and inflammation normally(Trinchieri 1995). IL17a has an impact on the regulation of immune functions via pro-inflammatory cytokines and chemokine generation and promotion of these chemokines and cytokines. IL17a is also followed by the interaction of macrophages and neutrophils at the site of inflammation(Jin and Dong 2013). Studies of IL-4 have revealed that it has a diverse role in disease pathogenesis, and it can be included in different and very alternatively regulator pathways(Luzina et al. 2012).

Interferons are linked to the cytokines which are especially described by their ability to benefit against infections of viruses and gaining resistance to viral infections(Ott and Ealy 2018). In this thesis study, it was demonstrated that Interferon-alpha and IFN- $\gamma$  were investigated and interestingly 2-month-old *Neu1*<sup>-/-</sup> mice and human patients' fibroblast sample results were decreased compared to *WT* of mice and human fibroblasts. However, in 5-month-old *Neu1*<sup>-/-</sup> mouse fibroblasts interferon results showed that interferon expression levels are increased compared to *WT* of 5-month-old mouse fibroblasts. Interferon-gamma (IFN- $\gamma$ ) and IL12b expression levels are correlated with each other and the low level of expression for IFN- $\gamma$  can be explained because of the low level of expression of IL12b for human fibroblasts and 2-month-old mouse fibroblasts. On the other hand, 5-month-old mice are phenotypically more severe than 2-month-old mice so according to the age, interferon expression ratio can vary because of the gradually increasing accumulation in sialidosis for mice.

Tnf receptor family members were investigated within this thesis study. It was reported that the *Tnfsf11* gene was decreased in both human and mouse fibroblasts of *Neu1*<sup>-/-</sup> samples compared to *WT*. The *Tnfsf11* gene plays an important role in encoding receptor activator of nuclear factor - $\kappa$ B (NF- $\kappa$ B) ligand (Guerrini et al. 2015). Also, *Tnfsf11* has an impact on the response of T cell-dependent immunity regulation and the protein which is expressed by this gene plays a critical role in the dendritic cell survival factor(Onal et al. 2016).

Growth factors were monitored in this study. Genes that are all related to the growing processes were investigated for both mice and human fibroblasts. According to our study, the OSM gene was monitored for expression ratio which was decreased. The level of the OSM gene is related to the IL-6 subfamily and it belongs to these chemokines. Oncostatin M (OSM) shows both anti-inflammatory effects and pro-inflammatory effects in cellular activities (Dumas et al. 2012). In the literature, OSM gene expression is linked to the reduction of IL-1 $\beta$  secretion and reduction of Cxcl8 expression, although it impacts the elevation of Ccl2 and IL-6 (Dumas et al. 2012). Because OSM is linked with the reduction of IL-1 $\beta$  and TNF- $\alpha$  which are pro-inflammatory cytokines, it plays a crucial role in the anti-inflammatory role, and its reduction in both human and mouse fibroblasts in our results showed that reduction in the OSM gene can correlate with the increase of inflammation in both human and mouse fibroblasts.

Other cytokines which are Adipoq, Ctf1, Spp1, and Tgfb2, and more cytokines were investigated under this topic. According to the results of the study, the Adipoq gene expression ratio was found that it was increase in both 5-month-old mouse fibroblasts and both human patients' fibroblasts compared to the *WT* of these fibroblasts however it was found a decrease in 2-month-old *Neul*<sup>-/-</sup> mouse fibroblasts compared to 2-month-old *WT* mouse fibroblasts. The Adipoq gene is expressed mostly and extremely in adipose tissues. This gene encodes a protein adiponectin which has an important impact on the breakdown of fatty acids and glucose level regulations(Ouchi and Walsh 2007). It is produced primarily in the tissue of adipose moreover, muscle, and brain. The results from the thesis monitored that the elevation of the Adipoq gene expression ratio mentioned above the inflammatory responses because the adipoq gene has an anti-inflammatory effect according to the literature and fibroblasts can react and produce more expression for the Adipoq gene to prevent and diminish inflammation via trying to decrease of inflammation.

The accumulation of complex sugars such as polysaccharides, glycoproteins, and glycolipids was detected using PAS staining. Previous studies have shown that several lysosomal storage disorders are associated with increased levels of glycosphingolipids, glycolipids, and secondary substances such as oligosaccharides. An overabundance of these compounds has been shown to disrupt the central nervous system, resulting in neurodegeneration in those with lysosomal storage disorders. For example, in the Pompei disease, it was investigated that there is a glycogen accumulation(Kamphoven et al. 2004), one of the other lysosomal storage disorders which is GM1 gangliosidosis also

investigated and glycosphingolipid accumulation in the cerebral cortex was monitored in this lysosomal storage disorder according to the literature (Breiden and Sandhoff 2020). In these investigations, PAS staining was already conducted. In this research, PAS staining was used for the investigation of accumulated glycoconjugates in both mice and human fibroblasts to comprehend the impact of potential accumulation of glycoconjugates on the cellular and structural alteration in fibroblasts and their survival rates. Our results indicated that the accumulation of glycoconjugates was monitored at any age of the mice fibroblast compared to *WT* mouse fibroblasts. In the *Neu1*<sup>-/-</sup> mouse fibroblasts, accumulation of a high amount of the glycoconjugate can be the result of the complex oligosaccharide accumulation and Neu1 sialidase substrates which are over-sialylated. The same type of accumulation for PAS staining was also observed in human patient fibroblasts compared to the human control fibroblasts. Histological staining of the PAS was indicated for human fibroblasts and the ratio of the accumulated glycoconjugates for patient human fibroblasts is elevated.

To comprehend lipid accumulations in mice and human fibroblasts, Oil-Red-O staining was performed. This dye which is Oil-Red-O can be soluble in fat molecules and attach to neutral lipids, cholesteryl esters, and lipoproteins (Bharati et al. 2022). According to figures 3.15 and figure 3.16, *Neu1*<sup>-/-</sup> mouse fibroblasts and human patient fibroblasts were observed for accumulation of neutral lipids or cholesterols compared to the *WT* fibroblasts results in these figures.

According to the literature, secondary accumulations for different molecules such as glycoaminoacids, and oligosaccharides have been published in different lysosomal storage disorders which are coming from the lysosomal enzyme deficiency, sialidases or hydrolases (Wraith and Imrie 2009). Moreover, oligosaccharide accumulation in the extracts of the urinary mixture was interpreted as a disease of the deficiency of the Neu1 gene also in other lysosomal storage disorders such as mucopolysaccharidosis or mannosidosis, there are also such accumulations which are glycosaminoglycans and glycoproteins in urinary samples, orderly (Xia et al. 2013). Lipidome analysis was conducted to reveal how secondary lipid alterations are affected in fibroblasts of *Neu1*<sup>-/-</sup> mice and human patient fibroblasts compared to the *WT* of mice and human fibroblasts. Different genotypes of mice were investigated to monitor patterns of the lipids in sialidosis. It was already published in the literature that there is a sialylated oligosaccharide accumulation in the urinary extract of sialidosis patients (Van Pelt et al. 1988). This accumulation can be linked to other secondary lipid accumulations and in

this research, an investigation of biomarkers using lipidome-based research analysis was conducted to find and reveal a link between the secondary lipid alterations and inflammation due to the sialidosis disease.

## CHAPTER 5

### CONCLUSION

Lysosomal Neu1 sialidase deficiency is the reason for Sialidosis which is a lysosomal storage disorder. Lysosomal Neu1 sialidase has a critical role in removing the residues of sialic acids which are found in sialoglycoconjugates. Oligosaccharide accumulation in the patient's urinary mixture is the most common and significant part of identifying this disease in patients. Also, ganglioside accumulations in different visceral organs are the main and most common identification point for sialidosis patients. In this study, the investigation of biomarkers using lipidome-based research analysis was conducted for the first time for in vitro and especially fibroblasts of the sialidosis for both mice and human fibroblasts. The link between the secondary lipid alterations and inflammation is our main idea to investigate and monitor under the condition of Neu1 gene deficiency. According to the results of Figure 3.2 and Figure 3.3, glycerophospholipid alterations were determined and the elevation in these lipids according to the sialidosis can result in the inflammatory response of the fibroblasts in vitro situation. According to the real-time PCR results, some of the pro-inflammatory chemokines are detected as elevated which are Ccl11, Cxcl1, and Cxcl16. Western blot and RT-PCR analysis for inflammatory markers monitored altered levels of expression in both mice and human fibroblasts. Although these inflammatory markers have been monitored in previously different lysosomal storage disorders, this research is the first study that provides the comprehension of specific expression levels of the inflammatory genes and their interaction with the secondary lipid alterations in fibroblasts of *Neu1*<sup>-/-</sup> human and mice samples.

The impact of the lipid alterations and metabolism of lipids on fibroblasts was investigated by histological staining which is Periodic acid–acid–Schiff stain (PAS) staining and Oil-Red-O staining to visualize lipid alteration between the fibroblasts of *Neu1*<sup>-/-</sup> human and mice samples. As a result of all analyses that we conducted at the level of gene and protein expression analysis and lipidomic analysis, the link between inflammation and secondary lipid alteration was investigated. According to the results of

this study, the correlation between inflammation and secondary lipid alteration was observed.

## 5.1. Future Directions

To completely comprehend the role of the *Neu1* gene in the link between inflammation and secondary lipid alterations, *in vivo*, experiments can be conducted. Also, according to the literature extensive vacuolization was monitored in the cell of epithelial in the *Neu1*<sup>-/-</sup> mice brain ((Pedersen et al. 2002). Because of the sialidosis also observed that degeneration in the macrophages and microglia cells can cause neurodegeneration and neuroinflammation. Comprehensive studies with *in vivo* experiments can reveal how neuroinflammation and neurodegeneration mechanisms proceed in several brain regions. Moreover, collecting information from both *in vitro* and *in vivo* experiments about inflammation and secondary lipid alterations can lead to the discovery of a therapeutic approach to ameliorate sialidosis. From this study, we found that there is a specific lipid molecule that is elevated in both mice and human fibroblasts of sialidosis patients compared with the *WT* fibroblasts. Coming from these results, these lipids can be chosen as a target to diminish inflammation via inhibitors of these specific lipids. Although these lipids are secondary accumulations that result from the disorder, there can be strong connections between inflammation. Inflammation and inflammatory responses are critical to balancing homeostasis in the human body. According to the literature, sialidosis is a systematic lysosomal storage disorder and it has a critical impact on visceral organs such as the kidney, liver, and spleen (Seyrantepe et al. 2003).

In a nutshell, all the details comprehensively how the *Neu1* gene impacts lipid alterations in mice and human fibroblasts may help to provide new therapeutic approaches and new target genes to diminish inflammation in sialidosis and that targeted lipid pathways with the inhibitors can support to ameliorate sialidosis.

## REFERENCES

- Bachmann, María Consuelo, Sofía Bellalta, Roque Basoalto, Fernán Gómez-Valenzuela, Yorschua Jalil, Macarena Lépez, Anibal Matamoros, and Rommy von Bernhardt. 2020. "The Challenge by Multiple Environmental and Biological Factors Induce Inflammation in Aging: Their Role in the Promotion of Chronic Disease." *Frontiers in Immunology*. <https://doi.org/10.3389/fimmu.2020.570083>.
- Bharati, Shikha, Km Anjaly, Shivani Thoidingjam, and Ashu Bhan Tiku. 2022. "Oil Red O Based Method for Exosome Labelling and Detection." *Biochemical and Biophysical Research Communications* 611. <https://doi.org/10.1016/j.bbrc.2022.04.087>.
- Breiden, Bernadette, and Konrad Sandhoff. 2020. "Mechanism of Secondary Ganglioside and Lipid Accumulation in Lysosomal Disease." *International Journal of Molecular Sciences* 21 (7). <https://doi.org/10.3390/ijms21072566>.
- Brocker, Chad, David Thompson, Akiko Matsumoto, Daniel W. Nebert, and Vasilis Vasiliou. 2010. "Evolutionary Divergence and Functions of the Human Interleukin (IL) Gene Family." *Human Genomics* 5 (1). <https://doi.org/10.1186/1479-7364-5-1-30>.
- Castaneda, Julian A., Ming J. Lim, Jonathan D. Cooper, and David A. Pearce. 2008. "Immune System Irregularities in Lysosomal Storage Disorders." *Acta Neuropathologica*. <https://doi.org/10.1007/s00401-007-0296-4>.
- Coutinho, Maria Francisca, Liliana Matos, and Sandra Alves. 2015. "From Bedside to Cell Biology: A Century of History on Lysosomal Dysfunction." *Gene* 555 (1). <https://doi.org/10.1016/j.gene.2014.09.054>.
- CUMINGS, J.N. 1962. "Abnormalities in Lipid Metabolism in Two Members of a Family with Niemann-Pick Disease." In *Cerebral Sphingolipidoses*. <https://doi.org/10.1016/b978-1-4831-9648-0.50018-3>.
- Dumas, Aline, Stéphanie Lagarde, Cynthia Laflamme, and Marc Pouliot. 2012. "Oncostatin M Decreases Interleukin-1  $\beta$  Secretion by Human Synovial Fibroblasts and Attenuates an Acute Inflammatory Reaction in Vivo." *Journal of Cellular and Molecular Medicine* 16 (6). <https://doi.org/10.1111/j.1582-4934.2011.01412.x>.
- Erazo, Anna B., Nancy Wang, Lena Standke, Adrian D. Semeniuk, Lorenz Fülle, Sevgi C. Cengiz, Manja Thiem, Heike Weighardt, Richard A. Strugnell, and Irmgard Förster. 2021. "CCL17-Expressing Dendritic Cells in the Intestine Are Preferentially Infected by Salmonella but CCL17 Plays a Redundant Role in Systemic Dissemination." *Immunity, Inflammation and Disease* 9 (3). <https://doi.org/10.1002/iid3.445>.
- Ferreira, Carlos R., and William A. Gahl. 2017. "Lysosomal Storage Diseases." In *Metabolic Diseases: Foundations of Clinical Management, Genetics, and Pathology*, 367–440. IOS Press. <https://doi.org/10.3233/978-1-61499-718-4-367>.

- Frisch, Amos, and Elizabeth F. Neufeld. 1979. "A Rapid and Sensitive Assay for Neuraminidase: Application to Cultured Fibroblasts." *Analytical Biochemistry* 95 (1). [https://doi.org/10.1016/0003-2697\(79\)90209-4](https://doi.org/10.1016/0003-2697(79)90209-4).
- Fung, Ka Yee, Cynthia Louis, Riley D. Metcalfe, Clara C. Kosasih, Ian P. Wicks, Michael D.W. Griffin, and Tracy L. Putoczki. 2022. "Emerging Roles for IL-11 in Inflammatory Diseases." *Cytokine* 149. <https://doi.org/10.1016/j.cyto.2021.155750>.
- Gordon, Simon. 2003. "Alternative Activation of Macrophages." *Nature Reviews Immunology*. <https://doi.org/10.1038/nri978>.
- Guerrini, Matteo M., Kazuo Okamoto, Noriko Komatsu, Shinichiro Sawa, Lynett Danks, Josef M. Penninger, Tomoki Nakashima, and Hiroshi Takayanagi. 2015. "Inhibition of the TNF Family Cytokine RANKL Prevents Autoimmune Inflammation in the Central Nervous System." *Immunity* 43 (6). <https://doi.org/10.1016/j.immuni.2015.10.017>.
- Harzer, K., W. Schlote, J. Peiffer, H. U. Benz, and A. P. Anzil. 1978. "Neurovisceral Lipidosis Compatible with Niemann-Pick Disease Type C: Morphological and Biochemical Studies of a Late Infantile Case and Enzyme and Lipid Assays in a Prenatal Case of the Same Family." *Acta Neuropathologica* 43 (1–2). <https://doi.org/10.1007/BF00685003>.
- Hawkins-Salsbury, Jacqueline A., Adarsh S. Reddy, and Mark S. Sands. 2011. "Combination Therapies for Lysosomal Storage Disease: Is the Whole Greater than the Sum of Its Parts?" *Human Molecular Genetics* 20. <https://doi.org/10.1093/hmg/ddr112>.
- Horst, G. T.J. Van der, N. J. Galjart, A. D'Azzo, H. Galjaard, and F. W. Verheijen. 1989. "Identification and in Vitro Reconstitution of Lysosomal Neuraminidase from Human Placenta." *Journal of Biological Chemistry* 264 (2). [https://doi.org/10.1016/s0021-9258\(19\)85088-3](https://doi.org/10.1016/s0021-9258(19)85088-3).
- Ivanovska, Mariya, Zakee Abdi, Marianna Murdjeva, Danielle Macedo, Annabel Maes, and Michael Maes. 2020. "Ccl-11 or Eotaxin-1: An Immune Marker for Ageing and Accelerated Ageing in Neuro-Psychiatric Disorders." *Pharmaceuticals*. <https://doi.org/10.3390/ph13090230>.
- Jerva, L. Fred, Gail Sullivan, and Elias Lolis. 1997. "Functional and Receptor Binding Characterization of Recombinant Murine Macrophage Inflammatory Protein 2: Sequence Analysis and Mutagenesis Identify Receptor Binding Epitopes." *Protein Science* 6 (8). <https://doi.org/10.1002/pro.5560060805>.
- Jeyakumar, M., R. Thomas, E. Elliot-Smith, D. A. Smith, A. C. Van der Spoel, A. D'Azzo, V. Hugh Perry, T. D. Butters, R. A. Dwek, and F. M. Platt. 2003. "Central Nervous System Inflammation Is a Hallmark of Pathogenesis in Mouse Models of GM1 and GM2 Gangliosidosis." *Brain* 126 (4). <https://doi.org/10.1093/brain/awg089>.
- Jin, Wei, and Chen Dong. 2013. "IL-17 Cytokines in Immunity and Inflammation." *Emerging Microbes and Infections*. <https://doi.org/10.1038/emi.2013.58>.

- Jmoudiak, Marina, and Anthony H. Futerman. 2005. "Gaucher Disease: Pathological Mechanisms and Modern Management." *British Journal of Haematology*. <https://doi.org/10.1111/j.1365-2141.2004.05351.x>.
- Kamoshita, Shigehiko, Alan M. Aron, Kinuko Suzuki, and Kunihiro Suzuki. 1969. "Infantile Niemann-Pick Disease: A Chemical Study With Isolation and Characterization of Membranous Cytoplasmic Bodies and Myelin." *American Journal of Diseases of Children* 117 (4). <https://doi.org/10.1001/archpedi.1969.02100030381001>.
- Kamphoven, Joep H.J., Martijn M. De Ruiter, Leon P.F. Winkel, Hannerieke M.P. Van Den Hout, Jan Bijman, Chris I. De Zeeuw, Hans L. Hoeve, Bert A. Van Zanten, Ans T. Van Der Ploeg, and Arnold J.J. Reuser. 2004. "Hearing Loss in Infantile Pompe's Disease and Determination of Underlying Pathology in the Knockout Mouse." *Neurobiology of Disease* 16 (1). <https://doi.org/10.1016/j.nbd.2003.12.018>.
- Khan, Aiza, and Consolato Sergi. 2018. "Sialidosis: A Review of Morphology and Molecular Biology of a Rare Pediatric Disorder." *Diagnostics*. <https://doi.org/10.3390/diagnostics8020029>.
- Komura, Naoko, Kenichi G.N. Suzuki, Hiromune Ando, Miku Konishi, Akihiro Imamura, Hideharu Ishida, Akihiro Kusumi, and Makoto Kiso. 2017. "Syntheses of Fluorescent Gangliosides for the Studies of Raft Domains." In *Methods in Enzymology*. Vol. 597. <https://doi.org/10.1016/bs.mie.2017.06.004>.
- Land, Walter G. 2015. "The Role of Damage-Associated Molecular Patterns (DAMPs) in Human Diseases Part II: DAMPs as Diagnostics, Prognostics and Therapeutics in Clinical Medicine." *Sultan Qaboos University Medical Journal*.
- Lanfranco, Maria Fe, Italo Mocchetti, Mark P. Burns, and Sonia Villapol. 2018. "Glial- and Neuronal-Specific Expression of CCL5 mRNA in the Rat Brain." *Frontiers in Neuroanatomy* 11. <https://doi.org/10.3389/fnana.2017.00137>.
- Luzina, Irina G, Achsah D Keegan, Nicola M Heller, Graham A W Rook, Terez Shea-Donohue, and Sergei P Atamas. 2012. "Regulation of Inflammation by Interleukin-4: A Review of 'Alternatives.'" *Journal of Leukocyte Biology* 92 (4). <https://doi.org/10.1189/jlb.0412214>.
- Malhotra, Renuka. 2012. "Membrane Glycolipids: Functional Heterogeneity: A Review." *Biochemistry & Analytical Biochemistry* 1 (2). <https://doi.org/10.4172/2161-1009.1000108>.
- Masquelier, Julien, Mireille Alhouayek, Romano Terrasi, Pauline Bottemanne, Adrien Paquot, and Giulio G. Muccioli. 2018. "Lysophosphatidylinositols in Inflammation and Macrophage Activation: Altered Levels and Anti-Inflammatory Effects." *Biochimica et Biophysica Acta - Molecular and Cell Biology of Lipids* 1863 (12). <https://doi.org/10.1016/j.bbalip.2018.09.003>.

- Matloubian, Mehrdad, Anat David, Sharon Engel, Jay E. Ryan, and Jason G. Cyster. 2000. "A Transmembrane CXC Chemokine Is a Ligand for HIV-Coreceptor Bonzo." *Nature Immunology* 1 (4). <https://doi.org/10.1038/79738>.
- Mohammad, Ahmed N., Katelyn A. Bruno, S. Hines, and Paldeep S. Atwal. 2018. "Type 1 Sialidosis Presenting with Ataxia, Seizures and Myoclonus with No Visual Involvement." *Molecular Genetics and Metabolism Reports* 15. <https://doi.org/10.1016/j.ymgmr.2017.12.005>.
- Moolenaar, Wouter H., and Timothy Hla. 2012. "SnapShot: Bioactive Lysophospholipids." *Cell*. <https://doi.org/10.1016/j.cell.2012.01.013>.
- Nathan, Carl. 2006. "Neutrophils and Immunity: Challenges and Opportunities." *Nature Reviews Immunology*. <https://doi.org/10.1038/nri1785>.
- Nilsson, Olle, Jan Eric Månsson, Gunilla Håkansson, and Lars Svennerholm. 1982. "The Occurrence of Psychosine and Other Glycolipids in Spleen and Liver from the Three Major Types of Gaucher's Disease." *Biochimica et Biophysica Acta (BBA)/Lipids and Lipid Metabolism* 712 (3). [https://doi.org/10.1016/0005-2760\(82\)90272-7](https://doi.org/10.1016/0005-2760(82)90272-7).
- Onal, M., H. C. St. John, A. L. Danielson, J. W. Markert, E. M. Riley, and J. W. Pike. 2016. "Unique Distal Enhancers Linked to the Mouse Tnfsf11 Gene Direct Tissue-Specific and Inflammation-Induced Expression of RANKL." *Endocrinology* 157 (2). <https://doi.org/10.1210/en.2015-1788>.
- Ott, Troy L., and Alan D. Ealy. 2018. "Interferons." In *Encyclopedia of Reproduction*. <https://doi.org/10.1016/B978-0-12-801238-3.64925-5>.
- Ouchi, Noriyuki, and Kenneth Walsh. 2007. "Adiponectin as an Anti-Inflammatory Factor." *Clinica Chimica Acta*. <https://doi.org/10.1016/j.cca.2007.01.026>.
- Pedersen, Inge Søkilde, Peter Dervan, Alo McGoldrick, Michèle Harrison, Frederique Ponchel, Valerie Speirs, John D. Isaacs, Thomas Gorey, and Amanda McCann. 2002. "Systemic and Neurologic Abnormalities Distinguish the Lysosomal Disorders Sialidosis and Galactosialidosis in Mice." *Human Molecular Genetics* 11 (12). <https://doi.org/10.1093/hmg/11.12.1455>.
- PELT, Johannes VAN, Daniëlle G.J.L. VAN BILSEN, Johannes P. KAMERLING, and Johannes F.G. VLIEGENTHART. 1988. "Structural Analysis of O-glycosidic Type of Sialyloligosaccharide-alditols Derived from Urinary Glycopeptides of a Sialidosis Patient." *European Journal of Biochemistry* 174 (1). <https://doi.org/10.1111/j.1432-1033.1988.tb14080.x>.
- Ransohoff, Richard M., and V. Hugh Perry. 2009. "Microglial Physiology: Unique Stimuli, Specialized Responses." *Annual Review of Immunology*. <https://doi.org/10.1146/annurev.immunol.021908.132528>.
- Rosales, Carlos. 2018. "Neutrophil: A Cell with Many Roles in Inflammation or Several Cell Types?" *Frontiers in Physiology*. <https://doi.org/10.3389/fphys.2018.00113>.

- Sally Hannoodee, Dian N. Nasuruddin. 2021. "Acute Inflammatory Response - PubMed." In: *StatPearls [Internet]. Treasure Island (FL): StatPearls Publishing; 2022 Jan. 2021 Nov 21.*
- Schmid, D., and C. Münz. 2005. "Immune Surveillance of Intracellular Pathogens via Autophagy." *Cell Death and Differentiation*.  
<https://doi.org/10.1038/sj.cdd.4401727>.
- Schmid, Dorothee, Jörn Dengjel, Oliver Schoor, Stefan Stevanovic, and Christian Münz. 2006. "Autophagy in Innate and Adaptive Immunity against Intracellular Pathogens." *Journal of Molecular Medicine*. <https://doi.org/10.1007/s00109-005-0014-4>.
- Sevastou, Ioanna, Eleanna Kaffe, Marios Angelos Mouratis, and Vassilis Aidinis. 2013. "Lysoglycerophospholipids in Chronic Inflammatory Disorders: The PLA 2/LPC and ATX/LPA Axes." *Biochimica et Biophysica Acta - Molecular and Cell Biology of Lipids* 1831 (1). <https://doi.org/10.1016/j.bbalip.2012.07.019>.
- Seyrantepe, Volkan, Helena Poupetova, Roseline Froissart, Marie Thérèse Zabet, Irène Maire, and Alexey V. Pshezhetsky. 2003. "Molecular Pathology of NEU1 Gene in Sialidosis." *Human Mutation*. <https://doi.org/10.1002/humu.10268>.
- Simonaro, Calogera M. 2016. "Lysosomes, Lysosomal Storage Diseases, and Inflammation." *Journal of Inborn Errors of Metabolism and Screening* 4.  
<https://doi.org/10.1177/2326409816650465>.
- Smith, David, Kerri Lee Wallom, Ian M. Williams, Mylvaganam Jeyakumar, and Frances M. Platt. 2009. "Beneficial Effects of Anti-Inflammatory Therapy in a Mouse Model of Niemann-Pick Disease Type C1." *Neurobiology of Disease* 36 (2). <https://doi.org/10.1016/j.nbd.2009.07.010>.
- Smutova, Victoria, Amgad Albohy, Xuefang Pan, Elena Korchagina, Taeko Miyagi, Nicolai Bovin, Christopher W. Cairo, and Alexey V. Pshezhetsky. 2014. "Structural Basis for Substrate Specificity of Mammalian Neuraminidases." *PLoS ONE* 9 (9).  
<https://doi.org/10.1371/journal.pone.0106320>.
- Trinchieri, Giorgio. 1995. "Interleukin-12: A Proinflammatory Cytokine with Immunoregulatory Functions That Bridge Innate Resistance and Antigen-Specific Adaptive Immunity." *Annual Review of Immunology*.  
<https://doi.org/10.1146/annurev.iy.13.040195.001343>.
- Vitner, Einat B., Frances M. Platt, and Anthony H. Futerman. 2010. "Common and Uncommon Pathogenic Cascades in Lysosomal Storage Diseases." *Journal of Biological Chemistry*. <https://doi.org/10.1074/jbc.R110.134452>.
- Walkley, S. U. 2009. "Pathogenic Cascades in Lysosomal Disease - Why so Complex?" In *Journal of Inherited Metabolic Disease*. Vol. 32. <https://doi.org/10.1007/s10545-008-1040-5>.
- Walkley, Steven U., and Marie T. Vanier. 2009. "Secondary Lipid Accumulation in Lysosomal Disease." *Biochimica et Biophysica Acta - Molecular Cell Research*.  
<https://doi.org/10.1016/j.bbamcr.2008.11.014>.

- Wang, Aozhe, Haifeng Zhang, Jianming Liu, Zhiyi Yan, Yaqi Sun, Wantang Su, Ji Guo Yu, Jing Mi, and Li Zhao. 2023. "Targeted Lipidomics and Inflammation Response to Six Weeks of Sprint Interval Training in Male Adolescents." *International Journal of Environmental Research and Public Health* 20 (4). <https://doi.org/10.3390/ijerph20043329>.
- Wang, Raymond Y., Olaf A. Bodamer, Michael S. Watson, and William R. Wilcox. 2011. "Lysosomal Storage Diseases: Diagnostic Confirmation and Management of Presymptomatic Individuals." *Genetics in Medicine* 13 (5). <https://doi.org/10.1097/GIM.0b013e318211a7e1>.
- Wehr, Alexander, Christer Baeck, Felix Heymann, Patricia Maria Niemietz, Linda Hammerich, Christian Martin, Henning W. Zimmermann, et al. 2013. "Chemokine Receptor CXCR6-Dependent Hepatic NK T Cell Accumulation Promotes Inflammation and Liver Fibrosis." *The Journal of Immunology* 190 (10). <https://doi.org/10.4049/jimmunol.1202909>.
- Wraith, James E., and Jackie Imrie. 2009. "New Therapies in the Management of Niemann-Pick Type C Disease: Clinical Utility of Miglustat." *Therapeutics and Clinical Risk Management*. <https://doi.org/10.2147/tcrm.s5777>.
- Wu, Junru, Anthony Cyr, Danielle S. Gruen, Tyler C. Lovelace, Panayiotis V. Benos, Jishnu Das, Upendra K. Kar, et al. 2022. "Lipidomic Signatures Align with Inflammatory Patterns and Outcomes in Critical Illness." *Nature Communications* 13 (1). <https://doi.org/10.1038/s41467-022-34420-4>.
- Wu, Yun Ping, and Richard L. Proia. 2004. "Deletion of Macrophage-Inflammatory Protein 1 $\alpha$  Retards Neurodegeneration in Sandhoff Disease Mice." *Proceedings of the National Academy of Sciences of the United States of America* 101 (22). <https://doi.org/10.1073/pnas.0400625101>.
- Xia, Baoyun, Ghazia Asif, Leonard Arthur, Muhammad A. Pervaiz, Xueli Li, Renpeng Liu, Richard D. Cummings, and Miao He. 2013. "Oligosaccharide Analysis in Urine by MALDI-TOF Mass Spectrometry for the Diagnosis of Lysosomal Storage Diseases." *Clinical Chemistry* 59 (9). <https://doi.org/10.1373/clinchem.2012.201053>.
- Zammarchi, Enrico, Maria Alice Donati, Amelia Morrone, Gian Paolo Donzelli, Xiao Yan Zhou, and Alessandra D'Azzo. 1996. "Early-Infantile Galactosialidosis: Clinical, Biochemical, and Molecular Observations in a New Patient." *American Journal of Medical Genetics* 64 (3). [https://doi.org/10.1002/\(SICI\)1096-8628\(19960823\)64:3<453::AID-AJMG2>3.0.CO;2-Q](https://doi.org/10.1002/(SICI)1096-8628(19960823)64:3<453::AID-AJMG2>3.0.CO;2-Q).
- Zigterman, B.G.R., and L. Dubois. 2022. "Inflammation and Infection: Cellular and Biochemical Processes." *Nederlands Tijdschrift Voor Tandheelkunde* 129 (3). <https://doi.org/10.5177/ntvt.2022.03.21138>.